January 2018

Discovery Of Piperlongumine Derivatives As Anti-Leukemic And Anti-Prostate Cancer Agents

Yi Liao
Wayne State University, fl9510@wayne.edu

DISCOVERY OF PIPERLONGUMINE DERIVATIVES AS ANTI-LEUKEMIC AND ANTI-PROSTATE CANCER AGENTS

by

YI LIAO

DISSERTATION

Submitted to the Graduate School

of Wayne State University,

Detroit, Michigan

in partial fulfillment of the requirements

for the degree of

DOCTOR OF PHILOSOPHY

2018

MAJOR: PHARMACEUTICAL SCIENCES

Approved By:

_____

Advisor Date

_____

_____

_____

DEDICATION

I dedicate this thesis to my beloved father (Shenggang Liao), mother (Xiuling Cao), and my wife (Di Kang), whose love, unselfish support, example over many years encouraged me in my study.

ACKNOWLEDGMENTS

I would like to give many thanks to my advisor, Dr. Zhihui Qin, who has always been with me. Thank him for giving me continuous support, guidance, and encouragement during my research; thank him for his patience, valuable time, motivation during my studying. Precisely because of this, I have not only developed professional skills but also grown up to be an independent and rigorous thinker. Besides, thank him for supporting my public presentation and poster printing, which has built my networking. There is no doubt that these experiences are unforgettable in my life and will motivate me to go forward all the time.

I am thankful for my dissertation committee members, Dr. Yubin Ge, Dr. Fei Chen, and Dr. Aloke Dutta. Thank them for giving me valuable suggestions, which help me solve every obstacle in my research. Thank them for their time and support as well.

Also, I would like to express my gratitude to previous and current lab members with whom I have worked over the past five years. Thank Dr. Bailing Chen for teaching and guiding my chemistry skills; thank Ms. Liping Xu for your careful instructions in various biological assays; thank Mr. Siyu Ou for sharing practical experimental skills; thank Katie Sorensen, Matthew T Kuntzman, and Floriana Bebri for choosing our lab, helping me gain mentoring experience.

I want to give special thanks to our collaborator, Dr. Yubin Ge, and his students, Dr. Xiaojia Niu and Dr. Jianyun Zhao, for their insightful advice, support, and contribution to my research projects. My research progress might not have gone smoothly without such a friendly and wonderful collaborative environment.

I would like to sincerely thank Department of Pharmaceutical Sciences, Wayne State University, for offering such an excellent study and research platform. I am extremely proud of being a member of this big family. Herein, I want to acknowledge all faculty, students, and administrative staff.

Finally, my great gratitude goes to my parent, my wife, and friends. Thank my father for his effort and encouragement, supporting my graduate education. Thank my mother for her generosity and unconditional love. Thank my lovely wife for her endless love and thoughtful care. Thank my friends for sharing happiness and sorrow with me. My accomplishment would not have been possible without their true love and support.

TABLE OF CONTENTS

LIST OF TABLES

LIST OF FIGURES

LIST OF SCHEMES

CHAPTER 1 INTRODUCTION

1.1. Anti-cancer activities of piperlongumine (PL)

a)

b)

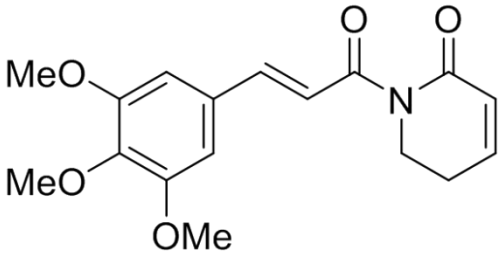

Figure 1. a) Pictures of long pepper, and PL was originally extracted from this plant. **b)** Chemical structure of PL.

The dried long pepper is usually used as a seasoning in Indian and Malaysian cuisine. Labeled with pippali, long pepper is readily available in many Indian grocery stores. Today, there are growing interest on Piperlongumine (PL), an alkaloid identified from the long pepper. PL was originally isolated from the root of *Piper longum L* (**Figure 1a**), and its structure and synthesis was elaborated in 1967[1] (**Figure 1b**). PL has multiple pharmacological activities[2], including anti-tumor, anti-depressant, anti-diabetic, anti-bacterial, anti-platelet aggregation,

etc. Among them, anti-cancer activities are very attractive, as demonstrated in a nature paper published in 2010[3]. As shown in **Figure 2**, PL affects various oncogenic pathways in multiple cancer cells, covalent protein modifications and induction of reactive oxygen species (ROS) are believed to be the key mediators of the observed anti-cancer effects[4].

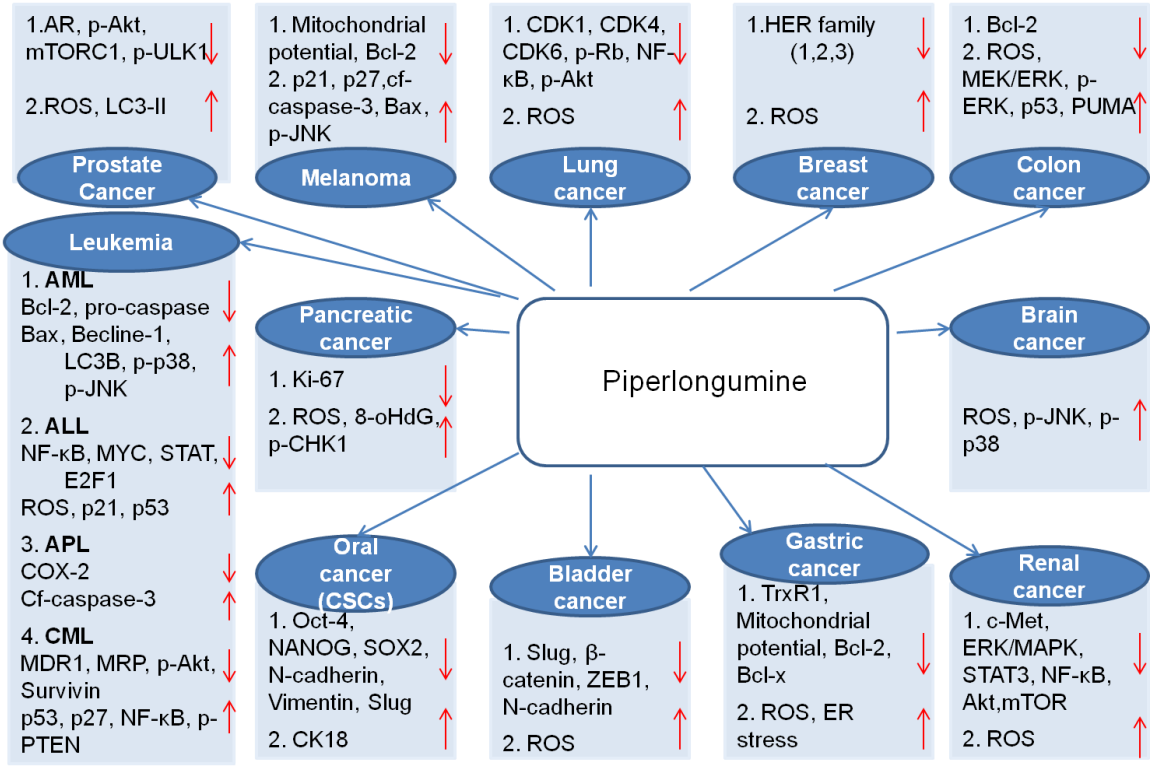

Figure 2. PL modules multiple oncogenic pathways and was studied in various cancer models, including prostate[5,6,7], melanoma[8], lung[9], breast[10], colon[11], leukemia[12,13,14,15], pancreatic[16], oral[17], bladder[18], gastric[19] and renal cancer[20].

1.1.1. PL is an anti-cancer electrophile

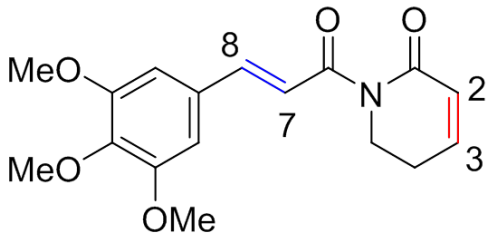

PL

C2-C3 olefin reacts with cellular thiols chemically or enzymatically via Michael addition.

Cellular thiols include GSH, GST, Keap1, TrxR, IKK, p65/p50 (NF-κB), etc.

C7-C8 olefin is necessary for protein glutathionylation, further enhancing cellular cytotoxicity

Figure 3. Structure-activity relationship and mechanisms of action of PL against cancer cells. Two Michael acceptors contribute to the overall anti-cancer activities. C2-C3 olefin correlates with ROS elevation, and C7-C8 enhances cytotoxicity. PL covalently interacts with cellular thiols such as GSH, GST, Keap1, TrxR, IKK, p65/p50(NF- NF-κB), etc. Abbreviations: GSH: glutathione; GST: glutathione *S*-transferase; Keap1: Kelch-like ECH-associated protein 1; TrxR: thioredoxin reductase; IKK: IκB kinase; p65/p50: two subunits of NF-κB transcriptional complex.

Anti-cancer activities of PL heavily rely on the unique electrophilic property. PL consists of two α, β-unsaturated moieties (C2-C3 and C7-C8 olefins) known as "Michael-acceptors," thereby harboring electrophilicity. The functionality of C2-C3 olefin and C7-C8 olefin is associated with GSH conjugation and glutathionylation of GSH-binding proteins[21], respectively (**Figure 3a**). Besides GSH-binding proteins, PL can also covalently modify other cellular proteins such as IKK[22], p65/p50 (NF-κB)[23] and Keap1[24] (**Figure 3b**). Current research points out that chlorine introduction at C2 of PL notably enhances PL's electrophilicity, thereby

leading to more potent anti-cancer activities[25,26]. C7-C8 olefin is primarily shown to increase protein glutathionylation, and its removal causes significant reductions in cytotoxicity[21]. Other modifications on either the trimethoxy group or the aromatic ring barely affect the potency of PL in cancer cells[21,25], demonstrating the tolerability and feasibility of PL structural modifications. In conclusion, C2-C3 and C7-C8 olefins are the most critical determinants for PL's actions, and modifications on other positions distal from these olefins are tolerable. Therefore, PL is a suitable research tool due to its favorable electrophilicity, and much effort has been continuously placed to explore the electrophilicity-based prooxidant anti-cancer strategy due to the intrinsic relationship between electrophilicity and oxidative stress[21].

The chemical reactivity of α,β-unsaturated carbonyl group of electrophiles decides PL's electrophilicity. Given the relatively reactive chemical property, α,β-unsaturated double bond of electrophiles generally reacts with many nucleophiles via Michael addition, including the amine group of Lys, the imidazole group of His, and the thiol group of Cys[27]. Among them, the reaction of electrophiles with Cys thiol is more readily and stable, especially the reaction with a more nucleophilic thiolate formed through deprotonation when Cys is located in basic environment or proximity to positively charged amino acids[27]. GSH is the

abundant source of cellular thiols and participates in antioxidant defense, so electrophiles are inevitable to react and consume intracellular GSH, thereby increasing oxidative stress[28]. In addition to antioxidant GSH depletion, they also covalently inhibit thiol-containing proteins (e.g., GST, TrxR, GCLC, GPX1 etc.) involved in the antioxidant defense system, attenuating ROS scavenging[12, 29]. Therefore, electrophilicity of electrophiles connects with oxidative stress through interfering with antioxidants or antioxidant defense systems.

1.1.2. Anti-leukemic activities of PL

PL reduced the viability of various AML cell lines (e.g., U937, MV4-11, etc.) with the IC_{50}s in low micromolar range (1-3 μM)[30], and was also effective in inhibiting $CD34^+$ AML stem cells through targeting glutathione metabolism[12]. PL induced apoptosis and autophagy in AML patient samples, as evidenced by the upregulation of Bax, Bcl-2, caspase-3, Becline-1, LC3B, p-p38, and p-JNK[31].

In addition to AML, PL inhibited the growth of B-cell acute lymphoblastic leukemia cell line through several mechanisms, including downregulation of multiple transcriptional factors (eg., AP1, MYC, NF-κB, Sp1, STAT1, STAT3, E2F1, etc.), p21 upregulation independent of p53, and ROS elevation[13]. Also, PL displayed anti-acute promyelocytic leukemic (APL) activities through inhibition of COX-2 and induction of caspase-3 cleavage[14]. PL was able to reverse drug

resistance of CML K562/A02 cells by reducing P-gp, MDR1, and MRP expression, and decreasing AKT phosphorylation as well as NF-κB transcriptional activity[15]. Moreover, p53 and p27 upregulation was observed in the same cell line following PL treatment[15].

1.1.3. Anti-prostate cancer activities of PL

PL exhibits diverse bioactivities against prostate cancer (PCa): 1) PL inhibited AR-positive LNCaP proliferation at low micromolar concentrations (IC_{50}<5uM) and effectively depletes full-length AR and AR variants through proteasome-mediated ROS-dependent mechanism[5]. 2) PL decreased phosphorylation of AKT at both S473 and T308 sites and downstream mTORC1 activity, thus promoting autophagy in AR-negative PC-3 cells[6]. 3) PL downregulated NF-κB signaling independently of AKT, leading to diminished adhesion and invasion of prostate cancer cells[7]. Besides these anti-prostate cancer mechanisms, PL also displays pleiotropic activities in other types of cancer through affecting JNK-EKR signaling pathway[32], GST Pi 1 activity[33], p38-JNK[31], TrxR1 activity[19], ubiquitin-proteasome system[34], and an array of transcriptional factors including c-Myc and Sp1, Sp3 and Sp4[35] (**Figure 2**). On the other hand, since PL serves as a versatile anti-cancer compound, it has been further combined with other chemotherapeutic agents such as cisplatin or paclitaxel[36],

auranofin[37], TRAIL[38], and SAHA[30].

1.2. Acute myeloid leukemia (AML)

Acute myeloid leukemia (AML) occurs in bone marrow and blood with the rapid growth of uncontrolled immature myeloid blast cells. AML is characterized by genetic heterogeneity and malignant clonal disorder of the hematopoietic system. Historically, the first report about AML was published by a Scottish physician, Peter Cullen, who described an unknown "milky blood" symptom in 1811[39]. In 1847, Rudolph Virchow named this disease "Leukemia"[40]. AML is one type of leukemia and is a highly acute and fatal malignancy. AML patients without treatments will typically die within six months or less[41]. 40 years ago, the overall survival of AML was less than 7%[42]. To date, breakthroughs in cytogenetic and hematopathologic advances lead to the significantly improved survival rate of AML to 35%-40% for adult patients[43], and 60%-70% for children patients[44]. However, although such efforts have been made to increase patient's survival, the overall remission rate of AML is still less than 50% for patients younger than 60 years old, and only 5-15% for patients older than 60 years old[45]. AML patients are often accompanied by several symptoms in a wide range, including pancytopenia, anemia, pale, fatigue, thrombocytopenia, sweet syndrome, blast proliferation, hyperleukocytosis, CNS infiltration, and intravascular coagulation, etc[46]. In 2015,

AML was affecting nearly 1 million people and was reported to be the most prevalent leukemia type among four types of leukemia (total 2.3 million patients with leukemia) in the world[47]. The current treatments for AML have not been changed dramatically over 30 years and mainly rely on chemotherapy and hematopoietic stem cell transplantation (HSCT)[43], while these treatments have limitations considering patient tolerance, AML fast relapse, and potential resistant occurrence.

1.2.1. Epidemiology

In the USA, estimated 62,130 cases were expected to be diagnosed with leukemia in 2017, which increased 19% than that in 2014[48,49]. The percentage of populations with AML accounted for 34-36% in total cases with leukemia in 2014-2017[48,49]. AML was the most common leukemia type among four types of leukemia and was also the fatal leukemia type, with the highest mortality (43% of all leukemia-causing deaths) and lowest overall 5-year survival rate. (26.8% of AML vs 65.9% CML vs 85.1% CLL vs 70.7% ALL)[48,49]. In gender, men were seen leukemia more common than women in 2017, with around 40.2 percent higher death rate for men than women[49]. Similar to the general gender trend, AML had 27% higher occurrence rate in men (estimated 11,960 cases) than women (9,420 cases) according to the 2017 statistics[49]. In race and ethnicity, AML was more

common in whites (85.6%) than in blacks (14.4%), as shown in 2016 report[50]. At age, people were usually diagnosed with AML within the age range from 65-74. The percentage of patients who die from AML was highest within the age of 75-84[51].

1.2.2. Pathogenesis

Multiple characteristics present in AML patients have been identified by using genome sequencing, flow cytometry, conventional cytogenetic testing, and genetic lesion screening. According to the latest revision of WHO classification of tumors of hematopoietic and lymphoid tissues in 2016[52], the major focus is on cytogenetic and molecular genetic abnormalities. These genetic abnormalities and molecular lesion are commonly detected and believed to drive the occurrence of AML.

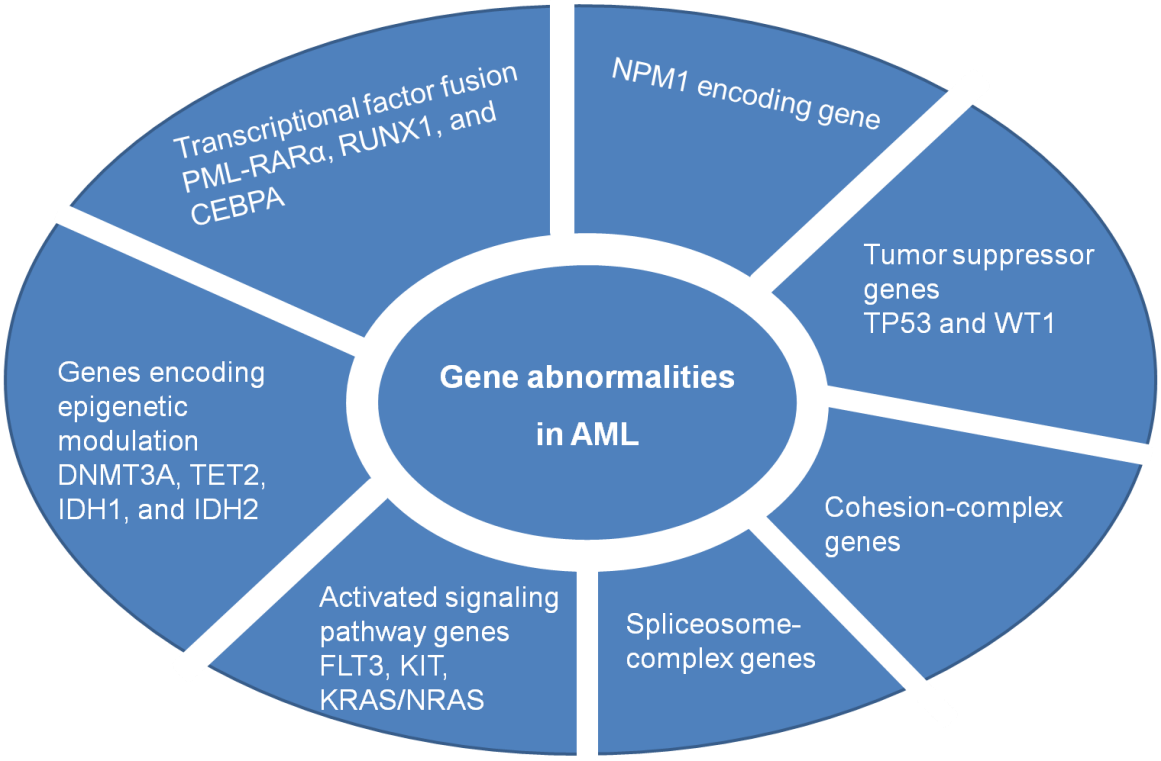

Figure 4. Cytogenetic abnormalities in AML. Abbreviations: PML-RARα: promyelocytic leukemia-retinoic acid receptor alpha fusion; RUNX1: Runt-related transcription factor 1; CEBPA: CCAAT/enhancer-binding protein alpha; DNMT3A: DNA (cytosine-5)-methyltransferase 3A; TET2: Tet methylcytosine dioxygenase 2; IDH1: IDH1/2: isocitrate dehydrogenase 1/2; FLT3: fms-like tyrosine kinase 3; KIT: mast/stem cell growth factor receptor; KRAS/NRAS: two members of RAS protein family; TP53: tumor suppressor p53 gene; WT1: WT1: Wilms' tumor suppressor gene; NPM1: nucleophosmin.

With many gene mutations revealed, not a single gene mutation accounts for AML pathogenesis. In normal hematopoiesis, the myeloblast cells can grow into mature white blood cells, however, they undergo differentiation arrest caused by genetic changes (e.g., production of a PML-PARα fusion protein) in AML[53]. This arrest, along with other gene disruption controlling cell proliferation, will result in

uncontrolled growth of immature myeloblasts and eventually lead to clinic entity and following clinical manifestations of AML. The percentage of blasts is important for the diagnosis of AML, with at least 20% myeloid blasts found in bone marrow and/or peripheral blood[46]. Cytogenetic abnormalities in AML can be classified into seven subsets[54,55,56,43,57]: 1) transcription factor fusion (PML-RARα, RUNX1, and CEBPA); 2) NPM1 encoding gene; 3) tumor-suppressor genes (TP53 and WT1); 4) genes encoding epigenetic modulation (DNMT3A, TET2, IDH1, and IDH2); 5) activated signaling pathway genes (FLT3, KIT, and KRAS/NRAS); 6) cohesion-complex genes; 7) spliceosome-complex genes. Regarding cellular effects, these gene mutations could also be mainly divided into three classes. Gene mutations in Class I affect cellular signal transduction such as FLT3, KIT, NRAS, KRAS, JAK2, and PTPN11; Class II disrupts cell differentiation, including RUNX1(AML-1), MLL, RARα, CBFβ, NPM1, etc. Class III includes TET2, IDH1 or IDH2, DNMT3A, EZH2, etc., and interferes with epigenetic modification. Other class includes WT1 and TP53, affecting tumor suppression[58,59]. Class I and class II are complicated and intertwined for initiation of AML, either class I or class II doesn't guarantee hematogenesis. For example, Dr. Gilliland group reported that FLT-ITD (Class I) could induce myeloporliferative disorder while not sufficient to initiate observed AML phenotype in humans, suggesting the necessary

participation of additional cooperative mutations[60]. Following the previous study, the same group demonstrated that Class II PML-RARα and FLT-ITD could cooperatively induce acute promyelocytic leukemia (APL) in the mouse model[61]. Different from class I and class II gene mutations, class III recurrent somatic mutations identified from genome-wide and candidate-gene studies are found to be a common genetic event in AML patients. They contribute to the pathogenesis of myeloid malignancies though regulating DNA methylation (e.g., TET2, DNMT3A) and histone post-modification (e.g., MLL, PRC)[62].

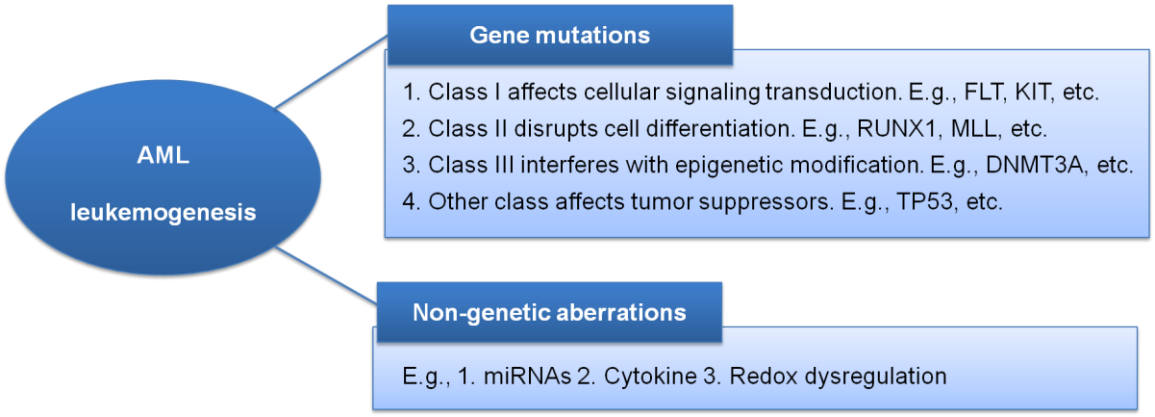

Figure 5. Genetic abnormalities and non-genetic aberrations contribute to the leukemogenesis of AML.

In addition to genetic aberrations, non-genetic alterations also play an important role in leukemogenesis. For instance, miR-125 is overexpressed in AML patient blasts and promotes the transformation of normal hematopoietic cells to AML[63]; Cytokine (IL-3) stimulation or PML-RARα alone only leads to limited effects on myelopoiesis, while IL-3 combined with PML-RARα can lead to fatal

diseases with AML phenotypes, suggesting the cooperation of cytokine with gene abnormalities in leukemogenesis[64]; Heightened endogenous ROS sustained by leukemic cells exacerbates oxidative damage, thereby leading to advantageous DNA mutation which promotes leukemogenesis[65]. Therefore, genetic abnormalities involving gene mutations and non-genetic changes (e.g., miRNA, cytokine, and redox dysregulation) are critical for leukemogenesis.

1.2.3. Potential therapeutic targets and treatments

In general, with the development of leukemic biology and molecular pathology, AML therapies are widely available and optimizing toward patient individualization. These therapies mainly contain intensive chemotherapy and allogeneic hematopoietic stem cell transplantation. Much effort has been made into the discovery of "targeted agents", development of novel drug combination and optimization of safer stem cell transplantation procedures. However, current AML management still heavily relies on chemotherapy in younger adult patients (<60 years of age). There are not effective agents available for older patients (>60 years of age) or patients unable to tolerate chemotherapy[66]. In this context, novel drugs or antibodies are discovered and developed by targeting a variety of cellular oncogenic signaling pathways, epigenetic modifications, antigens presenting on leukemic cells or leukemic stem cells, etc. These new drugs either approved by

FDA or under preclinical or clinical trials are summarized in the following table[45], and their potential targets are also shown.

Table 1 Drugs targets and therapeutic agents for the treatment of AML. The table was adapted from Dohner 2015[45].

Potential Targets/Action Mechanism	Agents	Clinical Status	Clinical Trials
Conventional drugs			
	Cytarabine	FDA approved in 1969	
	Daunorubicin	FDA approved in 1979	
	Arsenic Trioxide	FDA approved in 2000	
Epigenetic modifiers			
Hypomethylating agents	Decitabine	Phase IV	NCT03026842
	Azacitidine	Phase IV	NCT01806116
	Oral azacitidine	Phase III	NCT01757535
IDH1 inhibitor	AG-120	Phase III	NCT03173248
IDH2 inhibitor	AG-221	Phase III	NCT02577406
DOT1L inhibitor	EPZ-5676	Phase I	NCT02141828
Bromodomain inhibitor	OTX015	Phase I	NCT01713582
LSD1	GSK2879552	Phase I	NCT02177812
Histone deacetylase inhibitors	Vorinostat	Phase III	NCT01802333
	Panobinostat	Phase II	NCT00880269
	Valproic acid	Phase I/II	NCT01369368
Tyrosine kinase inhibitors			
FLT3 inhibitors	Midostaurin	Phase III	NCT03379727
	Sunitinib	Phase I/II	NCT00783653
	Sorafenib	Phase II/III	NCT02474290
KIT inhibitors	Dasatinib	Phase III	NCT02013648
	Midostaurin	Phase III	NCT03379727
Cell--cycle and			

signaling inhibitors			
MDM2 inhibitor	Idasanutlin	Phase III	NCT02545283
PLK inhibitor	Volasertib	Phase IV	NCT01721876
Aurora kinase inhibitor	Barasertib	Phase I/II	NCT03217838
CDK inhibitor	Alvocidib	Phase II	NCT02520011
PI3K inhibitor	Rigosertib	Phase I/II	NCT01167166
PIM kinase inhibitor	LGH447	Phase I	NCT02078609
Nuclear export inhibitor			
XPO1 (CRM1 inhibitor)	selinexor	Phase II	NCT03071276
Cytotoxic agents	Vosaroxin	Phase III	NCT01191801
Nucleoside analogs	Sapacitabine	Phase III	NCT01303796
	Clofarabine	Phase III	NCT00703820
	Cladribine	Phase III	NCT03384212

Abbreviations: IDH1/2: isocitrate dehydrogenase; DOT1L: DOT1-like histone H3K79 methyltransferase; LSD1: Lysine-specifi histone demethylase 1A; FLT3: FMS-like tyrosine kinase 3; MDM2: Mouse double minute 2 homolog; PLK: polo-like kinase; CDK: cycline-dependent kinase; PI3K: phosphoinositide 3-kinase inhibitor; PIM: proto-oncogene serine/threonine-protein kinase; XPO1: exportin 1, also known as chromosomal maintenance 1 (CRM1).

1.3. Castration-resistant prostate cancer (CRPC)

SEER cancer statistics review 1975-2014[67] and cancer statistic in 2017[68,49] reported that prostate cancer was the common type of cancer in men in the US, accounting for about 20-30% of all new cases of cancer. The mortality was 4.4%, and 26,730 people was projected to die from PCa in the US in 2017. Risk factors for prostate carcinogenesis included age, dietary habit (e.g., smoking), family history, and inherited genetic conditions (e.g., Lynch syndrome, BRCA1 and BRCA2 mutations). PCa was primarily localized in prostate (79%), partially spread

(12%), or metastasized (5%). For metastatic PCa, the 5-year survival rate was only 29.8%[67]. During cancer progression, symptoms include decreased urinary stream, frequent urination at night, pain, blood or burning with urination, nocturia or incomplete bladder emptying. In advanced or metastatic PCa, pain in spine, hips or bone may also be presented. Current treatments for PCa rely on surgery, hormonal therapy, radiation therapy or chemotherapy. Hormonal therapy may be used with surgery and radiation therapy is used for patients with more advanced PCa. Chemotherapy becomes a main option when hormone treatments or surgery are not effective. The standard treatment contains docetaxel/cabazitaxel along with steroid drug prednisone or androgen-deprivation therapy (ADT)[69].

Huggins and Hodges[70] for the first time identified and demonstrated reliance of prostate cancer on androgen. Since then, ADT has become the standard of care for patients, aiming to achieve disease stabilization by lowering the source of androgen. ADT can be achieved through surgical and medical castration. Surgical castration excises both testes and reduces major circulating androgen testosterone by 90%[71]. Medical castration pharmacologically reduces androgen production. For example, LHRH (luteinizing hormone-releasing hormone) agonists and antagonists are used to decrease luteinizing hormone, thus preventing testicular testosterone production. Despite the initial benefit,

patients who receive ADT frequently progress to castration-resistant prostate cancer (CRPC) within 2-3 years[72]. This progression is driven by several mechanisms including altered steroidogenesis, aberrant signaling activation, AR or AR co-regulators mutations, the presence of truncated AR, etc[73]. In CRPC, AR signaling continues to play the key role in PCa maintenance and progression[74]. Current treatments either approved by FDA or in clinical trials are mainly targeting AR, mutant AR, and androgen synthesis.

1.3.1. Epidemiology

According to latest cancer statistics in 2017 in USA[68], prostate cancer (PCa) was the third-leading cause of men deaths in 2017 with an estimated 26,730 cases in the USA. Nearly 161,360 men would be diagnosed with prostate cancer during 2017. 1 in 8 of men would be possibly diagnosed with PCa in their whole life in the US[68]. Prostate cancer was affecting around 1.1 million in the world and causing 0.3 million deaths in 2012, with the second highest incidence rate and fifth highest mortality in all cases of cancers in men[75]. In race and ethnicity, PCa was much more common in blacks (42.8%) than whites, with around twice higher risk rate than non-hispanic whites (18.7%), five-fold higher risk rate than Asian/Pacific islander (8.8%)[68]. Based on age-adjusted data from 2010-2014[67], people were usually diagnosed with PCa within an age range 65-74, with a

median age of 66 at diagnosis. The percent of patients who die from PCa was the highest within an age range 75-84, with a median age of 80 at death.

1.3.2. Pathogenesis

The specific pathogenesis of PCa is not fully understood, but several approaches (e.g., cellular signaling regulation mapping, genome-wide analysis, microRNAs profiling, etc.) have performed and identified potential causes for onset and advanced PCa. Many factors, including gene abnormalities and non-gene aberrations, contribute to the development of PCa.

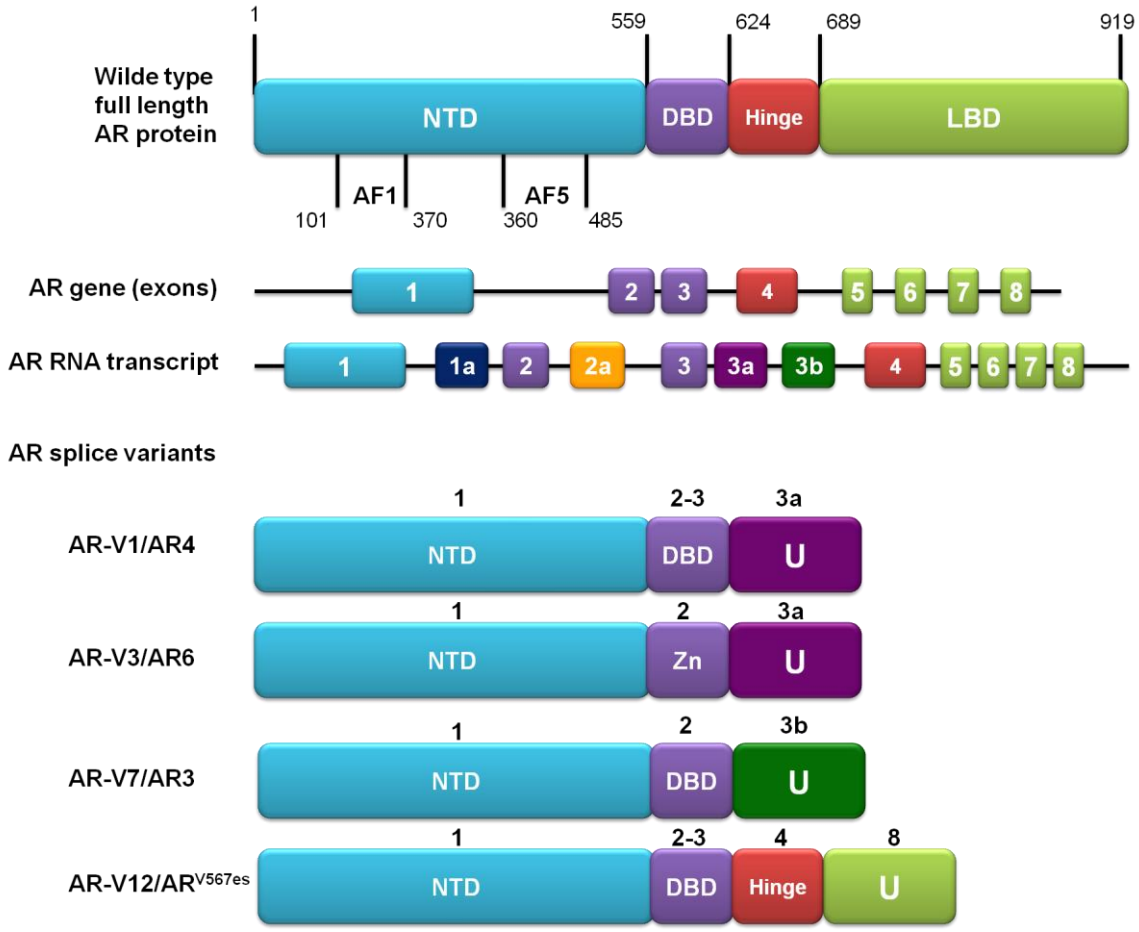

Figure 6. Structure of wild type AR protein, AR gene, AR RNA transcript, and common gain-of-function AR-Vs in CRPC. AR-V1, AR-V3, AR-V7, and AR-V12 are abundant and associated with resistance to hormonal therapy[76]. AR-V7 and AR-V3 may be the major androgen-independent drivers of AR-regulated gene expression in CRPC[77,78]. The picture was modified based on Brinkmann 1989[79] and Lallous 2013[80]. NTD= N-terminal domain; DBD= DNA-binding domain; LBD= ligand-binding domain; AR-Vs= AR splice variants; U= unique nucleic acid sequences not found in wild type AR; Zn= zinc finger; AF1/5= activation function 1/5.

AR signaling abnormalities are emphasized in the development and maintenance of androgen-dependent or independent PCa. As the initial mediator of AR signaling, approximately 33% of recurrent PCa and up to 80% CRPC show enhanced AR activity as a result of AR gene amplification, AR mRNA overexpression, and AR protein upregulation[81,82]. In androgen-dependent PCa, overexpressed AR renders PCa cells high sensitivity to sense and uptake androgen despite castration[83]. In androgen-independent PCa, AR activation is persistent, and driven by androgen-independent mechanisms such as MAP kinase[84] or HER family kinase[85]. Interestingly, AR protein itself is a transcriptional factor regulating expression of several miRNAs such as miR-19a[86], miR-27a[86], miR-133b[86], miR-148[87], miR-125b[88], etc. miR-125b is overexpressed either in PCa cell lines or PCa patient samples, and can induce androgen-independent PCa proliferation by downregulating Bak1[88], suggesting the oncogenic role of miR-125b. In CRPC, assessments of clinical patients with CRPC revealed that

androgen levels are not remarkably reduced when compared to control tissues[89], suggesting the intratumoral enhancement in androgen synthesis or maintenance[90]. In parallel with androgen level results, subsequent gene expression studies revealed the increased expression of androgen-synthesizing enzymes such as CYP17A1 and SRD5A1[91,92]. Currently, CRPC has been considered as "androgen-independent" or " hormone-refractory", and AR signaling axis still plays the central role in maintenance and progression of CRPC. In this context, two FDA-approved agents, abiraterone[93] (a CYP17A1 inhibitor) and enzalutamide[94] (an anti-androgen) are approved for the treatment of CRPC. Despite these current therapies, the treatment for CRPC is still challenging due to observed drug resistance[95]. Abiraterone or orteronel targeting androgen synthetic enzyme CYP17A1 with high affinity can reduce the circulating level of androgen, but the resistance has emerged in patients receiving these agents and is associated with the upregulation of CYP17A1, constitutively active full-length AR or the presence of AR splice variants (AR-Vs)[96] (**Figure 6**). Therefore, these resistances to CYP17A1 inhibitors observed in clinical samples limit their applications in patients with CRPC and encourage researchers to explore other targets. Targeting AR ligand binding domain (LBD) has become appealing. Given that AR signaling initiates by binding to dihydrotesterone (DHT), anti-androgens

are developed to compete with DHT with higher affinity, thus antagonizing AR signaling. However, compelling evidence has also shown resistant mechanisms to AR LBD agents such as bicalutamide and enzalutamide. The bicalutamide competes with AR substrate (DHT) and weakens AR binding to chromatin or coactivator proteins, but it fails to inhibit AR translocation into the nucleus; thereby, AR can still proceed transcription stimulation[97,98]. Furthermore, a mutation in codon 741 or AR overexpression confers bicalutamide agonistic activity instead of presumable antagonistic activity[99,100]. The other enzalutamide binds AR with high affinity and further blocks AR translocation into the nucleus, but it has no considerable efficacy in CRPC mouse model where increased AR-Vs are present[77]. Overall, multiple factors including promoted androgen biosynthesis, AR mutation, decreased recruitment of AR coactivators or corepressors, and increased AR-Vs level are implicated in resistance to current AR LBD-targeting agents. It is noted that these resistant mechanisms are closely related to CRPC's characteristics distinct from PCa cells. In CRPC cells, AR-Vs lacking C-terminal ligand-binding domain (LBD) are constitutively active and primarily present in the nucleus with AR transcriptional activities[101]. AR-V7 and ARv567es were commonly observed and linked to CRPC progression and metastasis[95]. Clinically, AR-Vs are implicated in 40%-50% CRPC patients[102]. Structurally, although AR-Vs

lack intact LBD and some even have incomplete DNA-binding domains (DBD)[78,77,103], AR and most AR-Vs share intact N-terminal domain (NTD) where activation function-1 region interacts with many partner proteins such as CBP[104] and RAP74[105] (**Figure 6**). It is AR NTD that is responsible for the formation of transcriptional complex, thus maintaining transcriptional activities of AR/AR-Vs regardless of LBD. Therefore, the regimen targeting both AR and AR-Vs is considered to be most effective in anti-CRPC therapy (**Figure 7**).

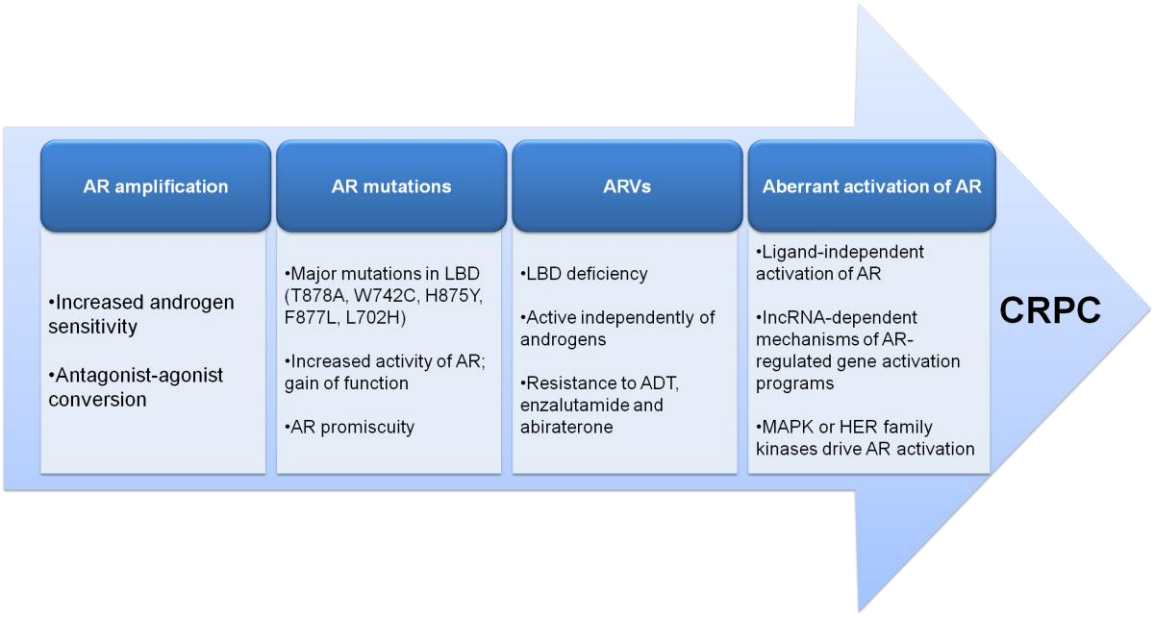

Figure 7. Summary of AR-dependent mechanisms of castration resistance. This picture was modified base on Tilki 2016[80]. Abbreviations: AR: androgen receptor; LBD: AR ligand-binding domain; ADT: androgen-deprivation therapy; MAPK: mitogen-activated protein kinase; HER family: epidermal growth factor receptor family.

Family inheritance and lifestyle difference have been recognized as important risk factors leading PCa, as indicated by world-wide epidemiological

studies[106,107]. PCa often occurs in familial aggregation, and 5%-10% of prostate cancer cases and up to 40% of early onset diseases are estimated to stem from inherited gene susceptibility[108]. Besides, the risk of developing PCa is 2-3 fold higher in men with family history than men without the family history[109]. Recent studies have further revealed that hereditary factor is the determinant of PCa instead of the lifestyle[110]. Approximately 42% risk leading to PCa could be explained by inherited genetic factors[110]. Therefore, much effort has been made to identify high-risk gene loci which are relevant to link PCa pathogenesis. Early PCa genetic linkage analysis identified *HPC1*, *HPCX*, *ELAC2*, *PCAP*, *HPC20*, etc[111] gene loci to be associated with familial PCa. Some studies have suggested their linkage with PCa predisposition, for example, *HPC1* is shown to be related to the advanced PCa within families[112], but clinic relevance between identified chromosome loci and PCa occurrence still needs to be established. Although the linkage analysis appeared to be a useful tool, it shows inconsistent results[113] and cannot recognize the low-moderate risk of developing PCa. Therefore, a new genome-wide association study (GWAS) is conducted and found 76 susceptibility loci with low penetrance, accounting for 30% familial risks of PCa[114]. Among 76 GWAS-selected loci, 8q24 is the firstly identified region and shown to harbor six (the largest number of) single nucleotide polymorphisms (SNPs)[115,116,117]. The

region where 8q24 locus is located is nearby *MYC* gene area known to be an oncogene which is associated with many types of cancers including the prostate cancer. Also, 8q24 was found to affect the *MYC* gene expression[118]. In addition to *MYC* gene, multiple genes including MSMB[119], KLK3[120], AR[121], etc., are also involved in pathogenesis of PCa. With advent of advanced genome-wide studies (e.g., GWAS), further validation at public health and personalized level is ongoing[114].

Additionally, PCa pathogenesis could be attributed to genome changes and lesions as a result of oxidative damage. Oxidative stress has been well studied as a connector linking exo/endogenous factors with carcinogenesis[122]. During chronic oxidative stress, many DNA changes may occur in cellular genome, including DNA base oxidation/mutation, DNA strands breaking, DNA-protein crosslink[123]. As a result of genetic aberrations, normal cells may start the transformation to neoplastic cells which subsequently progress to malignant cells. Since oxidative stress initiated by electrophiles or oxidants are detoxified or antagonized by antioxidant defense such as glutathione-S-transferase (GST)[124], these genes encoding antioxidant systems are highly susceptible to dysregulation[125] during carcinogenesis. Over recent years, π-class glutathione-S-transferase P1 (*GSTP1*) gene promotor methylation has been

recognized as a marker of the transformation of normal cells to prostatic intraepithelial neoplasia (PIN) and small PCa lesions[126,127]. *GSTP1* methylation leads to the declined expression of *GSTP1*[128] and is detected in 6% prostatic intraepithelial atrophy[129], 69% of PIN DNA specimens and 90% of PCa DNA specimens[127]. Besides, *GSTP1* repression occurs at the earliest stage of prostatic carcinogenesis and further correlates with the occurrence of prostate cancer[127]. Somatic genome damage resulting from *GSTP1* defects induces neoplastic transformation, and PCa carcinoma cells possessing loss of *GSTP1* function are subject to genome damage which leads to malignant progression[127,130]. Clinically, more than 40% of patients with the high-grade PIN will progress to PCa within three years[131]. These pre-cancerous events (*GSTP1* methylation, PIN, and PCa lesions) may provide the compelling evidence for elucidation of PCa pathogenesis and novel targets for PCa prevention or treatment. Interestingly, although *GSTP1* is downregulated in most of PCa cells (e.g., LNCaP, DU145)[132], it is overexpressed in androgen-independent CRPC PC-3 cells[132] and associated with chemoresistance in PCa[133]. Besides PCa, GSTP1 protein overexpression is associated with multiple drug resistance and tumor progression[134] in other types of cancer. Therefore, GSTP1 is a valuable target for the treatment of PCa, especially for androgen-independent PCa.

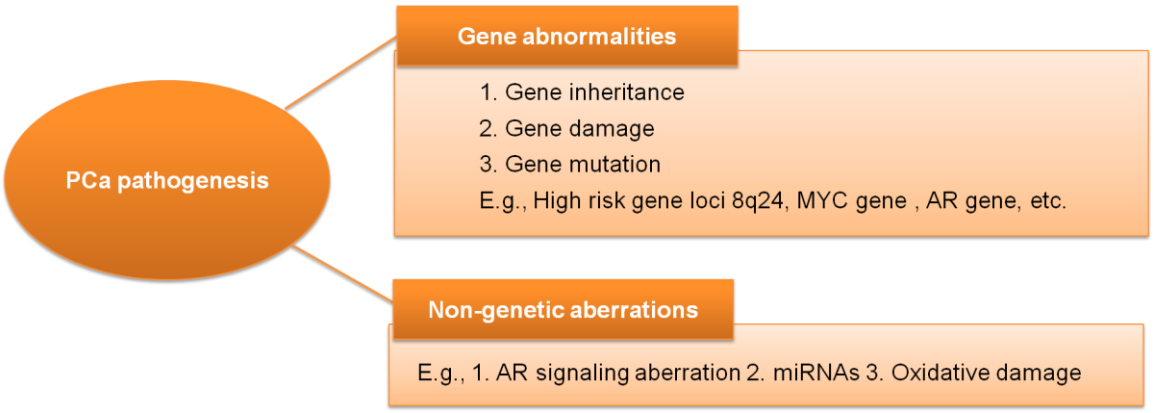

Figure 8. Gene abnormalities and non-genetic aberrations cause the pathogenesis of PCa.

Recent advances in explanation of PCa pathogenesis, including genome instability, damage, oxidative stress accumulation and AR signaling aberration, significantly contribute to the comprehensive molecular biological networking that modulates PCa initiation and progression (**Figure 8**). However, there is no clear answer fully unrolling this puzzle to date. Therefore, much clinical efforts and further functional clarification are being undertaken for connecting molecular characterization with PCa tumorigenesis.

1.3.3. Potential therapeutic targets and treatments

Treatment options of PCa depend on multiple factors such as diagnosis, stages of PCa development, age, overall health, life expectancy, quality, etc. They contain active monitoring, surgery, radiation, cryotherapy, hormone therapy, chemotherapy, vaccine treatment, bone-directed treatment[135]. In general, one treatment option will be used for one patient case, but sometimes they may be

combined. For example, surgery is the common treatment for patients with localized PCa, radiation and hormone therapy are usually combined for the treatment of metastatic PCa. Chemotherapy is applied when hormone therapy no longer works. Docetaxel alone or combination with prednisone is the first-line option. Recent advances in cancer biology of PCa revealed the essential role of AR signaling axis in progression and maintenance of CRPC[136] (**Figure 7**), so plenty of novel "AR signaling-targeting drugs" have been approved (e.g., enzalutamide and abiraterone) or under clinical investigation (e.g., EPI-506)[137]. Herein, we mainly focus on the chemotherapeutic drugs for the treatment of advanced PCa, especially CRPC, and summarized their targets and clinical status, as shown in the following table.

Table 2 Drugs targets and therapeutic agents for the treatment of PCa/CRPC. This table was adapted from Yoo 2016[137].

Potential Targets/Action Mechanism	Agents	Clinical Status	Clinical Trials
Cytotoxic chemotherapy			
	Carboplatin	Phase II	NCT02311764
	Docetaxel	Approved in 2004	
	Cabazitaxel	Approved in 2010	
Radiation therapy	Radium-223	Approved in 2013	
AR targeting			
	Bicalutamide	Approved in	

		1995	
	Nilutamide	Approved in 1996	
	Flutamide	Approved in 1989	
	Galeterone (AR&CYP17A1)	Phase II	NCT01709734
	Enzalutamide	Approved in 2012	
	ARN-509	Phase III	NCT01946204
	AZD-3514	Phase I	NCT01162395
	ODM-201	Phase III	NCT02200614
	SHR3680	Phase I/II	NCT02691975
	EPI-506	Phase I/II	NCT02606123
Androgen synthesis (CYP17A1)			
	Abiraterone	Approved in 2011	
	TAK-700	Phase III	NCT01707966
	TOK-001	Phase II	NCT01709734
	VT-464	Phase II	NCT02012920
	ODM-204 (dual inhibitor CYP17A1/AR)	Phase I/II	NCT02344017
Kinase inhibitors			
AKT inhibitor	AZD5363	Phase I/II	NCT02121639
PI3K inhibitor	LY3023414 (PI3K&mTOR)	Phase II	NCT02407054
	BKM120 (Buparlisib)	Phase I	NCT01634061
Aurora A kinase inhibitor	MLN8237 (Alisertib)	Phase I/II	NCT01848067
mTOR inhibitor	MLN0128	Phase II	NCT02091531
	Everolimus (RAD001)	Phase II	NCT00629525
CDK inhibitor	LEE011 (ribociclib)	Phase I/II	NCT02494921
Tyrosine kinase	TK1258 (Dovitinib)	Phase II	NCT01741116

inhibitors (FGFR)			
PARP inhibitor	Olaparib	Phase III	NCT02987543
Proteasome inhibitor	Carfilzomib	Phase II	NCT02047253
TGF-β inhibitor	Galunisertib	Phase II	NCT02452008
XPO-1	KPT-330	Phase II	NCT02215161
Immunotherapy			
Antibody	Ipilimumab	Phase III	NCT01057810
Antibody	177lu-J591	Phase III	NCT00916123
Vaccine	DCVAC	Phase III	NCT02111577
Vaccine	GX301	Phase II	NCT02293707

Abbreviations: AR: androgen receptor; CYP17A1: cytochrome P450 17A1; AKT: protein kinase B; PI3K: phosphoinositide 3-kinase; mTOR: mammalian target of rapamycin; CDK: cyclin-dependent kinase; FGFR: fibroblast growth factor receptor; PARP: poly (ADP-ribose) polymerase; TGF-β: transforming growth factor beta; XPO-1: exportin-1.

1.4. Overview of projects

Over the last few decades, the relationship between oxidative stress and electrophiles has been gradually unveiled. In addition to covalent modification of oncogenic effectors, electrophiles also exhibit multiple anti-cancer activities through elevating ROS. ROS such as hydroxyl radicals, superoxide anion, and hydrogen peroxide is found to be the direct mediator to regulate oxidative stress in cells[138]. ROS are generated in many organelles, including major mitochondria and endoplasmic reticulum[139]. The role of ROS is identified as "Good and Evil"[140]. The "Good" stems from its involvement in the regulation of many biological functions such as cell proliferation, apoptosis, and senescence. ROS overproduction, the "Evil", is linked to cytotoxicity through harmful effects on cellular DNA, lipids, and

proteins. These side effects of ROS are not only nontoxic but also fully exploited by cancer cells for cell proliferation, differentiation, and chemotherapeutic resistance[141]. Molecular mechanism studies reveal that increased activity or expression of oxidants and downregulation of antioxidant system contribute to ROS overproduction, while upregulation of some antioxidants is found to balance it[65]. Therefore, a dynamic redox homeostasis between oxidative stress and anti-oxidative defense is vital to maintaining phenotype of cancer cells. Given the aberrant redox status (e.g., vulnerability to higher ROS and dysregulation of antioxidant systems) in cancer cells, small molecular chemicals aimed to increase intracellular ROS levels have been explored in cancer therapy, which is referred to as electrophilicity-based anti-cancer prooxidant strategy[25]. ROS-inducing triggers include electrophiles (e.g., PL, β-phenylethyl isothiocyanate), acids (e.g., lactic acids), oxidants (e.g., hydrogen peroxide), enzyme inhibitors, (e.g., Buthionine sulfoximine) and GSH-depleting agents (e.g., diethylmaleate and DEM), etc. Among them, the class of electrophiles is the most attractive due to their high potency and great selectivity over cancer cells[142]. PL is a representative of electrophiles (**Figure 2**) and acts via covalent protein modification and ROS elevation, so we focus on exploitation of PL and PL chemical scaffolds to discover and develop novel drugs for the treatment of AML and PCa.

Chapter 2 focuses on PL combination with SAHA and following PL-HDACi hybrids for the treatment of AML. Chapter 3 focuses on the design, synthesis, and characterization of ROS/RNS-sensitive SAHA prodrugs, which in turn serves to increase the selectivity of PL-HDACi hybrids over cancer cells. Chapter 4 focuses on the structural modification of PL for enhancing the potency of PL and PL-HDACi hybrids against prostate cancer cells.

CHAPTER 2 DESIGN, SYNTHESIS, AND BIOLOGICAL CHARACTERIZATION OF PL-HDACi HYBRIDS AS ANTI-AML AGENTS

In this chapter, some of text were reprinted or modified from: Liao Y, Niu X, Chen B, et al. Synthesis and Antileukemic Activities of Piperlongumine and HDAC Inhibitor Hybrids against Acute Myeloid Leukemia Cells. *Journal of Medicinal Chemistry*, 2016, 59 (17): 7974-7990.

2.1. Rationale for the hybridization of PL and HDACi

The current treatment for almost all subtypes of AML (except acute promyelocytic leukemia) is to use a combination of cytosine arabinoside (Ara-C or cytarabine) and daunorubicin, which has not been changed for more than three decades. Treatment failure is mainly due to resistance to chemotherapy and disease relapse arising from leukemia stem cells (LSCs)[143]. The discovery of innovative therapeutic agents for AML treatment represents an urgent and essential medical need.

HDACs are implicated in tumorigenesis of acute leukemia and have been studied as therapeutic targets. HDAC inhibitors display attractive anti-cancer mechanisms of action, including transcriptional activation of p53[144], inactivation of NF-κB[145], upregulation of CDKN1A[146], downregulation of pro-angiogenic factors such as VEGF (Vascular endothelial growth factor)[147], and induction of caspase-3 protease activity[148]. A HDACs inhibitor (HDACi), suberoylanilide hydroxamic acid (Vorinostat, SAHA), was approved by FDA to treat cutaneous T-cell lymphoma (CTCL), and has been demonstrated anti-tumor activities as a single dose or in

combination with other agents in solid and hematological tumors at doses tolerated by normal cells[149]. HDACis not only induce leukemia cell death by DNA damage, ROS elevation, downregulation of DNA repair system (e.g., RAD51, CHK1, BRCA1 etc.)[150,151,152], and disruption of pro-/anti-apoptotic balance[153], but also reduce the population of LSCs linking to cancer relapse[154,155]. However, the clinical efficacy of SAHA as single agent drug in AML patients is poor, the reason might be associated with upregulation of antioxidant defense pathways in AML cells[156]. To overcome potential resistance and/or enhance efficacy, SAHA was combined with other potent anti-cancer agents. For example, SAHA was reported to synergistically interact with AZD1775 against null-p53 and wt p53 AML cells via inactivation of cell cycle regulator CHK1, upregulation of γH2A, and cell arrest at early S phase[157]. Besides, SAHA was paired with MK8776 (a CHK1 inhibitor), and this combination displayed synergistically inhibitory effects on multiple p53-wt or -deficient leukemia cell lines by impacting cell cycle checkpoints, downregulating expression of DNA replication (e.g., Cdt1) or repair-related proteins (e.g., CtIP and BRCA1)[158]. Taken together, HDACs could be rationally targeted for cancer treatment, and HDACi could be further exploited and combined with other DNA-damaging agents for the treatment of leukemia.

Piperlongumine (PL) extracted from long pepper was reported to

selectively kill cancer cells in low micromolar concentration and to inhibit tumor growth *in vivo*[3,21]. Because of electrophilicity, PL shows diverse mechanisms of actions against various cancers. PL-induced redox imbalance, such as ROS elevation and GSH depletion[3], plays a key role in its anti-cancer activities. For example, PL could kill primary myeloid leukemia[31] and CD34+ AML cells from patient samples[12] via increased oxidative stress. Besides, PL killed LSCs with an EC_{50} of 380 nM[159] by increasing ROS level, inducing various DNA lesions (mainly double-strand breaks), and inhibiting homologous recombination (HR) by using DNA repair-deficient DT40 cell lines[160]. PL could also reduce pancreatic tumor burden through ROS-mediated DNA damage, as suggested by increased level of 8-hydroxy-2`-deoxyguanosine (8-OHdG) in pancreatic tumor cells[161]. In triple-negative breast cancer cells, PL induced DNA fragmentation and p21 mRNA expression[162].

Consequently, HDACi SAHA-induced anti-AML activities, such as DNA damage, downregulation of DNA-related enzymes, and elevation of oxidative stress, overlap with the major properties of PL. Based on the understanding of the anti-cancer mechanisms of SAHA and PL, we hypothesized that SAHA and PL may synergistically increase ROS levels and enhance DNA damage in AML cells, and the SAHA resistance associated with antioxidant upregulation could be

potentially overcome by the electrophilic PL, which is known to decrease antioxidant defense[3]. The cooperative and complementary anti-AML properties of SAHA and PL form a scientific rationale to design new hybrid drugs against AML.

Different from co-treatment of SAHA and PL, we performed a "hybridization" strategy with HDACi and PL pharmacophores, affording single molecular entity (**1-58**) harboring both SAHA and PL activities. Compared to the simple combination of two drugs, this approach more efficiently co-localizes synergistic pharmacophores and greatly simplifies optimization of drug-like properties, PK and dose-toxicity profiles at advanced drug discovery/development stages[163]. We hypothesized that synergistic/additive anti-AML effects of SAHA and PL can be realized by PL-HDACi hybrid drugs through cooperatively enhanced DNA damage, upregulation of apoptotic, and downregulation of anti-apoptotic pathways.

2.2. Design and synthesis of PL-HDACi hybrid drugs

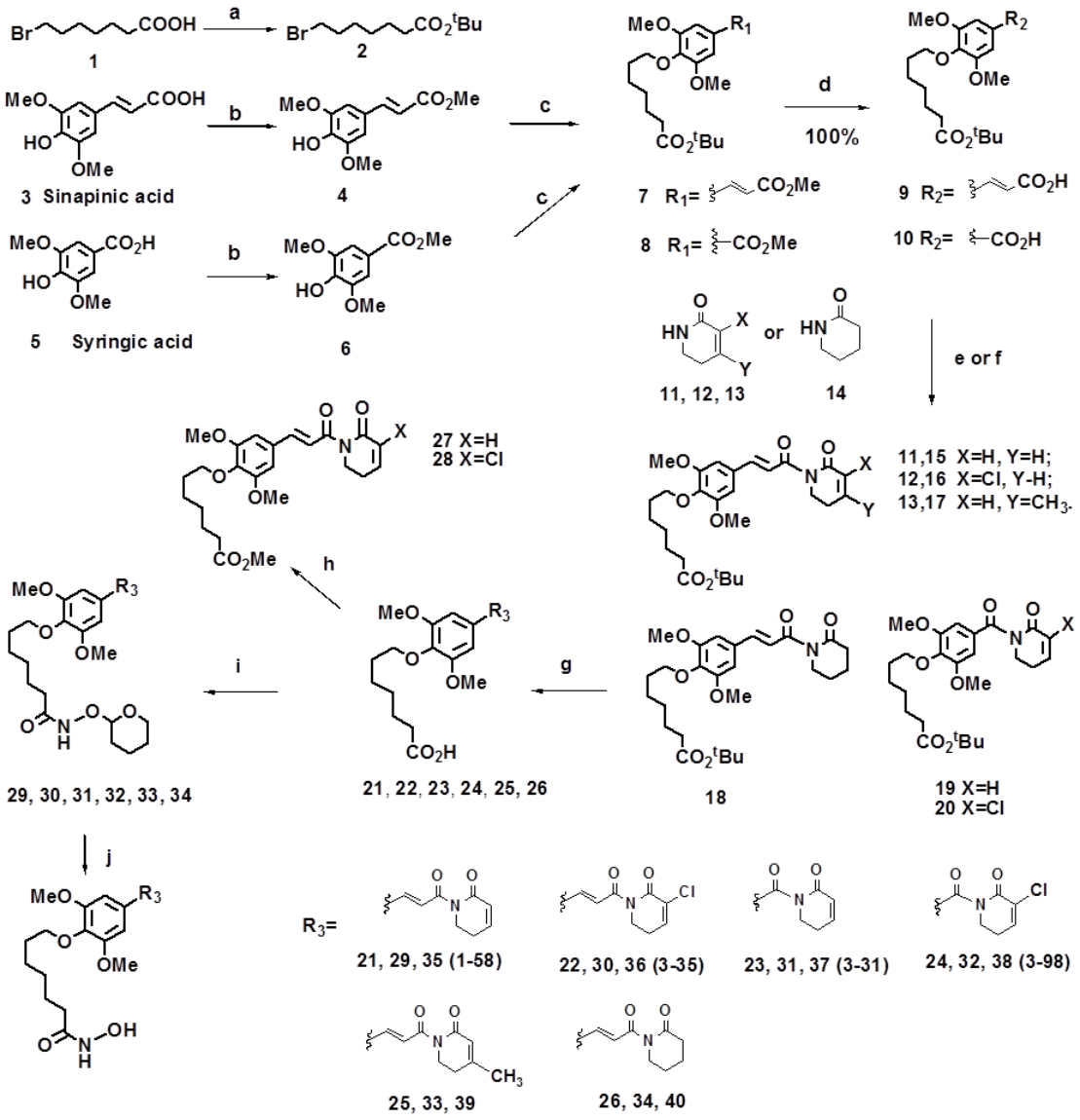

Scheme 1. Synthetic route of PL-HDACi hybrids. Reagents and conditions: (a) $(BOC)_2O$, DMAP, t-BuOH, THF; (b) concentrated sulfuric acid, MeOH, reflux; (c) K_2CO_3, DMF, 70 °C; (d) LiOH, THF, H_2O; (e) (1) pivaloyl chloride, TEA, THF, −20 °C; (2) lactam, *n*-BuLi, THF, −78 °C; (f) (1) oxalyl chloride, THF, −20 °C; (2) lactam, nBuLi, THF, −78 °C (g) 20% TFA, DCM; (h) diazomethane, DCM; (i) HBTU, NH_2OTHP, DIPEA, DMF; (j)10% TFA, MeOH.

In order to incorporate both PL and HDACi activities into a single chemical

entity, the prototype chimeric molecule **1-58** was designed by introducing a seven-carbon linker at the 4' position of PL. The linker was further connected to the hydroxamic acid moiety, a zinc binding group (ZBG), to mimic the partial structure of SAHA (**Scheme 1**). The modified PL structure served as a "cap" that could bind at the surface of HDAC enzymes. Published PL structure-activity relationship (SAR) studies suggested that the C2-C3 olefin was responsible for GSH conjugation via Michael addition and was vital for ROS induction. The C2 substituent could potentially affect the chemical reactivity of C2-C3 olefin and impact anticancer potency of PL. For instance, electron-withdrawing C2-chloride increases, while C2-methyl group decreases cytotoxicity of PL to cancer cells[21, 164]. After conjugation with cellular GSH, close interactions of PL-GSH conjugate with GSH-binding proteins could increase the availability of electrophilic C7-C8 olefin to protein thiol groups and therefore promote covalent protein modification. Elimination of the C7-C8 double bond has been shown to reduce cytotoxicity,[21] which might be a consequence of decreased PL covalent protein binding. To investigate how the C2 substituent and the C7-C8 olefin affect the overall anti-AML properties of **1-58**. Compound **3-35** with a C2-Cl substituent and **3-31/3-98** (**Scheme 1**) without the internal C7-C8 double bond were also synthesized and tested in cell culture models. Compared to parental drug, either

SAHA or PL, we expected that the C2-C3 olefin of **3-31** or **3-98** could partially retain anti-cancer properties of PL and still work cooperatively with the HDACi functional group to achieve improved anti-AML activities. Instead of having both HDACi and PL pharmacophores, compounds **27**, **28**, **35** and **36** are close structural analogues of **1-58** or **3-35** with just one active pharmacophore (**Scheme 1**), e.g., ZBG of **1-58** or **3-35** was replaced by a methyl ester in **27** and **28** respectively, and the electrophilic C2-C3 olefin of **1-58** was blocked by either a C3-methyl substituent (compound **39**) or hydrogen saturation (compound **40**). These compounds were used to make comparisons with **1-58** and **3-35** to demonstrate both PL and HDACi pharmacophores are required and contribute to the observed superior anti-AML properties.

The synthesis of **1-58**/**3-35** and **3-31**/**3-98** scaffold was accomplished from commercially available sinapinic acid **3** and syringic acid **5**, respectively (**Scheme 1**). Carboxylic acids **3** and **5** were first converted to corresponding methyl esters **4** and **6** followed by the alkylation of phenol hydroxyl groups with compound **2,** a *t*-butyl ester of 7-bromoheptanoic acid to afford **7** and **8** respectively. Free carboxylic acids **9** and **10** were obtained via basic hydrolysis of methyl esters **7** and **8**, while the *t*-butyl esters of these molecules were intact. In order to conduct SAR studies of PL-like pharmacophores, α,β-unsaturated lactam **11**[165], its

analogues **12**[164] which has a C2-Cl substituent, and **13**[166] with a C3-methyl group were synthesized according to published procedure with slight modifications and compound **14**, δ-valerolactam, was purchased. Different lactams **11**-**14** were de-protonated by *n*-BuLi and then coupled with pivaloyl chloride-activated **9** and **10** respectively, to afford **15**-**20**. In following steps, *t*-butyl esters were cleaved using TFA and the obtained acids **21**-**26** were coupled to THP-protected hydroxyl amine. Final acidic de-protection using 10% TFA in MeOH gave hydroxamic acid-containing **1-58**, **3-35**, **3-31**, **3-98, 39**, and **40**. Methyl esters **27** and **28** were prepared from **21** and **22** by using diazomethane as esterification reagent respectively. Synthetic intermediates and final products were characterized using ^{1}H, ^{13}C NMR and mass spectrometry; for the biological studies, purity of the compounds was further confirmed using HPLC analysis.

2.3. Chemistry

Tert-butyl 7-bromoheptanoate (2)

7-Bromoheptanoic acid (1.11 g, 5.3 mmol, 1.0 eq) and Boc anhydride (1.38 g, 6.3 mmol, 1.2 eq) were mixed in *tert*-butyl alcohol (5 mL). After the mixture was stirred at room temperature for 10 min, DMAP (195 mg, 1.6 mmol, 0.3 eq) was added and the reaction mixture was stirred for another 2 h. Upon completion, the solvent was removed under reduced pressure and the residue was re-dissolved in

ethyl acetate and was washed with water and brine, dried over anhydrous Na_2SO_4. Purification by flash chromatography (Hex/EA, 20/1) afforded product (colorless oil, 570 mg, 40%). ^{1}H NMR (600 MHz, $CDCl_3$): δ (ppm) 3.38 (t, *J*=6.6Hz, 2H), 2.19 (t, *J*=7.2Hz, 2H), 1.82-1.86 (m, 2H), 1.55-1.60 (m, 2H), 1.40-1.45 (m, 2H), 1.42 (s, 9H), 1.29-1.34 (m, 2H). ^{13}C NMR (125 MHz, $CDCl_3$): δ (ppm) 173.06, 80.01, 35.39, 33.81, 32.55, 28.16, 28.09, 27.81, 24.83.

(E)-Methyl 3-(4-hydroxy-3,5-dimethoxyphenyl)acrylate (4)

Sinapinic acid (1.03 g, 4.6 mmol, 1.0 eq) was dissolved in methanol (20 mL) followed by addition of several drops of conc. H_2SO_4. The reaction mixture was refluxed for 6 h. Upon completion, the reaction mixture was cooled to ambient temperature and solvent was removed under vacuum. The resulting residue was diluted with ethyl acetate and washed using sat. aq. $NaHCO_3$, water and brine, and dried over anhydrous Na_2SO_4. Purification by flash chromatography (Hex/EA, 2:1) afforded product (yellow oil, 1.1 g, 99%). ^{1}H NMR (600 MHz, $CDCl_3$): δ (ppm) 7.55 (d, *J*=15.6Hz, 1H), 6.72 (s, 2H), 6.26 (d, *J*=15.6Hz, 1H), 5.79 (s, 1H), 3.89 (s, 6H), 3.76(s, 3H). ^{13}C NMR (125 MHz, $CDCl_3$): δ (ppm) 167.61, 147.18, 145.15, 137.13, 125.77, 115.41, 105.00, 56.27, 51.62.

Methyl 3,5-dimethoxy-4-hydroxybenzoate (6)

^{1}H NMR (600 MHz, $CDCl_3$): δ (ppm) 7.32 (s, 2H), 6.04 (s, 1H), 3.93 (s, 6H),

3.90 (s, 3H). ^{13}C NMR (125 MHz, $CDCl_3$): δ (ppm) 166.85, 146.59, 139.16, 120.98, 106.57, 56.36, 52.07.

(E)-tert-butyl 7- (2,6-dimethoxy-4- (3-methoxy-3-oxoprop-1-enyl) phenoxy) heptanoate (7)

Compound **2** (570 mg, 2.1 mmol, 1.1 eq), compound **4** (476 mg, 2.0 mmol, 1.0 eq) and K_2CO_3 (838 mg, 6.0 mmol, 3.0 eq) were mixed in DMF (4 mL). The reaction mixture was stirred at 60^{o}C overnight. The reaction mixture was cooled to room temperature and diluted with water. After extraction using ethyl acetate three times, the combined organic phase was washed with water and brine, and dried over anhydrous Na_2SO_4. Purification by flash chromatography (Hex/EA, 6:1) afforded product compound **7** (colorless oil, 630 mg, 75%). ^{1}H NMR (600 MHz, $CDCl_3$): δ (ppm) 7.55 (d, *J*=15.6Hz, 1H), 6.69 (s, 2H), 6.28 (d, *J*=15.6Hz, 1H), 3.94 (t, *J*=6.6Hz, 2H), 3.81(s, 6H), 3.75 (s, 3H), 2.16 (t, *J*=7.2Hz, 2H), 1.67-1.72 (m, 2H), 1.53-1.68(m, 2H), 1.41-1.46(m, 2H), 1.38 (s, 9H), 1.28-1.33(m, 2H). ^{13}C NMR (125 MHz, $CDCl_3$): δ (ppm) 173.16, 167.36, 153.60, 144.89, 139.40, 129.57, 116.76, 105.23, 79.84, 73.41, 56.07, 51.61, 35.49, 29.86, 28.80, 28.04, 25.47, 25.01. HRMS (ESI): calcd for $[C_{23}H_{35}O_7+H]^+$, 423.2383; found, 423.2404.

Methyl 4-(7-tert-butoxy-7-oxoheptyloxy)-3,5-dimethoxybenzoate (8).

The flash was charged with compound **6** (1.8 g, 8.2 mmol) and compound

2 (2.4 g, 9.1 mmol). DMF (10 mL) and potassium carbonate (3.4 g, 24.7 mmol) were added at room temperature. The reaction was allowed to undergo at 80 ^{o}C overnight. Once completed, the resulting mixture was washed with water and extracted with DCM three times, and then the organic phase was dried over Na_2SO_4 for 30 min. Purification done by flash chromatography (Hex/EA, 8:1) produces compound **8** (colorless oil, 3.7 g, 94%). ^{1}H NMR (600 MHz, $CDCl_3$): δ (ppm) 7.26 (s, 2H), 3.99 (t, *J*=7.2Hz, 2H), 3.87 (s, 3H), 3.86 (s, 6H), 2.18 (t, *J*=7.2Hz, 2H), 1.70-1.75 (m, 2H), 1.55-1.60 (m, 2H), 1.42-1.47 (m, 2H), 1.41 (s, 9H), 1.31-1.36 (m, 2H). ^{13}C NMR (125 MHz, $CDCl_3$): δ (ppm) 173.20, 166.75, 153.12, 141.43, 124.88, 106.74, 79.88, 73.37, 56.16, 52.16, 35.52, 29.89, 28.82, 28.08, 25.48, 25.03. HRMS (ESI): calcd. for [$C_{21}H_{32}O_7 \cdot Na^+$], 419.2046; found, 419.2046.

(E)-3-(4-(7-tert-butoxy-7-oxoheptyloxy)-3,5-dimethoxyphenyl)acrylic acid (9).

Compound **7** (588 mg, 1.4 mmol, 1.0 eq) was dissolved in THF/H_2O (5 mL/5 mL) to which LiOH (40 mg, 1.7 mmol, 1.2 eq) was added. The reaction mixture was stirred at room temperature for overnight. Upon completion, 2N HCl was added to acidify the reaction and the solution was extracted with ethyl acetate three times. The collected organic phase was washed with water and brine, dried over anhydrous Na_2SO_4. Evaporation of solvent afforded product compound **9**

(yellow oil, 600 mg, 100%) which was used in the next step without further purification. ^{1}H NMR (600 MHz, $CDCl_3$): δ (ppm) 7.68 (d, *J*=15.6Hz, 1H), 6.75 (s, 2H), 6.33 (d, *J*=15.6Hz, 1H), 3.98 (t, *J*=6.6Hz, 2H), 3.85 (s, 6H), 2.19 (t, *J*=7.2Hz, 2H), 1.71-1.75 (m, 2H), 1.56-1.61 (m, 2H), 1.43-1.48 (m, 2H), 1.42 (s, 9H), 1.33-1.37 (m, 2H). ^{13}C NMR (125 MHz, $CDCl_3$): δ (ppm) 173.31, 172.21, 153.66, 147.04, 139.82, 129.26, 116.31, 105.57, 79.97, 73.50, 56.13, 35.54, 29.89, 28.83, 28.09, 25.49, 25.04.

4-(7-tert-butoxy-7-oxoheptyloxy)-3,5-dimethoxybenzoic acid (10)

Compound **10** was made from **8** (3.7 g, 7.7 mmol) as described for compound **9**. Product was obtained as yellow oil (1.7 g, 47%). ^{1}H NMR (600 MHz, $CDCl_3$): δ (ppm) 7.37 (s, 2H), 4.05 (t, *J*=7.2Hz, 2H), 3.90 (s, 6H), 2.23 (t, *J*=7.8Hz, 2H), 1.74-1.79(m, 2H), 1.59-1.64 (m, 2H), 1.46-1.51(m, 2H), 1.44 (s, 9H), 1.35-1.39 (m, 2H). ^{13}C NMR (125 MHz, $CDCl_3$): δ (ppm) 173.33, 171.37, 153.17, 142.18, 124.04, 107.34, 79.99, 73.44, 56.18, 35.53, 29.90, 28.82, 28.08, 25.47, 25.04.

(E)-tert-butyl 7-(2,6-dimethoxy-4-(3-oxo-3-(2-oxo-5,6-dihydropyridin-1(2H)-yl)prop-1-enyl)phenoxy)heptanoate (15)

Step 1: compound **9** (540 mg, 1.3 mmol, 1.0 eq) was dissolved in DCM (12 mL) followed by addition of oxalyl chloride (0.6 mL, 6.5 mmol, 5.0 eq) and catalytic

amount of DMF (two drops). The reaction mixture was stirred at room temperature for 1 h after which the solvent was removed under reduced pressure. The residue was dissolved in THF (3 mL) and directly used in the next step without purification. Step 2: compound **11** (150 mg, 1.6 mmol, 1.2 eq) was dissolved in anhydrous THF (5 mL) and *n*-BuLi (2.5 M in hexane, 0.7 mL, 1.7 mmol, 1.3 eq) was added dropwise via syringe at -78^{o}C. The reaction mixture was stirred for 15 min at the same temperature followed by the dropwise addition of the THF solution in the first step. TLC showed the completion of the reaction within about 30 min at -78°C. Sat. aq. NH_4Cl was added to quench this reaction and the resulting solution was extracted with ethyl acetate three times. The combined organic phase was washed with water and brine, and dried over anhydrous Na_2SO_4. Flash chromatography (Hex/EA, 4:1) purification afforded product as yellow oil (358 mg, 56%). ^{1}H NMR (600 MHz, $CDCl_3$): δ (ppm) 7.66 (d, *J*=15.6Hz, 1H), 7.39 (d, *J*=15.6Hz, 1H), 6.91-6.94 (m, 1H), 6.77 (s, 2H), 6.02 (m, 1H), 4.02 (t, *J*=6.6Hz, 2H), 3.96 (t, *J*=6.6Hz, 2H), 3.85 (s, 6H), 2.45-2.47 (m, 2H), 2.19 (t, *J*=7.8Hz, 2H), 1.70-1.75 (m, 2H), 1.56-1.61(m, 2H), 1.48-1.44 (m, 2H), 1.42 (s, 9H), 1.32-1.37 (m, 2H). ^{13}C NMR (125 MHz, $CDCl_3$): δ (ppm) 173.24, 168.90, 165.84, 153.55, 145.49, 143.94, 139.31, 130.37, 125.83, 120.83, 105.55, 79.90, 73.46, 56.15, 41.63, 35.56, 29.91, 28.86, 28.10, 25.52, 25.07, 24.79. HRMS (ESI): calcd. for

[$C_{27}H_{37}NO_7 \cdot Na^+$], 510.2468; found, 510.2455.

(E)-tert-butyl 7-(4-(3-(3-chloro-2-oxo-5,6-dihydropyridin-1(2H)-yl)-3-oxoprop-1-enyl)-2,6-dimethoxyphenoxy)heptanoate (16)

Compound **16** was synthesized from compounds **9** (360 mg, 0.9 mmol) and **12** (139 mg, 1.1 mmol) following the procedure described for compound **15**, except **9** was activated using pivaloyl chloride (0.2 mL, 1.0 mmol) in the presence of TEA (0.2 mL, 1.8 mmol) in THF (5 mL) at -10°C. Flash chromatography (Hex/EA, 2:1) purification afforded product as colorless oil (150 mg, oil, 33%). ^{1}H NMR (600 MHz, $CDCl_3$): δ (ppm) 7.68 (d, *J*=15.0Hz, 1H), 7.38 (d, *J*=15.6Hz, 1H), 7.07 (t, *J*=4.8Hz, 1H), 6.77 (s, 2H), 4.06 (t, *J*=6.6Hz, 2H), 3.99 (t, *J*=6.6Hz, 2H), 3.85 (s, 6H), 2.53-2.56 (m, 2H), 2.19 (t, *J*=7.2Hz, 2H), 1.71-1.74 (m, 2H), 1.57-1.59 (m, 2H), 1.43-1.63 (m, 2H), 1.41 (s, 9H), 1.33-1.36 (m, 2H). ^{13}C NMR (125 MHz, $CDCl_3$): δ (ppm) 173.21, 168.50, 161.37, 153.59, 145.12, 141.10, 139.58, 130.09, 128.20, 119.99, 105.69, 79.89, 73.46, 56.20, 41.77, 35.55, 29.90, 28.85, 28.09, 25.51, 25.28, 25.05. HRMS (ESI): calcd. for [$C_{27}H_{36}NO_7Cl \cdot Na^+$], 544.2078; found, 544.2054.

(E)-tert-butyl 7-(2,6-dimethoxy-4-(3-(4-methyl-2-oxo-5,6-dihydropyridin-1(2H)-yl)-3-oxoprop-1-enyl)phenoxy)heptanoate (17)

Compound **17** was synthesized from compounds **9** and **13** following the

procedure described for compound **16**. **9** (141 mg, 0.3 mmol) was activated using pivaloyl chloride (0.1 mL, 0.4 mmol, 1.1 eq) in the presence of TEA (0.1 mL, 2.0 eq) in THF (5 mL) at -10°C. Compound **13** (44 mg, 0.4 mmol) was deprotonated by using *n*-BuLi (2.0 eq) in THF and then reacted with activated **9** to afford product **17** (24 mg, 23%). ^{1}H NMR (600 MHz, $CDCl_3$): δ (ppm) 7.63 (d, *J*=15.6Hz, 1H), 7.40 (d, *J*=15.6Hz, 1H), 6.76 (s, 2H), 5.81 (d, *J*=1.2Hz, 1H), 4.00 (t, *J*=6.6Hz, 2H), 3.96 (t, *J*=6.6Hz, 2H), 3.84 (s, 6H), 2.37 (d, *J*=6.6Hz, 2H), 2.19 (t, *J*=7.2Hz, 2H), 1.99 (s, 3H), 1.72 (m, 2H), 1.58 (m, 2H), 1.43-1.48 (m, 2H), 1.41 (s, 9H), 1.33-1.36 (m, 2H).^{13}C NMR (125 MHz, $CDCl_3$): δ (ppm) 173.25, 168.87, 166.09, 157.85, 153.54, 143.61, 139.21, 130.46, 121.29, 120.97, 105.50, 79.89, 73.44, 56.13, 41.53, 35.55, 29.90, 29.89, 28.84, 28.09, 25.50, 25.05, 22.97. HRMS (ESI): calcd for $[C_{28}H_{40}NO_7+H]^+$, 502.2805; found, 502.2807.

(E)-tert-butyl 7-(2,6-dimethoxy-4-(3-oxo-3-(2-oxopiperidin-1-yl)prop-1-enyl) phenoxy)heptanoate (18)

Compound **18** was synthesized from compounds **9** and **14** following the procedure described for compound **16**. Compound **9** (900 mg, 2.2 mmol) was activated using pivaloyl chloride (0.4 mL, 2.4 mmol, 1.1 eq) in the presence of TEA (0.6 mL, 2.0 eq) in THF (5 mL) at -10°C. Compound **14** (263 mg, 2.7 mmol) was deprotonated by using *n*-BuLi (2.0 eq) in THF (5 mL) and then reacted with

activated **9** to afford product **18** (760 mg, 75%). ^{1}H NMR (600 MHz, $CDCl_3$): δ (ppm) 7.59 (d, *J*=15.0Hz, 1H), 7.31 (d, *J*=15.6Hz, 1H), 6.74 (s, 2H), 3.95 (t, *J*=6.6Hz, 2H), 3.83(s, 6H), 3.76 (t, *J*=4.8Hz, 2H), 2.57(t, *J*=6.6Hz, 2H), 2.18 (t, *J*=7.2Hz, 2H), 1.84-1.86 (m, 4H), 1.69-1.72 (m, 2H), 1.55-1.58 (m, 2H), 1.42-1.46 (m, 2H), 1.40 (s, 9H), 1.31-1.35 (m, 2H). ^{13}C NMR (125 MHz, $CDCl_3$): δ (ppm) 173.86, 173.21, 169.59, 153.53, 143.53, 139.23, 130.39, 121.07, 105.48, 79.87, 73.42, 56.12, 44.60, 35.53, 34.92, 29.88, 28.84, 28.08, 25.50, 25.04, 22.54, 20.60. HRMS (ESI): calcd. for [$C_{27}H_{39}NO_7 \cdot Na^+$], 512.2624; found, 512.2625.

tert-butyl 7-(2,6-dimethoxy-4-(6-oxo-1,2,3,6-tetrahydropyridine-1-carbonyl) phenoxy)heptanoate (19)

Compound **19** was synthesized from compounds **10** and **11** following the procedure described for compound **16**. **10** (1.0 g, 2.6 mmol) was activated using pivaloyl chloride (0.5 mL, 2.9 mmol, 1.1 eq) in the presence of TEA (0.7 mL, 2.0 eq) in THF (5 mL) at -10°C. Compound **11** (304.9 mg, 3.1 mmol) was deprotonated by using *n*-BuLi (2.0 eq) in THF(5 ml) and then reacted with activated **10** to afford product **19** (340 mg, 28%). ^{1}H NMR (600 MHz, $CDCl_3$): δ (ppm) 6.96-6.99 (m, 1H), 6.85 (s, 2H), 5.98-6.00 (m, 1H), 4.01 (t, *J*=6.6Hz, 2H), 3.96 (t, *J*=6.6Hz, 2H), 3.84 (s, 6H), 2.59-2.61 (m, 2H), 2.22 (t, *J*=7.8Hz, 2H), 1.73-1.77 (m, 2H), 1.58-1.63 (m, 2H), 1.45-1.49 (m, 2H), 1.44 (s, 9H), 1.33-1.39

(m, 2H). ^{13}C NMR (125 MHz, $CDCl_3$): δ (ppm) 173.64, 173.22, 165.56, 152.96, 145.48, 140.82, 130.66, 125.71, 106.24, 79.87, 73.39, 56.18, 43.72, 35.54, 29.91, 28.84, 28.08, 25.49, 25.05, 24.88. HRMS (ESI): calcd for $[C_{25}H_{36}NO_7+H]^+$, 462.2492; found, 462.2491.

tert-butyl 7-(4-(5-chloro-6-oxo-1,2,3,6-tetrahydropyridine-1-carbonyl)-2,6-dimethoxyphenoxy)heptanoate (20)

Compound **20** was synthesized from compounds **10** and **12** following the procedure described for compound **16**. **10** (1.0 g, 2.6 mmol) was activated using pivaloyl chloride (0.5 mL, 2.9 mmol, 1.1 eq) in the presence of TEA (0.7 mL, 2.0 eq) in THF (5 mL) at -10°C. Compound **12** (413 mg, 3.1 mmol) was deprotonated by using *n*-BuLi (1.5 eq) in THF and then reacted with activated **10** to afford product **20** (350 mg, 27%). ^{1}H NMR (600 MHz, $CDCl_3$): δ (ppm) 7.11 (t, *J*=4.2Hz, 1H), 6.83 (s, 2H), 3.99-4.02 (m, 4H), 3.84 (s, 6H), 2.67-2.70 (m, 2H), 2.22 (t, *J*=7.8Hz, 2H), 1.73-1.77 (m, 2H), 1.58-1.63 (m, 2H), 1.46-1.48 (m, 2H), 1.44 (s, 9H), 1.34-1.39 (m, 2H). ^{13}C NMR (125 MHz, $CDCl_3$): δ (ppm) 173.25, 173.15, 161.18, 153.07, 141.19, 140.88, 130.02, 127.75, 106.28, 79.90, 73.47, 56.26, 43.90, 35.55, 29.92, 28.84, 28.09, 25.49, 25.42, 25.06. HRMS (ESI): calcd. for $[C_{25}H_{34}NO_7Cl\cdot Na^+]$, 518.1922; found, 518.1922.

(E)-7-(2,6-dimethoxy-4-(3-oxo-3-(2-oxo-5,6-dihydropyridin-1(2H)-yl)prop-1-e

nyl)phenoxy)heptanoic acid (21)

Compound **15** (350 mg, 0.7 mmol) was dissolved in a mixture of DCM/TFA (10 mL/1 mL) and the reaction mixture was stirred at room temperature for overnight. Upon completion shown by TLC, the reaction mixture was diluted with DCM and washed with water and brine, dried over anhydrous Na_2SO_4. Evaporation of solvent afforded product compound **21** (yellow oil, 311 mg, 99%) which was used in the next step without purification.

***(*E)-7-(4-(3-(3-chloro-2-oxo-5,6-dihydropyridin-1(2H)-yl)-3-oxoprop-1-enyl)-2, 6-dimethoxyphenoxy)heptanoic acid (22)**

Compound **22** was synthesized from **16** following the procedure described for compound **21**. Compound **16** (130 mg, 0.3 mmol) was dissolved in DCM (5 mL) followed by the addition of TFA (1 mL) to afford compound **22** (110 mg, 95%). ^{1}H NMR (600 MHz, $CDCl_3$): δ (ppm) 7.69 (d, *J*=15.6Hz, 1H), 7.39 (d, *J*=15.0Hz, 1H), 7.08 (t, *J*=4.8Hz, 1H), 6.78 (s, 2H), 4.07 (t, *J*=6.6Hz, 2H), 3.98 (t, *J*=6.6Hz, 2H), 3.85 (s, 6H), 2.54-2.57 (m, 2H), 2.35 (t, *J*=7.2Hz, 2H), 1.71-1.76 (m, 2H), 1.62-1.67 (m, 2H), 1.45-1.50 (m, 2H), 1.36-1.41 (m, 2H). ^{13}C NMR (125 MHz, $CDCl_3$): δ (ppm) 179.33, 168.59, 161.41, 153.57, 145.19, 141.15, 139.51, 130.12, 128.19, 119.98, 105.70, 73.38, 56.20, 41.79, 35.85, 29.84, 28.78, 25.44, 25.29, 24.61.

7-(2,6-dimethoxy-4-(6-oxo-1,2,3,6-tetrahydropyridine-1-carbonyl)phenoxy)heptanoic acid (23)

Compound **23** was synthesized from **19** following the procedure described for compound **21**. Compound **19** (340 mg, 0.7 mmol) was dissolved in DCM (10 mL) followed by the addition of TFA (2 mL) to afford compound **23** (242 mg, 81%). ^{1}H NMR (600 MHz, $CDCl_3$): δ (ppm) 9.32 (s, 1H), 6.99-7.02 (m, 1H), 6.84 (s, 2H), 6.00-6.03 (m, 1H), 4.03 (t, *J*=6.6Hz, 2H), 3.97 (t, *J*=6.6Hz, 2H), 3.84 (s, 6H), 2.60-2.63 (m, 2H), 2.36 (t, *J*=7.2Hz, 2H), 1.73-1.77 (m, 2H), 1.63-1.68 (m, 2H), 1.46-1.51 (m, 2H), 1.36-1.41 (m, 2H). ^{13}C NMR (125 MHz, $CDCl_3$): δ (ppm) 179.71, 173.77, 166.01, 152.94, 145.99, 140.88, 130.44, 124.97, 106.29, 73.35, 56.19, 43.83, 33.89, 29.80, 28.69, 25.36, 24.85, 24.59.

7-(4-(5-chloro-6-oxo-1,2,3,6-tetrahydropyridine-1-carbonyl)-2,6-dimethoxyphenoxy)heptanoic acid (24)

Compound **24** was synthesized from **20** following the procedure described for compound **21**. Compound **20** (310 mg, 0.6 mmol) was dissolved in DCM (10 mL) followed by the addition of TFA (1.5 mL) to afford compound **24** (275 mg, 99%). ^{1}H NMR (600 MHz, $CDCl_3$): δ (ppm) 7.09 (t, *J*=4.2Hz, 1H), 6.80 (s, 2H), 4.00 (t, *J*=6.6Hz, 2H), 3.98 (t, *J*=6.6Hz, 2H), 3.81 (s, 6H), 2.65-2.68 (m, 2H), 2.35 (t, *J*=7.2Hz, 2H), 1.70-1.75 (m, 2H), 1.61-1.66 (m, 2H), 1.43-1.48 (m, 2H),

1.34-1.39 (m, 2H). ^{13}C NMR (125 MHz, $CDCl_3$): δ (ppm) 180.10, 173.35, 161.43, 153.01, 141.28, 141.04, 129.97, 127.59, 106.29, 73.47, 56.26, 43.98, 33.89, 29.76, 28.67, 25.37, 25.34, 24.55.

(E)-7-(2,6-dimethoxy-4-(3-(4-methyl-2-oxo-5,6-dihydropyridin-1(2H)-yl)-3-oxo prop-1-enyl)phenoxy)heptanoic acid (25)

Compound **25** was synthesized from **17** following the procedure described for compound **21**. Compound **17** (136 mg, 0.3 mmol) was dissolved in DCM (10 mL) followed by the addition of TFA (1.5 mL) to afford compound **25** (120 mg, amber oil, 99%). ^{1}H NMR (600 MHz, $CDCl_3$): δ (ppm) 7.63 (d, *J*=15.6Hz, 1H), 7.37 (d, *J*=15.6Hz, 1H), 6.77 (s, 2H), 5.84 (s, 1H), 3.96-4.00 (m, 4H), 3.83 (s, 6H), 2.39 (t, *J*=6.0Hz, 2H), 2.33 (t, *J*=7.2Hz, 2H), 2.00 (s, 3H), 1.69-1.74 (m, 2H), 1.61-1.65 (m, 2H), 1.43-1.48 (m, 2H), 1.34-1.39 (m, 2H). ^{13}C NMR (125 MHz, $CDCl_3$): δ (ppm) 179.72, 169.28, 166.85, 159.21, 153.49, 144.23, 139.15, 130.37, 120.78, 120.71, 105.58, 73.41, 56.09, 41.72, 33.90, 29.85, 29.76, 28.74, 25.40, 24.58, 23.03.

(E)-7-(2,6-dimethoxy-4-(3-oxo-3-(2-oxopiperidin-1-yl)prop-1-enyl)phenoxy)h eptanoic acid (26)

Compound **26** was synthesized from **18** following the procedure described for compound **21**. Compound **18** (400 mg, 0.8 mmol) was dissolved in DCM (10

mL) followed by the addition of TFA (2.0 mL) to afford compound **26** (354 mg, yellow oil, 99%). ^{1}H NMR (600 MHz, $CDCl_3$): δ (ppm) 10.15 (s, 1H), 7.61 (d, *J*=15.6Hz, 1H), 7.31 (d, *J*=15.6Hz, 1H), 6.76 (s, 2H), 3.97 (t, *J*=6.6Hz, 2H), 3.84 (s, 6H), 3.76 (t, *J*=6.0Hz, 2H), 2.59 (t, *J*=6.6Hz, 2H), 2.34 (t, *J*=7.2Hz, 2H), 1.84-1.87 (m, 4H), 1.70-1.75 (m, 2H), 1.61-1.66 (m, 2H), 1.44-1.49 (m, 2H), 1.35-1.40 (m, 2H). ^{13}C NMR (125 MHz, $CDCl_3$): δ (ppm) 179.54, 174.14, 169.71, 153.52, 143.71, 139.20, 130.39, 121.07, 105.51, 73.34, 56.13, 44.68, 34.88, 33.90, 29.82, 28.77, 25.44, 24.60, 22.52, 20.57.

(E)-methyl 7-(2,6-dimethoxy-4-(3-oxo-3-(2-oxo-5,6-dihydropyridin-1(2H)-yl) prop-1-enyl)phenoxy)heptanoate (27)

Compound **21** was dissolved in diethyl ether/MeOH (6 mL/0.6 mL) and trimethylsilyldiazomethane (2 M in diethyl ether, 0.2 mL, 1.2 eq) was added at 0°C. The reaction mixture was stirred at room temperature overnight. Solvent was removed under reduced pressure and the residue was re-dissolved in ethyl acetate, washed with water and brine, dried over anhydrous Na_2SO_4. Crude product was purified by flash chromatography (Hex/EA, 2:1) to afford **27** (90 mg, yellow oil, 64%). ^{1}H NMR (600 MHz, $CDCl_3$): δ (ppm) 7.62 (d, *J*=15.6Hz, 1H), 7.36 (d, *J*=15.6Hz, 1H), 6.88-6.90 (m, 1H), 6.75 (s, 2H), 5.98 (m, 1H), 3.98 (t, *J*=6.6Hz, 2H), 3.93 (t, *J*=6.6Hz, 2H), 3.82 (s, 6H), 3.61 (s, 3H), 2.41-2.44 (m, 2H), 2.27 (t,

J=7.2Hz, 2H), 1.67-1.72 (m, 2H), 1.58-1.63 (m, 2H), 1.41-1.46 (m, 2H), 1.30-1.35 (m, 2H). ^{13}C NMR (125 MHz, $CDCl_3$): δ (ppm) 174.20, 168.85, 165.82, 153.53, 145.53, 143.82, 139.25, 130.38, 125.76, 120.87, 105.51, 73.35, 56.12, 51.42, 41.61, 33.99, 29.86, 28.86, 25.46, 24.88, 24.77. HRMS (ESI): calcd. for $[C_{24}H_{32}NO_7+H]^+$, 446.2179; found, 446. 2188.

(E)-methyl 7-(4-(3-(3-chloro-2-oxo-5,6-dihydropyridin-1(2H)-yl)-3-oxoprop-1-enyl)-2,6-dimethoxyphenoxy)heptanoate (28)

Compound **28** was synthesized from **22** following the procedure described for compound **27**. Compound **22** (70 mg, 0.15 mmol) was reacted with trimethylsilyldiazomethane (2M in diethyl ether, 0.13 mL, 1.2 eq) in a mixture of diethyl ether and MeOH (5 mL : 0.5 mL) to afford compound **28** (22 mg, colorless oil, 31%). ^{1}H NMR (600 MHz, $CDCl_3$): δ (ppm) 7.70 (d, *J*=15.6Hz, 1H), 7.41 (d, *J*=15.6Hz, 1H), 7.09 (t, *J*=4.2Hz, 1H), 6.80 (s, 2H), 4.09 (t, *J*=6.0Hz, 2H), 3.99 (t, *J*=6.0Hz, 2H), 3.88 (s, 6H), 3.67 (s, 3H), 2.57 (q, *J*=6.0Hz, 2H), 2.32 (t, *J*=7.2Hz, 2H), 1.73-1.78 (m, 2H), 1.63-1.68 (m, 2H), 1.46-1.51 (m, 2H), 1.35-1.40 (m, 2H). ^{13}C NMR (125 MHz, $CDCl_3$): δ (ppm) 174.25, 168.51, 161.38, 153.58, 145.11, 141.11, 139.55, 130.11, 128.20, 120.00, 105.69, 73.40, 56.20, 51.45, 41.78, 34.02, 29.88, 28.88, 25.47, 25.29, 24.90. HRMS (ESI): calcd. for $[C_{24}H_{31}NO_7Cl+H]^+$, 480.1789; found, 480.1795.

General procedure for compounds **29-34.** To a flask were added carboxylic acids **21**-**26** (1.0 eq), THP protected hydroxyl amine (2.5 eq) and condensing reagent HBTU (2.0 eq) and filled with argon. DMF and DIPEA (2.0 eq) were added via syringe. The reaction mixture was stirred at room temperature overnight and was diluted with water, extracted with ethyl acetate three times. The combined organic phase was washed with brine, dried over anhydrous Na_2SO_4. Crude products were purified by flash column chromatography (EA/DCM, 1:1) to afford compounds **29**-**34** with yields from 50% to 80%.

(E)-7-(2,6-dimethoxy-4-(3-oxo-3-(2-oxo-5,6-dihydropyridin-1(2H)-yl)prop-1-enyl) phenoxy)-N-hydroxyheptanamide (1-58)

Compound **29** (100 mg, 0.2 mmol, 1.0 eq) was dissolved in MeOH (10 mL) and then TFA (2 mL) was added. The reaction mixture was continued to stir at room temperature for 1 h. Solvent was removed under reduced pressure. Crude product was purified by flash column chromatography (DCM/MeOH, 20:1) to afford product **1-58** (white solid, 57 mg, 67%). ^{1}H NMR (600 MHz, $CDCl_3$): δ (ppm) 8.77 (br, s 1H), 7.64 (d, *J*=15.0Hz, 1H), 7.37 (d, *J*=15.6Hz, 1H), 6.92-6.95 (m, 1H), 6.77 (s, 2H), 6.02 (d, *J*=9.6Hz, 1H), 4.02 (t, *J*=6.6Hz, 2H), 3.97 (t, *J*=6.6Hz, 2H), 3.84 (s, 6H), 2.46 (m, 2H), 2.12 (m, 2H), 1.67-1.70 (m, 2H), 1.60-1.63 (m, 2H), 1.43-1.45 (m, 2H), 1.31-1.34 (m, 2H). ^{13}C NMR (125 MHz, $CDCl_3$): δ (ppm)

171.45, 168.95, 165.92, 153.48, 145.64, 143.85, 139.15, 130.42, 125.75, 120.93, 105.58, 73.27, 56.17, 41.66, 32.71, 29.72, 28.59, 25.27, 25.16, 24.78. HRMS (ESI): calcd. for $[C_{23}H_{31}N_2O_7+H]^+$, 447.2131; found, 447.2129.

(E)-7-(4-(3-(3-chloro-2-oxo-5,6-dihydropyridin-1(2H)-yl)-3-oxoprop-1-enyl)-2, 6-dimethoxyphenoxy)-N-hydroxyheptanamide (3-35)

Compound **30** (100 mg, 0.2 mmol) was reacted with TFA (0.5 mL) in MeOH (10 mL). After removing all the solvent, crude product was purified by flash column chromatography (DCM/MeOH, 20:1) to afford compound **3-35** (50 mg, colorless oil, 67%). ^{1}H NMR (600 MHz, $CDCl_3$): δ (ppm) 7.69 (d, *J*=15.6Hz, 1H), 7.39 (d, *J*=15.6Hz, 1H), 7.09 (t, *J*=4.8Hz, 1H), 6.79 (s, 2H), 4.08 (t, *J*=6.6Hz, 2H), 3.99 (t, *J*=6.6Hz, 2H), 3.86 (s, 6H), 2.57 (q, *J*=6.0Hz, 2H), 2.14 (t, *J*=7.8Hz, 2H), 1.69-1.73 (m, 2H), 1.62-1.67 (m, 2H), 1.43-1.48 (m, 2H), 1.34-1.37 (m, 2H). ^{13}C NMR (125 MHz, $CDCl_3$): δ (ppm) 171.55, 168.55, 161.43, 153.50, 145.04, 141.19, 139.39, 130.17, 128.16, 120.09, 105.73, 73.30, 56.23, 41.81, 32.70, 29.72, 28.57, 25.29, 25.25, 25.15. HRMS (ESI): calcd. for $[C_{23}H_{30}N_2O_7Cl+H]^+$, 481.1742; found, 481.1734.

7-(2,6-dimethoxy-4-(6-oxo-1,2,3,6-tetrahydropyridine-1-carbonyl)phenoxy)-N -hydroxyheptanamide (3-31)

Compound **31** (184 mg, 0.4 mmol) was dissolved in MeOH (10 mL)

following addition of TFA (1 mL) at room temperature. After stirring for 1h, solvent was removed under reduced vacuum. Crude product was purified by flash column chromatography (DCM/MeOH, 20:1) to afford product **3-31** (58.5 mg, colorless oil, 40%). ^{1}H NMR (600 MHz, $CDCl_3$): δ (ppm) 8.89 (s, 1H), 6.96-6.99 (m, 1H), 6.83 (s, 2H), 5.99 (d, *J*=9.6Hz, 1H), 4.04 (t, *J*=6.6Hz, 2H), 3.95 (t, *J*=6.6Hz, 2H), 3.82 (s, 6H), 2.58-2.60 (m, 2H), 2.06 (t, *J*=7.2Hz, 2H), 1.67-1.71 (m, 2H), 1.57-1.62 (m, 2H), 1.39-1.44 (m, 2H), 1.28-1.31 (m, 2H). ^{13}C NMR (125 MHz, $CDCl_3$): δ 173.61, 171.22, 165.93, 152.84, 145.86, 140.73, 130.58, 125.09, 106.28, 73.02, 56.25, 43.76, 32.53, 29.69, 28.36, 25.10, 25.03, 24.88. HRMS (ESI): calcd for $[C_{21}H_{29}N_2O_7+H]^+$, 421.1975; found, 421.1975.

7-(4-(5-chloro-6-oxo-1,2,3,6-tetrahydropyridine-1-carbonyl)-2,6-dimethoxyphenoxy)-N-hydroxyheptanamide (3-98)

Compound **3-98** was synthesized by treating **32** (80 mg, 0.2 mmol) with TFA (0.4 mL) in MeOH (5 mL) at room temperature. Crude product was purified by flash column chromatography (DCM/MeOH, 20:1) to afford pure compound (lightly yellow solid, 38 mg, 56%). ^{1}H NMR (600 MHz, $CDCl_3$): δ (ppm) 9.08 (s, 1H), 7.09 (t, *J*=4.8Hz, 1H), 6.78 (s, 2H), 3.96-4.00 (m, 4H), 3.80 (s, 6H), 2.65-2.68 (m, 2H), 2.06 (t, *J*=6.6Hz, 2H), 1.66-1.70 (m, 2H), 1.57-1.62 (m, 2H), 1.38-1.42 (m, 2H), 1.26-1.32 (m, 2H). ^{13}C NMR (125 MHz, $CDCl_3$): δ (ppm) 173.13, 171.51,

161.38, 152.99, 141.19, 141.04, 130.02, 127.61, 106.28, 73.24, 56.31, 43.94, 32.59, 29.71, 28.46, 25.39, 25.21, 25.16. HRMS (ESI): calcd. for $[C_{21}H_{28}N_2O_7Cl+H]^+$, 455.1590; found, 455.1585.

(E)-7-(2,6-dimethoxy-4-(3-(4-methyl-2-oxo-5,6-dihydropyridin-1(2H)-yl)-3-oxo prop-1-enyl)phenoxy)-N-hydroxyheptanamide (35)

Compound **35** was synthesized by treating **33** (67 mg, 0.1 mmol) with TFA (0.5 mL) in MeOH (6.0 mL) at room temperature. Crude product was purified by flash column chromatography (DCM/MeOH, 30:1) (lightly yellow solid, 20 mg, 36%). ^{1}H NMR (600 MHz, $CDCl_3$): δ (ppm) 8.77 (bs, 1H), 7.63 (d, *J*=15.6Hz, 1H), 7.39 (d, *J*=15.0Hz, 1H), 6.77 (s, 2H), 5.82 (s, 1H), 3.99 (t, *J*=6.0Hz, 2H), 3.97 (t, *J*=6.0Hz, 2H), 3.84 (s, 6H), 2.38 (t, *J*=5.4Hz, 2H), 2.12 (m, 2H), 2.00 (s, 3H), 1.68-1.70 (m, 2H), 1.61-1.64 (m, 2H), 1.40-1.46 (m, 2H), 1.30-1.36 (m, 2H). ^{13}C NMR (125 MHz, $CDCl_3$): δ (ppm) 171.37, 168.92, 166.18, 158.01, 153.46, 143.55, 139.06, 130.51, 121.24, 121.05, 105.55, 73.25, 56.16, 41.57, 32.72, 29.91, 29.71, 28.58, 25.27, 25.16, 22.99. HRMS (ESI): calcd for $[C_{24}H_{33}N_2O_7+H]^+$, 461.2288; found, 461.2299.

(E)-7-(2,6-dimethoxy-4-(3-oxo-3-(2-oxopiperidin-1-yl)prop-1-enyl)phenoxy)-N -hydroxyheptanamide (36)

Compound **36** was synthesized by treating **34** (70 mg, 0.1 mmol) with TFA

(0.4 mL) in MeOH (10 mL) at room temperature. Crude product was purified by flash column chromatography (DCM/MeOH, 20:1) (colorless oil, 15 mg, 26%). ^{1}H NMR (400 MHz, DMSO-d_6): δ (ppm) 10.32 (s,1H), 7.32 (d, *J*=16.0Hz, 1H), 6.85 (s, 2H), 6.54 (d, *J*=15.6Hz, 1H), 3.82 (t, *J*=6.4Hz, 2H), 3.77 (s, 6H), 3.12-3.17 (m, 2H), 2.31 (t, *J*=7.6Hz, 2H), 1.93 (t, *J*=7.6Hz, 2H), 1.36-1.61 (m, 10H), 1.20-1.28 (m, 2H). ^{13}C NMR (75 MHz, DMSO-d_6): δ (ppm) 173.73, 169.57, 165.39, 153.68, 139.06, 138.21, 130.80, 121.97, 105.33, 72.80, 56.33, 38.63, 33.36, 32.70, 29.94, 28.99, 28.78, 25.60, 25.54, 22.38. HRMS(ESI): calcd. for $[C_{23}H_{32}N_2O_7+Na]^+$, 471.2107; found, 471.2100.

2.4. Biological characterization

In this collaborative project, the following biological characterization of newly synthesized compounds was done by our collaborator, Dr.Yubin Ge group. Herein, key points of their anti-leukemic activities are listed and noted.

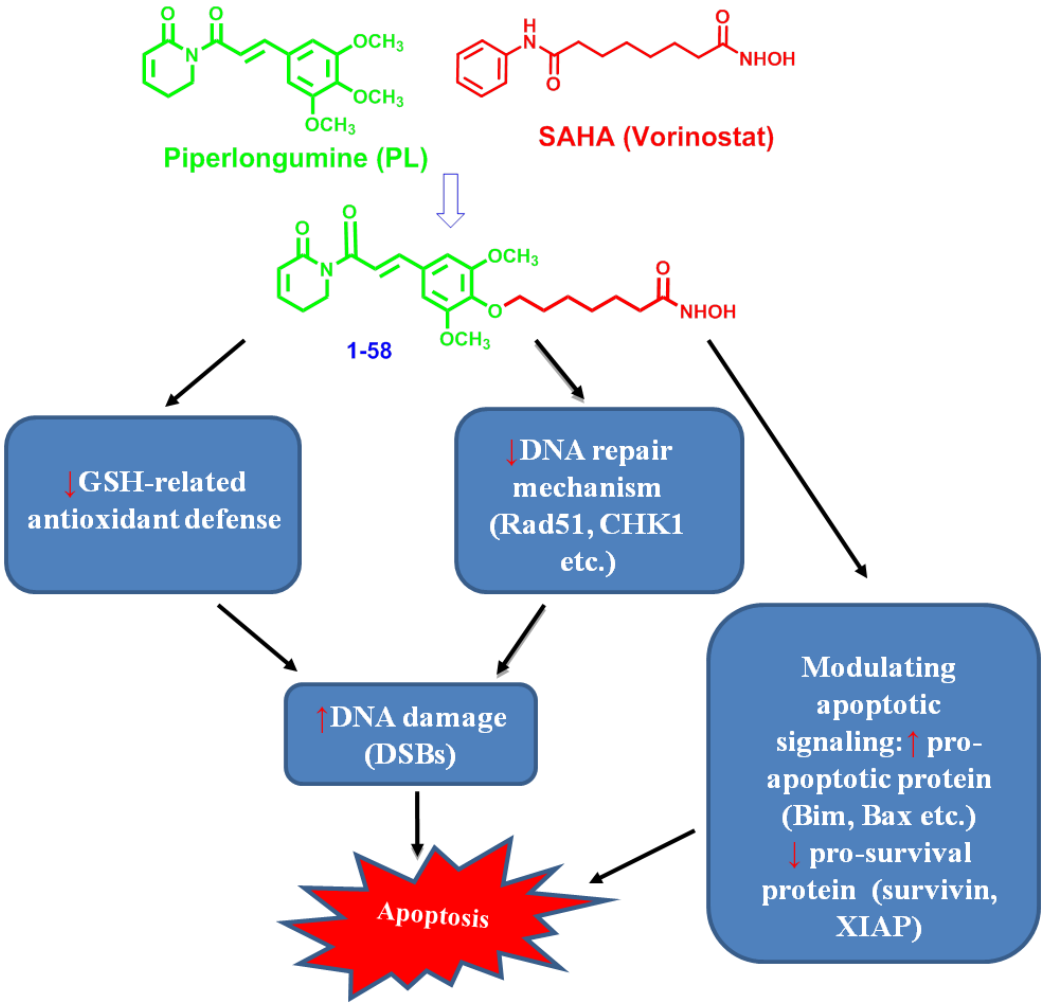

Figure 9. Schematic summary of biological activities of **1-58** in AML cells.

2.4.1. Synergy between SAHA and PL

The synergistic-to-additive anti-leukemic interactions between PL and SAHA provide a compelling rationale to construct PL-HDACi chimeric molecules against AML cells.

2.4.2. Anti-AML activities of the PL-HDACi hybrid 1-58

On the basis of favorable anti-AML interactions between PL and SAHA, we

explored a “hybrid drug” approach to discover a single chemical entity possessing both HDACi and PL-related activities. The chimeric compound **1-58** triggered concentration-dependent apoptotic cell death, as indicated by a significant increase of Annexin V-positive cells and cleavage of PARP and caspase-3. EC_{50}s of **1-58** mimicked those of the PL and SAHA combination and were significantly lower than those of single agents, indicating improved anti-AML potency. **1-58** was further tested in other AML cell lines representing various disease subtype and status, for instance, in pediatric AML cell lines CMS, CMK, and CMY and in Ara-C-resistant HL60/ARC and CMK/ARC cells. **1-58** IC_{50}s were sub-micromolar for the cell lines tested and were equivalent or substantially lower than combined PL and SAHA treatment. In conclusion, **1-58** shows a broad spectrum of anti-AML activities regardless of many disease-specific molecular characteristics, such as p53 and FLT3-ITD mutational status.

2.4.3. SAR of 1-58

Cellular HDACi activities. Designed as multifunctional anticancer agents, chimeric molecules were expected to retain HDACi activities. Results show that hybrid molecules **1-58**, **3-35**, **3-31** and **3-98** maintain strong pan-HDACi activity. Comparisons between **1-58**/**3-35** and **3-31**/**3-98** demonstrated that the absence of C7-C8 olefin in **3-31** and **3-98** did not change HDACi efficacy. **27** and **28,** which

lack the hydroxamic acid functional group, didn't affect acetylation of H4 and α-tubulin. The cellular HDACi activity of compound **35** with C3-methyl group was better than that of compound **36** in which C2-C3 olefin was saturated. Compared to **1-58**, structural modification of the 5,6-dihydro-2(*1H*)-pyridinone ring of PL, by introducing a C3-methyl group (compound **35**) or saturation of C2-C3 olefin (compound **36**), decreased cellular HDACi activities. On the contrary, C2-Cl substitution and elimination of C7-C8 olefin were well tolerated for cellular HDACi activities. These results suggested that the PL or partial PL scaffold was an acceptable "cap" group to render effective HDACi activities to the chimeric molecules.

Dual-acting mode. First, to clarify the contributions of HDACi and PL moieties to the overall anti-AML effects of chimeric molecule **1-58**, close structural analogues, i.e. compounds **27**, **35** and **36**, were tested in U937 cells. Hydroxamic acid, the ZBG of **1-58**, was replaced by a methyl ester in **27** to eliminate HDACi activity. On the other hand, compounds **35** and **36** retained the ZBG but the electrophilic C2-C3 olefin of PL was blocked by using C3-methyl substituent in compound **35** or via hydrogen saturation in compound **36**. The **1-58** and **27** pair illustrated the contribution of HDAC inhibition to the anti-leukemic activity of the hybrid **1-58**. Compound **35** or **36** emphasized C2-C3 olefin-provoked PL-like

cellular activities, such as GSH depletion and/or protein alkylation. These results suggested that the integration of intact HDACi and PL moieties into one chemical entity is necessary for the observed superior anti-AML effects, blocking either pharmacophore in close structural analogues significantly decreased their apoptotic induction activity. Once getting into AML cells, **1-58** may have a dual action mode: some drug molecules act as HDAC inhibitors, and others may induce PL-like effects. **3-35** was designed as an analogue of **1-58** with a C2-chloro substituent and was used to test if the chemical reactivity of the C2-C3 olefin plays a role in the biological properties of chimeric molecules. The **1-58** and **3-35** pair demonstrated that introducing an electron-withdrawing group at the C2 position of PL enhanced the potency of chimeric molecules, which could be attributed to the electron-deficiency of C2-C3 olefin that facilitates the conjugation with cellular nucleophiles. **3-31** and **3-98** were synthesized as **1-58** and **3-35** analogues without the C7-C8 double bond. It has been reported that disrupting the electrophilicity of the C7-C8 olefin by saturation, steric blockade or cyclization into a heterocycle could substantially diminish PL's cytotoxicity and covalent modification of GSH-binding protein[21]. Interestingly, these modifications did not interfere with ROS production and GSH depletion properties as long as an active C2-C3 olefin was intact. **3-31**/**3-98** had weaker cellular HDACi activities in

contrast to **1-58**/**3-35**, which is likely attributed to the absence of C7-C8 olefin. Interestingly, **3-31** and **3-98** showed similar potency without C7-C8 olefin involved whereas much difference with C7-C8 involved. This observation indicates that C2-chloro substituent might heavily rely on C7-C8 olefin to enhance the cytotoxicity of hybrid compound.

2.4.4. Cytotoxicity vs. selectivity

Since both cytotoxicity and selectivity (i.e., sparing non-cancer cells) are important for an anticancer compound, we further evaluated PL, SAHA, PL plus SAHA, and chimeric compounds **1-58**, **3-31, 3-35** and **3-98** in non-cancer cells. PL has been shown to be non-toxic to MCF-10A, a non-cancerous breast epithelial cell line, at concentrations up to 15 μM in 24 h treatments[3], which makes it an interesting model for comparison. **1-58** was more selective than PL + SAHA and **3-35**. Similar to **1-58**, **3-31** and **3-98** also showed selectivity. **3-35** was highly toxic and barely showed selectivity because **3-35** may efficiently cause cellular GSH depletion and trigger massive protein glutathionylation which may be responsible for the non-selective toxicity. Since C2 reactivity is tightly linked to overall effects of hybrid compound through GSH conjugation, we conducted an *N*-acetyl cysteine (NAC) rescue experiment. The result emphasized the role of GSH depletion and/or ROS induction played in the overall apoptotic effects.

2.4.5. DNA damage caused by PL, HDACi and their hybrid drug 1-58

Since both PL[160-161] and HDACis (e.g., SAHA[150]) are able to induce DNA damage and inhibit DNA repair mechanisms, we investigated their impact on the integrity of DNA in U937 cells by using alkaline comet assay and western blotting assay. The results showed that the reduction of Rad51 and CHK1 contributes to the observed significant DNA damage induced by SAHA and PL combination and hybrid drug **1-58**. Rad51 was up-regulated 1.4-fold by PL (2 μM), which could be a cellular adaptive reaction to the PL-induced DNA damage. Strikingly, this increase was abolished by the combination with SAHA or by the hybrid compound **1-58**.

2.4.6. Apoptotic proteins affected by PL-HDACi 1-58

The balance between the expression/activity of the pro- and anti-apoptotic pathways could ultimately determine the fate of a given cell. Western blotting revealed up-regulation of pro-apoptotic Bim (EL isoform, 1.8 fold) and down-regulation of anti-apoptotic protein XIAP (to 0.6 fold) by **1-58**. Because PL itself didn't change the expression of Bim and XIAP, the observed modulations were mainly attributed to the retained HDACi activity of **1-58**. PL and SAHA combination, as well as SAHA alone, showed similar effects.

2.5. Chemistry methods

General Methods for Chemistry. ^{1}H and ^{13}C NMR spectra were obtained

using Varian Mercury 600MHz and Advance 300 MHz spectrometers. Chemical shifts are reported as δ values in parts per million (ppm) relative to tetramethylsilane (TMS) for all recorded NMR spectra. All reagents and solvents were obtained commercially from Acros, Aldrich or Fisher and were used without purification. Flash column chromatography was performed over 200−300 mesh silica gel. High resolution mass spectral data were collected using a LCT Premier XE KD128 instrument. All compounds submitted for biological testing were found to be >95% pure by analytical HPLC. HPLC analysis of incubations were conducted using a Phenomenex (Luna^{R}) C18, 3.5 µm, 100 mm × 3.0 mm column on either a Shimadzu UFLC or Agilent 1100 series HPLC instrument. HPLC parameters were: 0.1% formic acid (FA) in 10% CH_3OH (solvent A); 0.1% FA in CH_3CN (solvent B); flow rate 0.5 mL/min; gradient, t = 0 min, 10% B; t = 1 min, 10% B; t = 18 min, 80% B; t = 20 min, 80% B; t = 21 min, 95% A.

CHAPTER 3 DESIGN, SYNTHESIS, AND BIOLOGICAL CHARACTERIZATION OF HYDROXAMIC HDACi PRODRUGS AS ANTI-AML AGENTS

3.1. Rationale

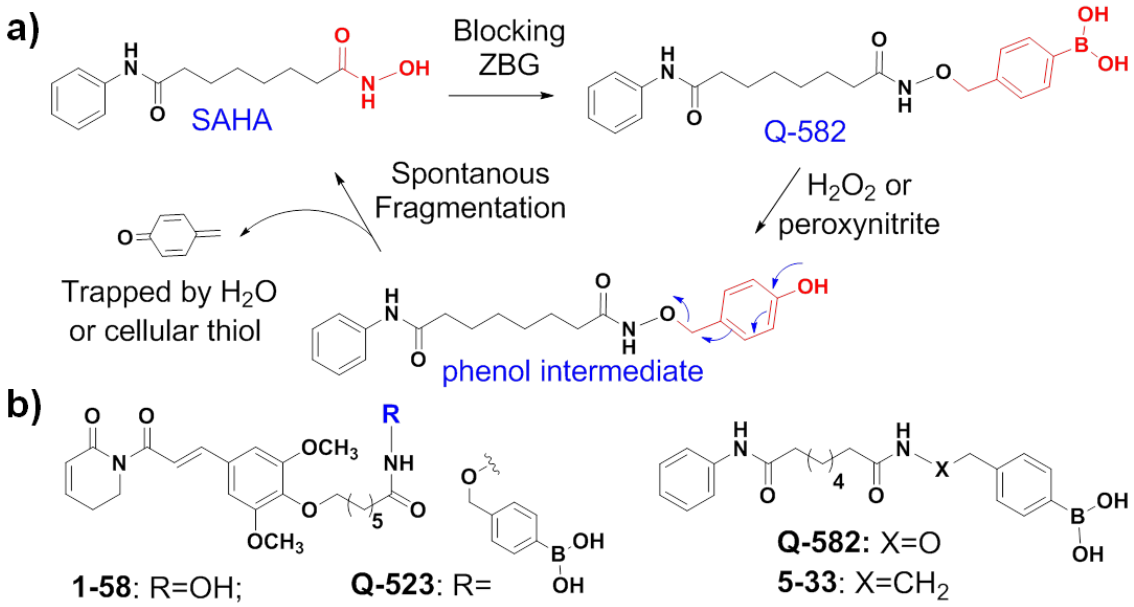

Scheme 2. Activation mechanism and structure of Prodrugs. **a)** The design of arylboronic acid-masked hydroxamic acid prodrug and the mechanism of activation, exemplified using SAHA and **Q-582**. **b)** Chemical structures of HDACi **1-58**, prodrug **Q-523**, and **Q-582** derivative **5-33**.

Acute myeloid leukemia (AML) remains a challenging disease, overall 5-year survival is less than 5% in patients over the age of 65[167]. AML is frequently characterized by epigenetic deregulation. Histone deacetylase inhibitors (HDACis) target aberrant epigenetic modifications of cancer and have been studied as an attractive "targeted" drug class for AML treatment[168]. Although very promising in preclinical models, HDACis as monotherapy only resulted in modest[156] or poor[169] clinical activities in AML trials. Multiple factors, such as undesired cardiovascular

and gastrointestinal toxicity[170], fast elimination, and poor tissue penetration caused by metabolic labile and high polar hydroxamic acid zinc binding group (ZBG)[171], hindered the clinical use of HDACi in AML and other cancer indications. To overcome these shortcomings, several prodrug approaches, such as carbamate[171a, 172]- and quinone[171b]-protected hydroxamic acid prodrugs have been proposed with aims to increase metabolic stability and membrane permeability of hydroxamic acid-based drugs[171a].

3.2. Design and synthesis of hydroxamic acid HDACi prodrugs

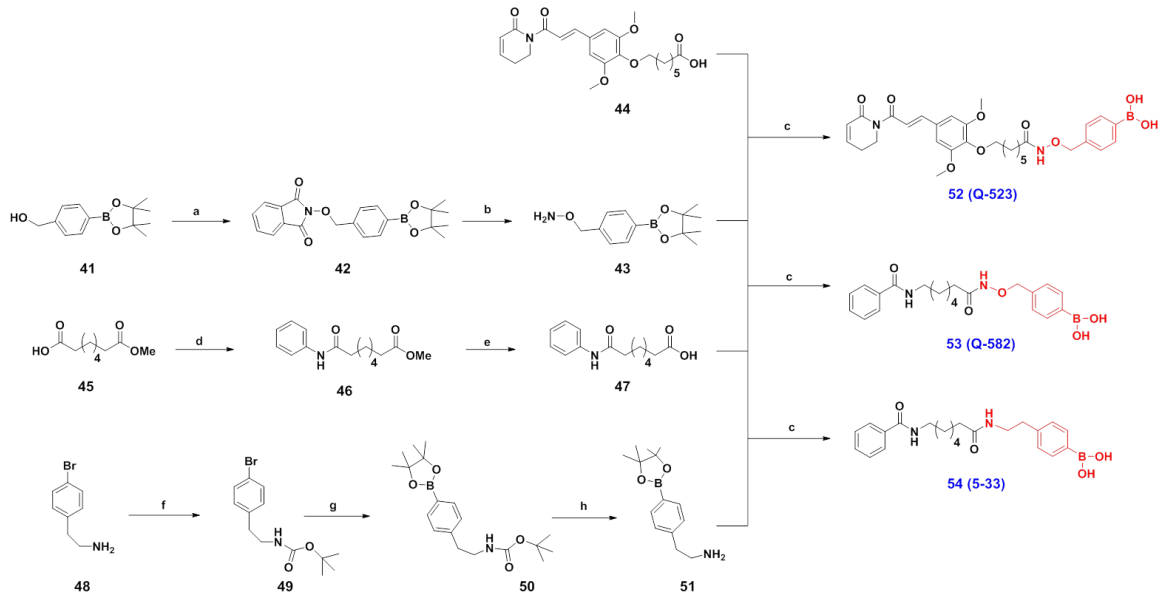

Scheme 3. Synthetic route of prodrugs. Reagents and conditions: (a) PPh_3, DEAD, THF, 82%; (b) Methylhydrazine, THF, 0°C, 77%; (c) 1. HBTU, DIPEA, THF; 2. $NaIO_4$, NH_4OAc, acetone/H_2O (1:1); 57% for **Q-523**, 60% for **Q-582**; 75% for **5-33**; (d) Aniline, BOP, DIPEA, DCM, 70%; (e) LiOH, THF/H_2O (1:1), 80%; (f) $(BOC)_2O$, Et_3N, 95%; (g) Bis(pinacolato)diboron, AcOK, $Pd(dppf)Cl_2$, 1,4-dioxane, 80°C, 80%; (h) Trifluoroacetic acid, DCM, 91%.

Herein, we designed a novel HDACi prodrug class by masking the hydroxamic acid ZBG with hydrogen peroxide (H_2O_2)/peroxynitrite (PNT)-sensitive, self-immolative aryl boronic acid promoiety. The chemical reactions between aromatic boronate/boronic acid and H_2O_2 (a reactive oxygen species, ROS)[173] or PNT (a reactive nitrogen species, RNS)[174] are specific and bioorthogonal and give phenol as the major product. Via 1,6-elimination, the phenol intermediate is expected to release free hydroxamic acid and a short-lived quinone methide which can be further quenched by H_2O or cellular thiols (**Scheme 2a**). In this study, two HDACis, SAHA (vorinostat), an FDA-approved drug to treat cutaneous T cell lymphoma[175] and **1-58**, a piperlongumine-HDACi hybrid molecule with potent anti-AML activity[30], were converted to prodrugs **Q-582** and **Q-523,** respectively (**Scheme 2a** and **2b**). Boronic acid instead of boronic acid ester was used as promoiety to improve water solubility of **Q-582** and **Q-523**.

Besides chemical properties, the design of ROS/RNS-activated HDACi prodrugs is also reasoned by abundant endogenous ROS/RNS sources in AML cells and in disease-relevant microenvironments. Due to malfunctioned redox homeostasis pathways, e.g., mitochondrial DNA mutation-induced electron transfer chain alteration, FLT3-ITD-caused NADPH oxidase (NOX) upregulation and the elevated xanthine oxidoreductase activity[65], AML blasts display higher

levels of ROS compared to normal leukocytes[176]. PNT is formed from the reaction of nitric oxide (NO) and superoxide ($O_2^{\cdot -}$) and it reacts with boronic acid up to a million-fold faster than H_2O_2[174, 177]. The occurrence of AML abnormally upregulates and activates NOX4 (an $O_2^{\cdot -}$ generating enzyme) and nitric oxide synthase 3 (also known as eNOS) in bone marrow (BM) endothelial cells and results in overproduction of NO and ROS[178]. This event could eventually generate higher levels of PNT in the AML BM microenvironment. Compared with the healthy tissue, the elevated ROS (e.g., H_2O_2) and PNT could activate boronic acid-based HDACi prodrug and release higher levels of cytotoxic HDACi in AML cells and in AML-relevant, ROS/RNS-enriched microenvironments.

Starting from the pinacol ester **41**, hydroxylamine **43** was made by deprotecting Mitsunobu reaction product **42** with methylhydrazine. Coupling of **43** with carboxylic acids **44**[30] and **47**[179], followed by the treatment of $NaIO_4/NH_4OAc$[180] gave prodrugs **Q-523** and **Q-582** respectively (**Scheme 3**). To study the potential biological effects of aryl boronic acid, we prepared a close structural analogue of **Q-582**, i.e. compound **54** (**5-33**) which does not release HDACi functionality due to replacing oxygen of ZBG with a methylene group. Similar to the synthesis of **Q-582**, **54** (**5-33**) was made by condensing **47** with amine **51**. This intermediate was synthesized from **48** via sequential amine

protection, palladium-catalyzed borylation and acidic deprotection (**Scheme 3**).

3.3. Chemistry

2-((4-(4,4,5,5-tetramethyl-1,3,2-dioxaborolan-2-yl)benzyl)oxy)isoindoline-1,3-dione (42)

4-(Hydroxymethyl)phenylboronic acid pinacol ester (**41**, 2.8 g, 12.0 mmol, 1.0 eq) and *N*-Hydroxyphthalimide (2.34 g, 14.36 mmol, 1.2 eq) were dissolved in anhydrous THF (15 mL) and cooled in ice bath. A mixture of DIAD (2.9 g, 14.4 mmol, 1.2 eq) and PPh_3 (3.76 g, 14.4 mmol, 1.2 eq) in anhydrous THF (15 mL) was added dropwise over 15 min. The reaction mixture was allowed to gradually warm up to room temperature and stirred overnight. Solvent was removed under reduced pressure and diluted with DCM. The organic layer was washed with saturated aqueous NaCl and dried over anhydrous Na_2SO_4. After concentration, residue was purified by flash chromatography (Hexane/ethyl acetate, 10:1) to afford product (white solid, 3.7 g, 82%). ^{1}H NMR (600 MHz, $CDCl_3$): δ (ppm) 7.79 (d, *J*=7.2Hz, 2H), 7.76-7.78 (m, 2H), 7.69-7.71 (m, 2H), 7.51 (d, *J*=7.8Hz, 2H), 5.21 (s, 2H), 1.32 (s, 12H). ^{13}C NMR (125 MHz, $CDCl_3$): δ (ppm) 163.44, 136.51, 134.91, 134.43, 128.96, 128.81, 123.49, 83.89, 79.61, 77.26, 77.05, 76.84, 24.87.

O-(4-(4,4,5,5-tetramethyl-1,3,2-dioxaborolan-2-yl)benzyl)hydroxylamin e (43)

To a stirred solution of **42** (3.7 g, 9.8 mmol, 1.0 eq) in anhydrous THF (10 mL) was added methyhydrazine (500 mg, 10.7 mmol, 1.1 eq) at 0°C. The reaction was completed in 30min accompanied by forming white precipitate. After filtration through celite, the filtrate was concentrated and the residue was purified by flash chromatography (DCM/MeOH, 10:1) to afford product (colorless oil, 1.9 g, 77%). ^{1}H NMR (600 MHz, $CDCl_3$): δ (ppm) 7.80 (d, *J*=7.8Hz, 2H), 7.36 (d, *J*=7.8Hz, 2H), 5.39 (bs, 2H), 4.70 (s, 2H), 1.33 (s, 12H). ^{13}C NMR (125 MHz, $CDCl_3$): δ (ppm) 140.59, 134.94, 127.49, 83.79, 77.83, 24.85.

(E)-(4-(((7-(2,6-dimethoxy-4-(3-oxo-3-(6-oxo-3,6-dihydropyridin-1(2H)-yl)prop-1-en-1-yl)phenoxy)heptanamido)oxy)methyl)phenyl)boronic acid (Q-523)

To a stirred solution of **44** (156 mg, 0.36 mmol, synthesized as previously described [30]) were added HBTU (164 mg, 0.43 mmol, 1.2 eq), DIPEA (0.13 mL, 0.72 mmol, 2.0 eq) in anhydrous THF (5.0 mL), **43** (98 mg, 0.40 mmol, 1.1 eq), and the reaction was stirred at room temperature overnight. The reaction was quenched with water and diluted with DCM.

The organic layer was separated, washed with water and concentrated to give a white solid that was directly used for next step without further purification. The crude coupling product was mixed with NH_4OAc (58.5 mg, 0.76 mmol, 2.1 eq) and $NaIO_4$ (231 mg, 1.08 mmol, 3.0 eq) in acetone/water (1:1, 10 mL) at room temperature and the reaction was stirred overnight. The resulting mixture was diluted with DCM and washed with brine. The organic fraction was collected and concentrated. The residue was purified by flash chromatography (Hexane/DCM/MeOH, 4:4:0.1) to afford product (colorless oil, 120 mg, 57%). ^{1}H NMR (600 MHz, CD_3OD): δ (ppm) 7.76 (m, 1H), 7.59-7.61 (m, 2H), 7.35-7.40 (m, 3H), 7.05-7.08 (m, 1H), 6.88 (s, 2H), 6.00 (d, *J*=10.2Hz, 1H), 4.84 (s, 2H), 3.98 (t, *J*=6.6Hz, 2H), 3.95 (t, *J*=6.6Hz, 2H), 3.85 (s, 6H), 2.49-2.51 (m, 2H), 2.06 (t, *J*=7.2Hz, 2H), 1.66-1.70 (m, 2H), 1.58-1.62 (m, 2H), 1.46-1.49 (m, 2H), 1.28-1.33 (m, 2H). ^{13}C NMR (125 MHz, $CDCl_3$): δ (ppm) 172.95, 170.59, 167.76, 155.02, 148.36, 144.45, 140.36, 135.08, 134.70, 132.12, 129.48, 129.37, 125.98, 122.48, 106.71, 74.38, 56.74, 54.83, 43.05, 33.80, 30.98, 29.81, 26.67, 26.65, 25.79. HRMS (ESI): calcd. for $[C_{30}H_{37}BN_2O_9\text{-}H]^-$, 578.2550; found, 578.2537.

Methyl 8-oxo-8-(phenylamino)octanoate (46)

Intermediate **47** was synthesized through **46** according to literature[179] with modifications. Aniline (1.0 g, 10.8 mmol, 1.1 eq) and suberic acid monomethyl ester (**45**, 1.75 mL, 9.8 mmol, 1.0 eq) were dissolved in DCM (20 mL) and cooled in an ice bath. To the above stirred solution, BOP (5.71 g, 12.9 mmol, 1.2 eq) and DIPEA (2.27 mL, 12.9 mmol, 1.2 eq) were slowly added. The reaction was stirred at room temperature overnight. The reaction was quenched with water and diluted by adding DCM. The resulting organic layer was washed with water, and dried over anhydrous Na_2SO_4. Crude product was purified by flash chromatography (Hexane/Ethyl acetate, 1:1) to afford **46** (yellow solid, 1.8 g, 70%). ^{1}H NMR (600 MHz, $CDCl_3$): δ (ppm) 7.50 (d, *J*=7.8Hz, 2H), 7.40 (bs, 1H), 7.29 (t, *J*=7.8Hz, 2H), 7.08 (t, *J*=7.8Hz, 1H), 3.65 (s, 3H), 2.33 (t, *J*=7.2Hz, 2H), 2.30 (t, *J*=7.2Hz, 2H), 1.69-1.74 (m, 2H), 1.59-1.64 (m, 2H), 1.33-1.38 (m, 4H). ^{13}C NMR (125 MHz, $CDCl_3$): δ (ppm) 174.29, 171.36, 137.97, 128.95, 124.14, 119.75, 51.51, 37.55, 33.93, 28.73, 28.70, 25.32, 24.66.

8-oxo-8-(phenylamino)octanoic acid (47)

The methyl ester **46** (2.0 g, 7.6 mmol, 1.0 eq) was dissolved in THF/H_2O (1:1, 20 mL), followed by addition of LiOH (273 mg, 11.4 mmol, 1.5 eq). The reaction was vigorously stirred at room temperature for 12h.

THF was removed under reduced pressure, and pH of the aqueous solution was adjusted to 2-3 using HCl (2 M). DCM was added to re-dissolve the precipitated white solid. DCM solution was separated and dried over anhydrous Na_2SO_4. The crude product was purified using flash chromatography (DCM/MeOH, 40:1) to afford **47** (white solid, 1.5 g, 80%). ^{1}H NMR (600 MHz, CD_3OD): δ (ppm) 7.52 (d, *J*=7.2Hz, 2H), 7.28 (t, *J*=7.8Hz, 2H), 7.06 (t, *J*=7.8Hz, 1H), 2.35 (t, *J*=7.8Hz, 2H), 2.28 (t, *J*=7.8Hz, 2H), 1.67-1.70 (m, 2H), 1.60-1.63 (m, 2H), 1.37-1.39 (m, 4H).

(4-(((8-oxo-8-(phenylamino)octanamido)oxy)methyl)phenyl)boronic acid (Q-582)

A flask was charged with carboxylic acid **47** (200 mg, 0.80 mmol, 1.0 eq), anhydrous THF (15 mL) and cooled to 0°C in an ice bath. HBTU (365 mg, 0.96 mmol, 1.2 eq), DIPEA (0.28 mL, 1.60 mmol, 2.0 eq) and **43** (220 mg, 0.88 mmol, 1.1 eq) were added and reaction mixture was stirred overnight. The reaction was quenched with water and diluted with DCM. The organic layer was separated, washed with water and concentrated to give a white solid that was directly used for next step. The crude product (112 mg) was dissolved in acetone/water mixture (1:1, 10 mL), followed by the addition of NH_4OAc (38 mg, 0.49 mmol) and $NaIO_4$ (148 mg, 0.69 mmol).

The reaction mixture was stirred at room temperature overnight. The resulting mixture was extracted with DCM and washed with water. The crude product was purified using flash chromatography (DCM/ Hexane/MeOH, 4:4:0.5) to afford **Q-582** (white solid, 190 mg, 60%). ^{1}H NMR (ppm) (600 MHz, CD_3OD): δ (ppm) 7.75 (d, *J*=6.6Hz, 1H), 7.60 (d, *J*=7.8Hz, 1H), 7.51 (d, *J*=7.8Hz, 2H), 7.40 (d, *J*=7.8Hz, 1H), 7.35 (d, *J*=7.2Hz, 1H), 7.27 (t, *J*=7.8Hz, 2H), 7.06 (t, *J*=7.8Hz, 1H), 4.83 (s, 2H), 2.34 (t, *J*=7.2Hz, 2H), 2.03 (t, *J*=7.2Hz, 2H), 1.65-1.69 (m, 2H), 1.57-1.60 (m, 2H), 1.35-1.36 (m, 2H), 1.27-1.32 (m, 2H). ^{13}C NMR (125 MHz, CD_3OD): δ (ppm) 174.67, 172.97, 139.98, 135.13, 134.76, 129.86, 129.53, 129.42, 125.20, 121.33, 78.89, 37.93, 33.75, 29.96, 29.83, 26.78, 26.54. HRMS (ESI): calcd. for $[C_{21}H_{27}BN_2O_5\text{-}H]^-$, 396.1971; found, 396.1973.

Tert-butyl (4-bromophenethyl)carbamate (49)

To a stirred solution of 4-bromophenethylamine (**48**, 5.0 g, 3.87 mmol, 1.0 eq) in DCM (20 mL) were added Di-*tert*-butyl dicarbonate (8.2 g, 37.5 mmol, 1.5 eq) and triethylamine (10.23 mL, 75 mmol, 3.0 eq). The reaction was stirred for overnight at room temperature. Upon completion, the reaction was diluted with DCM and washed with water. The DCM solution was concentrated. The crude product was purified using flash

chromatography (Hexane/Ethyl acetate, 20:1) to afford **49** (white solid, 7.1 g, 95%). ^{1}H NMR (600 MHz, $CDCl_3$): δ (ppm) 7.40 (d, *J*=8.4Hz, 2H), 7.04 (d, *J*=8.4Hz, 2H), 4.53 (bs, 1H), 3.12-3.34 (m, 2H), 2.74 (t, *J*=7.2Hz, 2H), 1.41(s, 9H). ^{13}C NMR (125 MHz, $CDCl_3$): δ (ppm) 155.80, 137.97, 131.60, 130.55, 120.22, 79.33, 41.57, 35.62, 28.37.

Tert-butyl (4-(4,4,5,5-tetramethyl-1,3,2-dioxaborolan-2-yl)phenethyl) carbamate (50)

Intermediate **49** (3.0 g, 10 mmol, 1.0 eq), bis(pinacolato)diboron (5.1 g, 20 mmol, 2.0 eq) and AcOK (3.92 g, 40 mmol, 4.0 eq) were mixed in dioxane (100 mL) in a flask purged with nitrogen. The reaction was stirred at 80°C overnight. The resulted mixture was diluted with hexane (100 mL), filtrated through celite. After concentration, the crude product was purified using flash chromatography (Hexane/EA, 10:1) to afford **50** (white solid, 2.8 g, 80%). ^{1}H NMR (600 MHz, $CDCl_3$): δ (ppm) 7.72 (d, *J*=7.8Hz, 2H), 7.19 (d, *J*=7.8Hz, 2H), 4.52 (bs, 1H), 3.34-3.36 (m, 2H), 2.78 (t, *J*=7.2Hz, 2H), 1.40 (s, 9H), 1.32 (s, 12H). ^{13}C NMR (125 MHz, $CDCl_3$): δ (ppm) 155.82, 142.34, 135.05, 128.24, 83.71, 83.47, 41.61, 36.29, 28.37, 24.99, 24.83.

2-(4-(4,4,5,5-tetramethyl-1,3,2-dioxaborolan-2-yl)phenyl)ethan-1-amine (51)

Intermediate **50** (1.2 g, 3.5 mmol, 1.0 eq) was dissolved in DCM (20 mL), cooled in an ice bath. TFA (1.32 mL, 17.3 mmol, 5.0 eq) was added. The reaction was gradually warmed up to room temperature and was complete in about 3h. Solvent was removed and the crude product was purified using flash chromatography (DCM/MeOH, 10:1) to afford **51** (white solid, 0.78 g, 91%). ^{1}H NMR (600 MHz, $CDCl_3$): δ (ppm) 8.00 (bs, 2H), 7.74 (d, *J*=7.8Hz, 2H), 7.18 (d, *J*=8.4Hz, 2H), 3.13 (t, *J*=7.2Hz, 2H), 2.96 (t, *J*=7.2Hz, 2H), 1.31 (s, 12H). ^{13}C NMR (125 MHz, $CDCl_3$): δ (ppm) 139.20, 135.40, 128.01, 83.79, 40.87, 33.72, 24.80.

(4-(2-(8-oxo-8-(phenylamino)octanamido)ethyl)phenyl)boronic acid (5-33)

Carboxylic acid **47** (147 mg, 0.59 mmol, 1.0 eq), HBTU (269 mg, 0.71 mmol, 1.2 eq) and DIPEA (0.21 mL, 1.18 mmol, 2.0 eq) were dissolved in anhydrous THF (10 mL), followed by the addition of **51** (160 mg, 0.65 mmol, 1.1 eq) at 0 °C. The reaction was stirred at room temperature overnight. The resulted mixture was diluted with DCM, washed with water and dried over anhydrous Na_2SO_4. The crude coupling product was directly subjected to deprotection without further purification. The coupling product (82 mg, 1.0 eq) was stirred with NH_4OAc (26 mg, 0.34 mmol, 2.0 eq) and $NaIO_4$ (109 mg, 0.51 mmol, 3.0 eq) in acetone/water (1:1, 10 mL) at room temperature

overnight. The resulted mixture was diluted with DCM, washed with water and dried over anhydrous Na_2SO_4. The crude product was purified using flash chromatography (DCM: Hex: MeOH 4:4:0.5) to afford **5-33** (white solid, 50 mg, 75%). ^{1}H NMR (600 MHz, CD_3OD): δ (ppm) 7.94 (d, *J*=4.2Hz, 1H), 7.66 (d, *J*=7.2Hz, 1H), 7.52 (d, *J*=7.8Hz, 2H), 7.26 (t, *J*=7.8Hz, 1H), 7.19 (d, *J*=7.2Hz, 1H), 7.15 (d, *J*=7.8Hz, 1H), 7.05 (t, *J*=7.8Hz, 1H), 3.38 (t, *J*=6.0HZ, 2H), 2.77-2.78 (m, 2H), 2.33 (t, *J*=7.8Hz, 2H), 2.12 (t, *J*=2.12Hz, 2H), 1.64-1.69 (m, 2H), 1.55-1.57 (m, 2H), 1.33-1.36 (m, 2H), 1.29-1.31 (m, 2H). ^{13}C NMR (125 MHz, CD_3OD): δ (ppm) 176.16, 174.58, 139.84, 135.15, 134.84, 129.77, 129.18, 129.06, 126.11, 121.25, 41.73, 37.89, 37.04, 36.57, 29.95, 29.91, 26.86, 26.72. HRMS (ESI): calcd. for $[C_{22}H_{29}BN_2O_4\text{-}H]^-$, 394.2178; found, 394.2176.

3.4. Biological characterization

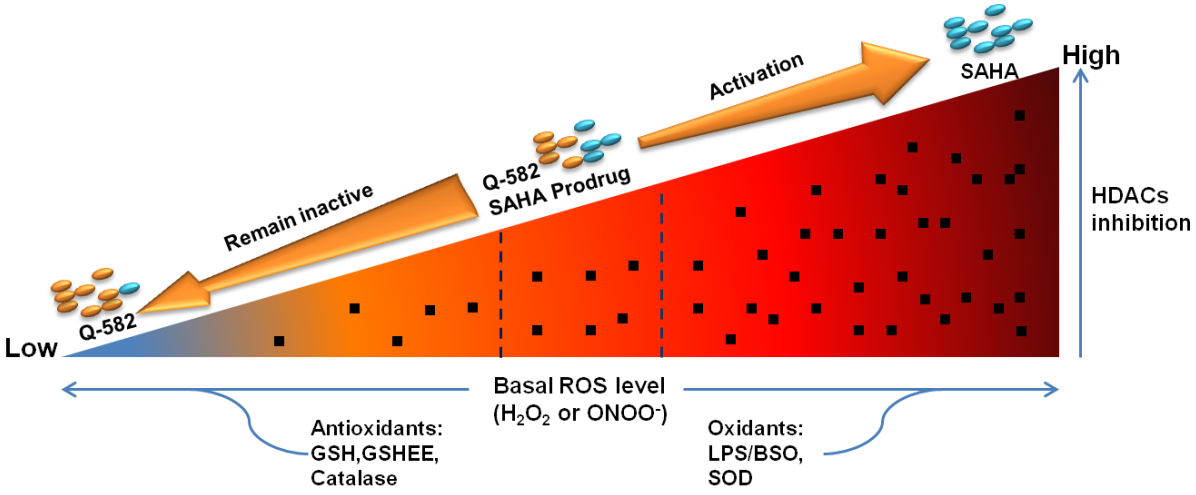

Figure 10. Schematic summary of mechanisms of prodrug activation.

3.4.1. Prodrug activation by H_2O_2 or PNT

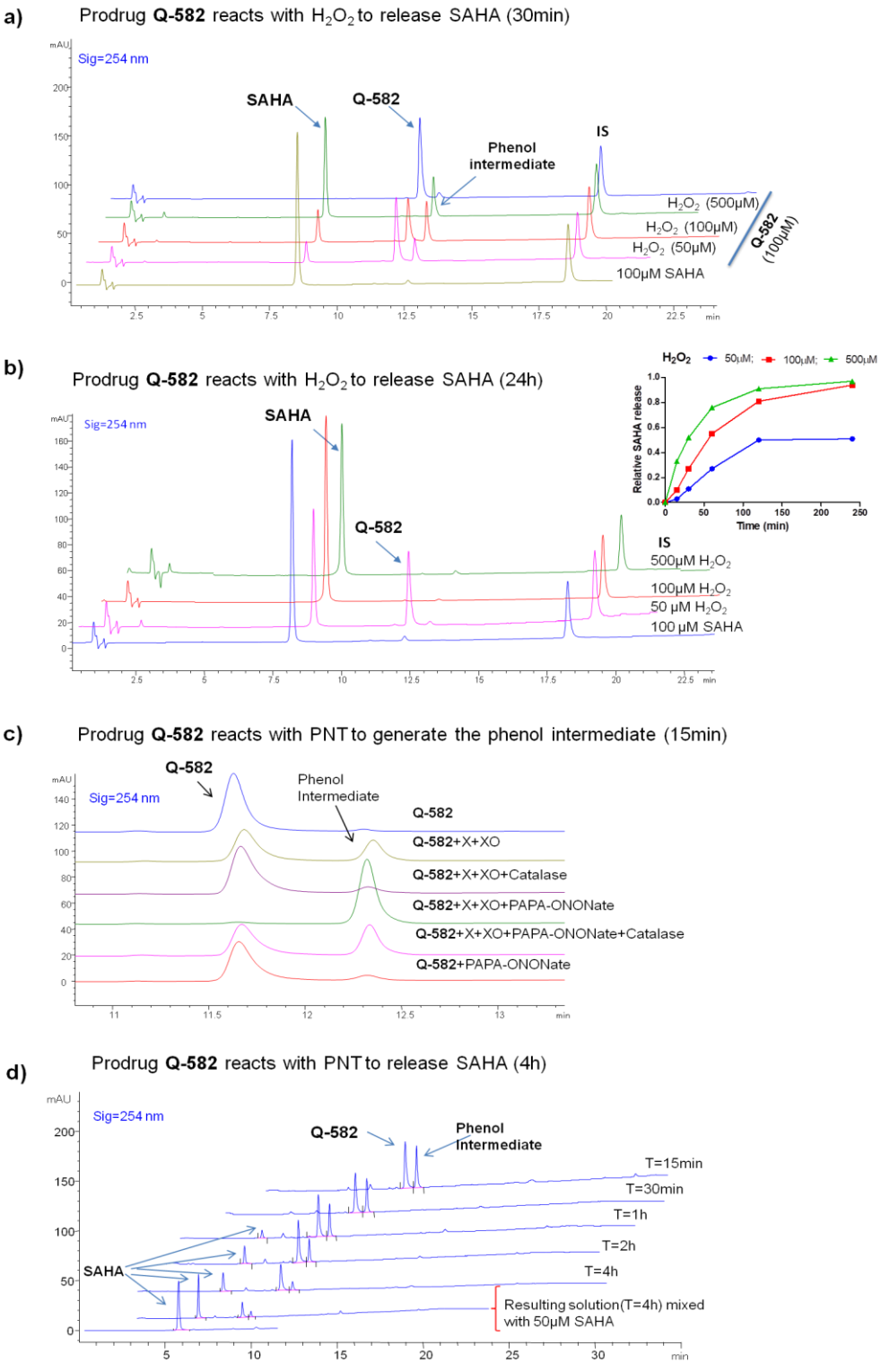

Figure 11. Prodrug **Q-582** activation with H_2O_2 or PNT and SAHA release in cell-free incubations. **a)** Prodrug **Q-582** was activated by H_2O_2. **Q-582** (100 μM) was incubated with H_2O_2 in PBS (pH 7.4) at 37°C for 30 min. Aliquots were analyzed by HPLC. **b) Q-582** (100 μM) time-dependently released SAHA in the presence of H_2O_2 in 4h in PBS (pH 7.4) at 37°C. **c)** Prodrug **Q-582** was activated by peroxynitrite. **Q-582** (100 μM) was incubated with indicated reagents in PBS (pH 7.4) at room temperature for 15 min. Aliquots of the resulted mixture was analyzed using HPLC. **d)** Prodrug **Q-582** was activated by peroxynitrite to release SAHA. **Q-582** (100 μM) was incubated with peroxynitrite produced by X/XO/catalase/PAPA-NONOate system in PBS (pH 7.4) at 37^{o}C. Co-injection of SAHA with 4 h sample was used to further confirm SAHA release under enzymatic incubation conditions. Benzophenone was used as internal standard (IS). X: xanthine; XO: xanthine oxidase; Cat.: catalase; PAPA/NO: PAPA-NONOate.

Following the synthesis (**Scheme 3**), by using SAHA prodrug **Q-582** as model compound, we first investigated if the designed prodrug can be activated by H_2O_2 or PNT in cell-free incubations. **Q-582** was incubated with H_2O_2 at various concentrations in PBS buffer (pH 7.4) at 37°C. As revealed by HPLC analysis (**Figure 11a**), **Q-582** reacted with H_2O_2 within 30 min to form two new peaks: the retention time of A (8.2 min) was identical to that of SAHA, and peak B (12.2 min) was assigned as the phenol intermediate since it eventually disappeared within 4 h, and the disappearance was accompanied by the increased peak area of SAHA. At a given time point (e.g., at 30 min, **Figure 11a**), the formation of phenol intermediate and SAHA were proportional to H_2O_2 concentration. **Q-582** (100 μM) was completely converted to SAHA by equivalent (100 μM) or excessive (500

μM) H_2O_2, whereas only half of the **Q-582** was consumed by 50 μM of H_2O_2 as determined by comparison of the peak area of SAHA with the standard sample (**Figure 11b**). These observations suggest that **Q-582** is rapidly oxidized by H_2O_2 in a stoichiometric manner to release SAHA through a phenol intermediate.

Q-582 was also activated by PNT. PNT was generated by a mixture of xanthine (X, 200 mM), xanthine oxidase (XO, 10 mU/mL) and NO donor PAPA-NONOate (100 μM) as described in the literature[174]. X and XO produce fluxes of superoxide anion which further reacts with NO to form PNT. Even at room temperature, **Q-582** was completely converted to a phenol intermediate by X/XO/PAPA-NONOate within 15 min (**Figure 11c**). In sharp contrast, PAPA-NONOate itself barely induced any change of **Q-582**, emphasizing the specific reaction between boronic acid and PNT. X/XO alone partially consumed **Q-582** to generate the phenol, and this conversion was abrogated by the addition of catalase (100 U/mL), indicating that **Q-582** was specifically oxidized by H_2O_2, a disproportionated product of $O_2^{\cdot-}$ yielded from the X/XO system (**Figure 11c**). The addition of catalase also reduced consumption of **Q-582** in the X/XO/PAPA-NONOate system, suggesting that both H_2O_2 and PNT were generated and were responsible for the oxidation of aryl boronic acid to form the

phenol intermediate in X/XO/PAPA-NONOate incubation. Since catalase removes H_2O_2, **Q-582** was mainly consumed by PNT in the X/XO/PAPA-NONOate/catalase system. Consistent with H_2O_2 incubations, the X/XO/PAPA-NONOate/catalase system converted **Q-582** to the phenol intermediate that gradually released SAHA in 4 h (**Figure 11d**). Taken together, we conclude that **Q-582** rapidly reacts with either H_2O_2 or PTN to form a phenol intermediate which subsequently turns into SAHA in PBS buffer.

3.4.2. Intracellular activation of prodrugs

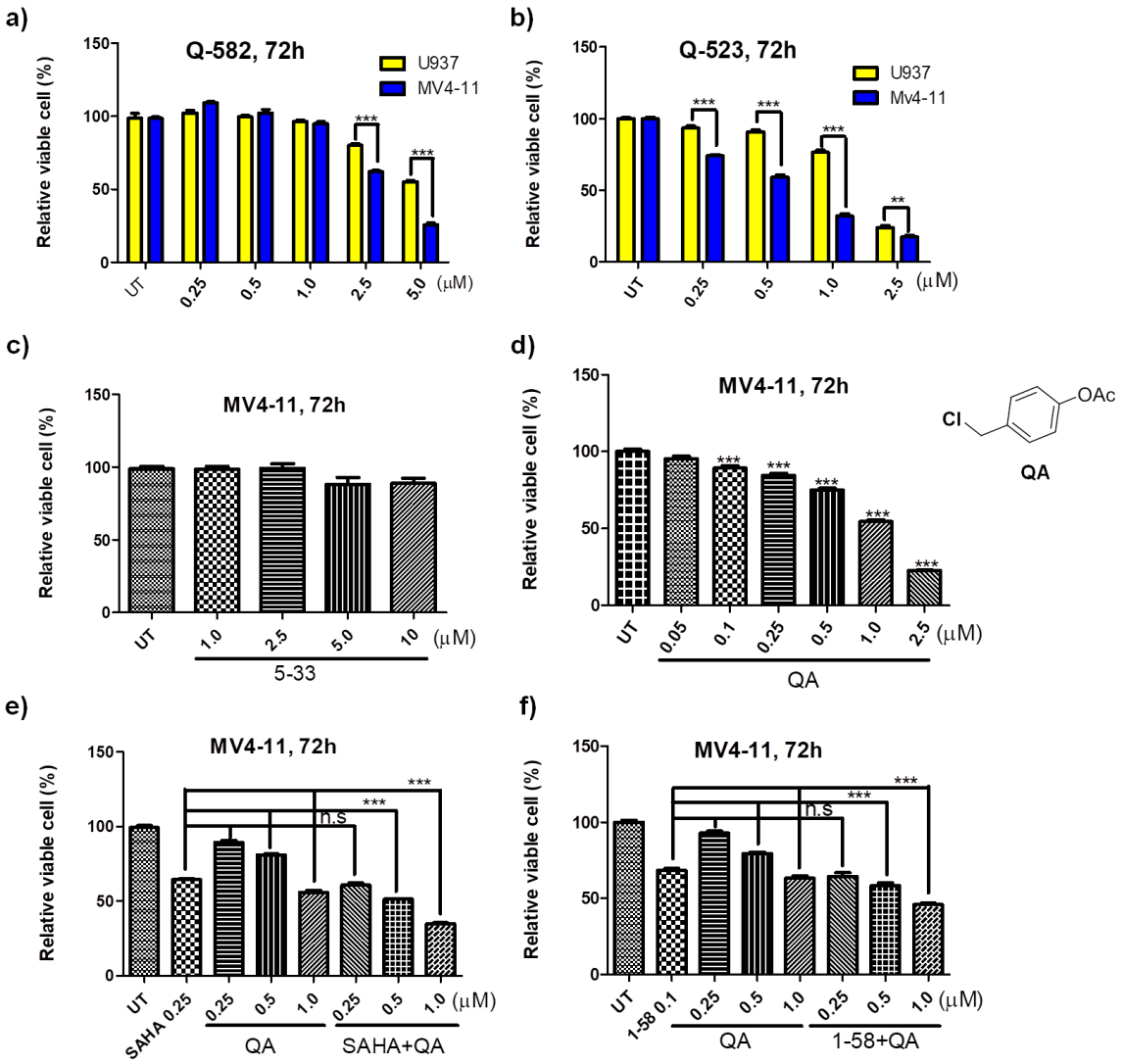

Figure 12. Prodrugs are activated and reduce AML cell viability. **a)** Prodrugs **Q-582** and **b) Q-523** reduced viability of both U937 and MV4-11 AML cells. **c) 5-33** didn't affect cell growth of MV4-11 cells. **d)** The chemical structures of QA and the potency of QA against MV4-11 cell viability. QA was tested in MV4-11 cells at indicated concentrations for 72h. **e)** SAHA or **f) 1-58** was used alone or combined with QA in MV4-11 cells. Cells were treated with each compound alone or drug combinations at indicated concentrations for 72h. Cell viability was analyzed by using MTT assay. Bars represent mean ± SEM. n.s indicates no statistical significance, ** indicates P < 0.01, *** indicates P<0.001. QA: 4-(Chloromethyl)phenyl acetate.

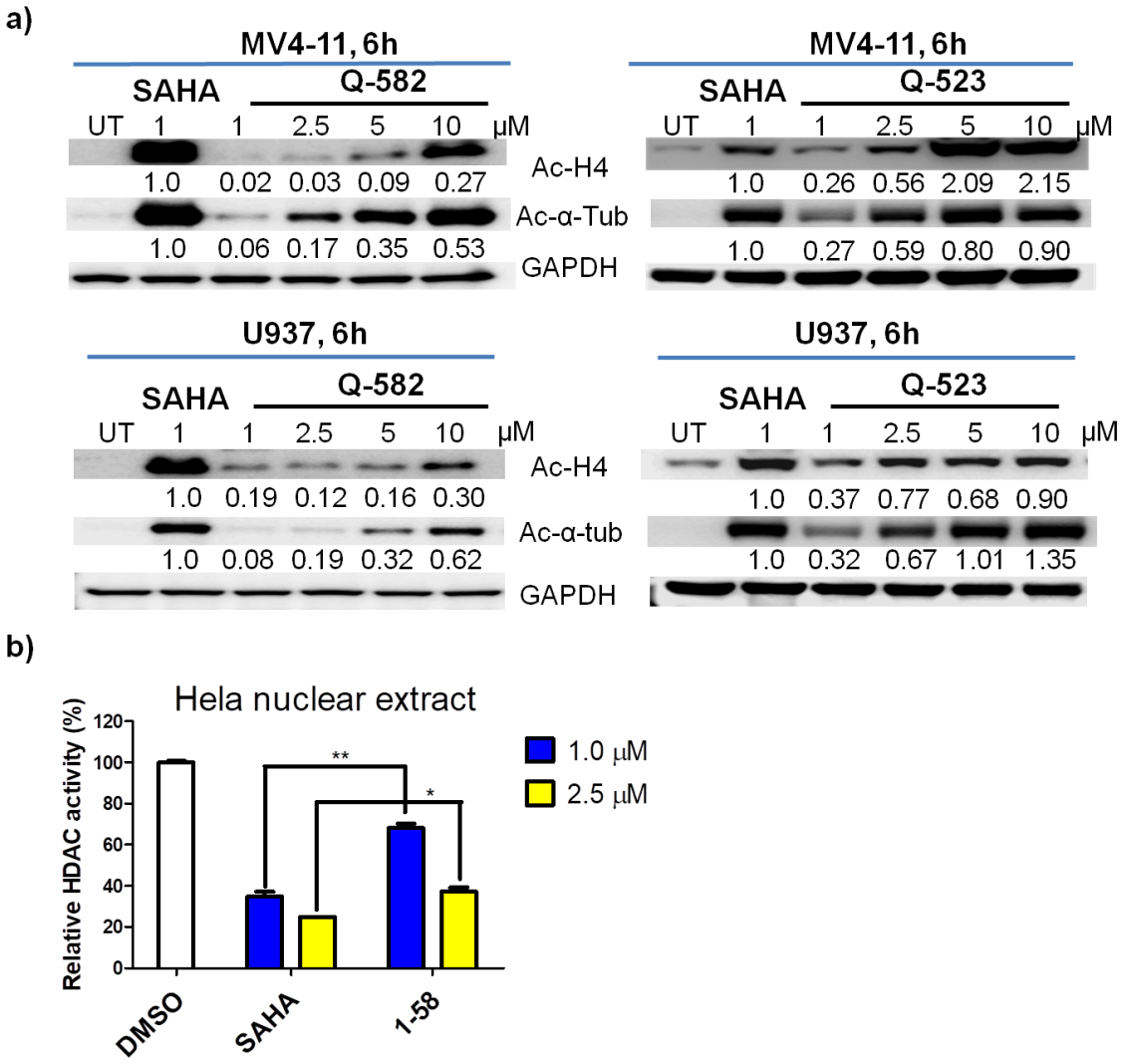

Figure 13. Prodrugs **Q-582** and **Q-523** concentration-dependently increase acetylation of histone H4 (Ac-H4) and α-tubulin (Tub) in MV4-11 cells determined by Western Blotting. **a)** MV4-11 cells were treated with **Q-582** or **Q-523** at indicated concentrations for 6 h. The fold changes for the Ac-H4 and Ac-α-Tub were determined by densitometry measurements, normalized to GAPDH, and then compared to SAHA treatment. One representative blot from three experiments is shown. **b) 1-58** is less potent than SAHA in inhibiting nuclear HDACs. Following the manufacturer's standard protocol, SAHA (1.0 or 2.5 μM) or **1-58** (1.0 or 2.5 μM) was incubated with HeLa nuclear extract and substrate for 15min. The reaction was stopped by adding *Fluor de Lys*® developer, and fluorescence was measured at Ex/Em=360 nm/ 460nm. The HDACs activity was

normalized by vehicle control. Bars represent mean ± SEM. * indicates P< 0.05, ** indicates P < 0.01.

We next tested prodrug activation and anti-proliferative activity of **Q-582** and **Q-523** in AML cell culture models. Both prodrugs concentration-dependently reduced the viability of U937 and MV4-11 cells, with IC_{50}s in sub μM to low μM range (**Figure 12a and 12b**). MV4-11 was more sensitive to prodrug treatments than U937 cells, consistent with their sensitivity to parental HDACis SAHA and **1-58**[30]. Boronic acid is a structural component of several approved (e.g., proteasome inhibitor Bortezomib) or clinically tested drugs[181]. To assess potential biological effects of aryl boronic acid in the designed prodrugs, we prepared **5-33** (**Scheme 2b**), a close structural analogue of **Q-582**. Because of the replacement of the oxygen of ZBG with a methylene group, **5-33** cannot release HDACi functionality. In contrast to **Q-582**, **5-33** didn't affect the viability of MV4-11 cells at concentrations up to 10μM (**Figure 12c**).

In addition, since QM is released upon prodrug activation, we also investigated the role of QM in overall anti-leukemic activities of **Q-582** or **Q-523**. QA (4-(Chloromethyl)phenyl acetate)[182] (**Figure 12d**) and QB (4-Chloromethylphenylboronic acid)[183,184] were selected because they were reported to be activated and converted to QM inside cells. QB, the same H_2O_2/PNT-sensitive promoiety as **Q-582** and **Q-523**, has negligible effect on cell

viability even if the concentration was increased up to 50 μM (data are not shown), while QA efficiently decreased cell viability with IC_{50} value (1.13 ± 0.11 μM) (**Figure 12d**). To further clarify, we combined QA with SAHA or **1-58** and tested each drug or drug combo in MV4-11 cells. The result (**Figure 12e** and **12f**) shows that SAHA/QA combo performed, when QA concentration is less than one or two equivalents of SAHA concentration, as nearly same effect as SAHA, suggesting the effect of **Q-582** on cell viability comes from activated SAHA instead of combinatory effect of SAHA and QM, which is also applicable for **Q-523**. Although combinations of QA (up to 500 nM) and SAHA didn't outperform SAHA alone when used in 1:1 ratio to mimic prodrug setting, QA enhanced **1-58**'s or SAHA's cytotoxicity when its concentration is increased up to 2-4 fold relative to SAHA's, or 5-10 fold relative to **1-58**'s concentration (**Figure 12e** and **12f**), suggesting QM may become a positive contributor to the overall cytotoxicity especially when the released HDACis are less cytotoxic than QM. In conclusion, **Q-582/Q-523**-induced growth inhibition is solely due to the released SAHA or **1-58**, respectively. Since acetylation of histones and α-tubulin is negatively regulated by nuclear HDACs or by cytosolic HDAC6, respectively, we measured these HDAC inhibition markers to further confirm intracellular activation of prodrugs. Both **Q-582** and **Q-523** concentration-dependently increased acetylation of histone H4

and α-tubulin within 6h in MV4-11 and U937 cells (**Figure 13a**). Compared to the same standard SAHA, densitometry analyses revealed that the **1-58** (a hybrid HDACi) prodrug **Q-523** caused more prominent global acetylation than SAHA prodrug **Q-582** in MV4-11 and U937 cells (**Figure 13a**). To understand this observation, we measured intrinsic HDAC inhibition activity of parental HDACis using enzymatic assay against nuclear HDACs extracted from Hela cells. Interestingly, 1 μM **1-58** and SAHA treatment resulted in 32% and 65% inhibition, respectively (**Figure 13b**), demonstrating that **1-58** is weaker HDACi than SAHA at nuclear HDACi inhibition. Therefore, compared to **Q-582**, the increased H4 acetylation induced by **Q-523** (**Figure 13a**) was likely attributed to the higher levels of intracellular free HDACi (but not higher intrinsic HDACi activity), potentially caused by: 1) increased intracellular prodrug concentration since **Q-523** is more lipophilic than **Q-582** (ClogP 4.73 vs. 3.26); and 2) the presence of ROS-inducing piperlongumine functionality[3] enhances oxidative stress in AML cells, which facilitates prodrug activation. Besides enhanced acetylation of histone H4 and α-tubulin, **Q-523** was also more potent than **Q-582** in inhibiting cell proliferation, reflected by the IC_{50}s of the two prodrugs: 0.70 μM vs. 3.07 μM in MV4-11 cells and 1.61 μM vs. 6.13 μM in U937 cells. At least two factors, the higher intracellular free HDACi concentration and the stronger anti-proliferative

activity of **1-58** than SAHA[30], may have contributed to the greater anti-leukemic activity of **Q-523** than **Q-582**.

3.4.3. Intracellular activation of prodrug is under the control of redox status

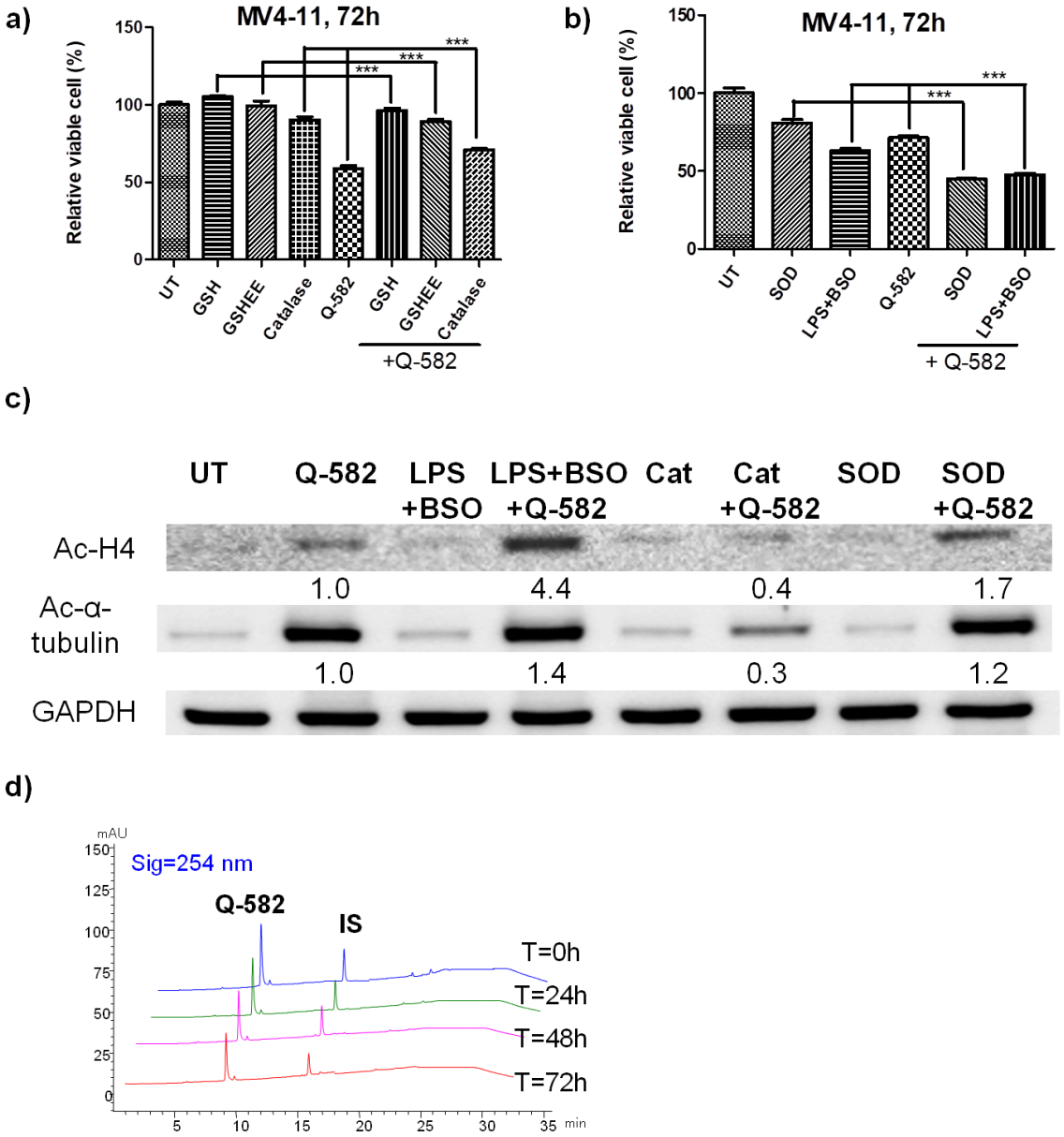

Figure 14. Intracellular activation of prodrug **Q-582** is influenced by ROS/RNS inducers and scavengers. **a)** and **b)** MV4-11 cells were pre-treated with GSH (5 mM), GSHEE (5 mM), catalase (0.125 mg/mL), SOD (0.05 mg/mL) or the

combination of LPS (10 ug/mL) and BSO (2.5 μM), respectively, for 2h, followed by **Q-582** (2.5 μM) treatment for 72h. Viable cells were measured using MTT assay. Bars represent mean ± SEM. *** indicates $P < 0.001$. **c)** MV4-11 cells were pretreated with catalase (Cat, 0.5 mg/mL), SOD (0.1 mg/mL), LPS (10 ug/mL) and BSO (10 μM) for 2h, followed by **Q-582** (2.5 μM) treatment for 24h. Acetylation of histone H4 and α-tubulin were analyzed using Western Blotting. The fold changes for the Ac-H4 and Ac-α-Tub were obtained by using densitometry measurements, normalized to GAPDH, and then compared to **Q-582** treatment. One representative blot from three experiments is shown. **d) Q-582** (100 μM) was incubated with GSH (5 mM) in PBS (pH 7.4) at 37 ℃ for 24 h, 48 h and 72 h. The reaction was monitored using HPLC. Benzophenone served as the internal standard (IS).

We then investigated if prodrug activation is affected by cellular redox status. Pretreatment (2 h) with an antioxidant, such as GSH (5 mM), GSH ethyl ester (GSHEE, 5 mM) or catalase (0.125 mg/mL), significantly reduced inhibitory effect of **Q-582** treatment on MV4-11 cell proliferation (**Figure 14a**). **Q-582** was stable in GSH co-incubation up to 72h (**Figure 14b)**, suggesting that the rescue of MV4-11 cells from **Q-582** treatment by GSH or GSHEE was due to scavenging intracellular ROS/RNS instead of potential reaction between nucleophilic GSH/GSHEE and the electrophilic boron center of **Q-582**. Catalase exerted the rescue function by reducing intracellular H_2O_2 concentration. On the contrary to the antioxidants, H_2O_2 and/or PNT inducers, such as superoxide dismutase (SOD) and a combination of lipopolysaccharide (LPS) and buthionine-(S,R)-sulfoximine (BSO), notably enhanced inhibitory effect of **Q-582** treatment on the proliferation of MV4-11 cells (**Figure 14b**). SOD catalyses the conversion of $O_2^{\cdot-}$ to H_2O_2, one

of the major sources for prodrug activation. LPS induces iNOS expression and BSO depletes cellular GSH, their combination could boost ROS (e.g., H_2O_2) and RNS (e.g., PNT) production and generate oxidative environment favoring intracellular prodrug activation. The cell proliferation results (**Figure 14a**) are well correlated with the acetylation levels of histone H4 and α-tubulin in MV4-11 cells (**Figure 14b**): the addition of SOD, the combination of LPS and BSO increased whereas adding catalase decreased acetylation of histone H4 and α-tubulin. Taken together, our results demonstrate that prodrug activation is under the control of cellular redox status: the exogenous ROS/RNS inducers enhance whereas antioxidants weaken anti-leukemic activity by influencing prodrug activation.

3.4.4. Prodrug enhances the potency of cytarabine in MV4-11 cells

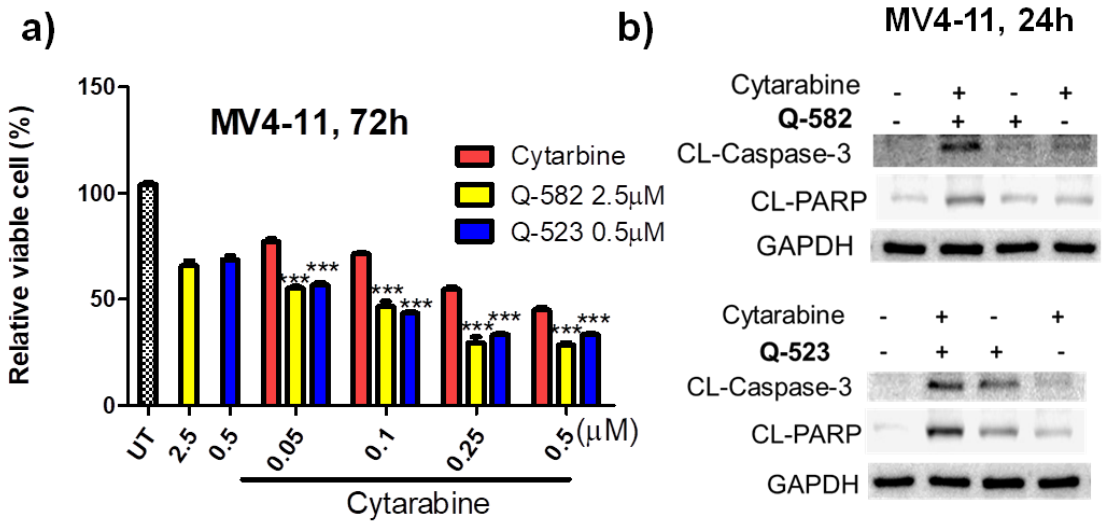

Figure 15. Prodrugs **Q-582** (2.5 μM) and **Q-523** (0.5 μM) enhance the effect of

cytarabine on the viability of MV4-11 cells. **a)** MV4-11 cells were treated with drugs at indicated concentrations for 72 h, cell viability was measured using MTT assay. Bars represent mean ± SEM. *** indicates $P < 0.001$. **b)** MV4-11 cells were treated with prodrugs and/or cytarabine (0.5 µM) for 24h, expression of cleaved caspase-3 and PARP-1 was analyzed by Western Blotting. One representative blot from three experiments is shown.

Because of pleiotropic anti-cancer mechanisms, HDACis are a versatile component for combinatorial AML treatments to improve overall potency and response rate over individual anti-AML agents[185]. For instance, SAHA was combined with chemotherapy drug idarubicin and cytarabine in an AML clinical trial[186]. To explore the possibility of using HDACi prodrugs in combination therapies in AML, we investigated the anti-leukemic activities of prodrug **Q-582** or **Q-523** in combination with cytarabine in MV4-11 cells. Both **Q-582** (2.5 µM) and **Q-523** (0.5 µM) significantly enhanced the potency of cytarabine (0.05-0.5 µM) (**Figure 15a**), measured using MTT assay. Consistently, the inhibitory effects on proliferation was accompanied by substantially increased PARP-1 and caspase-3 cleavage induced by the combination compared to individual drug treatment (**Figure 15b**).

3.4.5. Selectivity vs toxicity

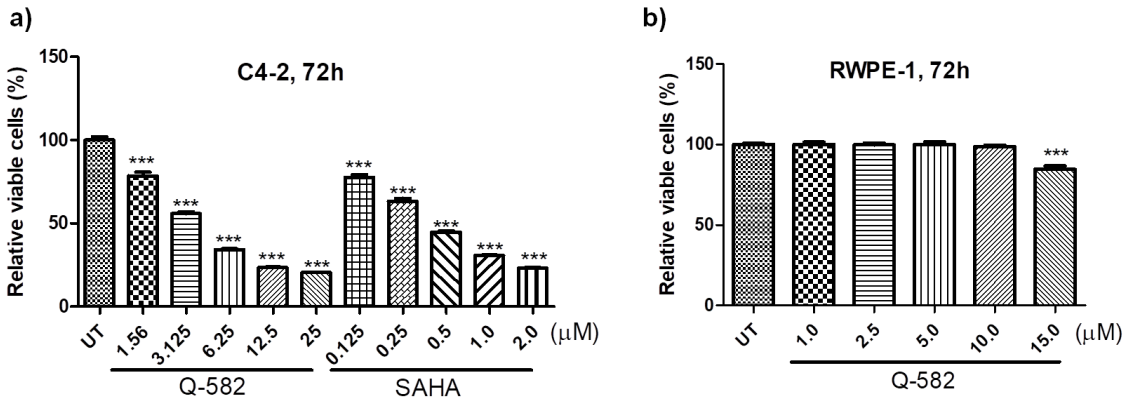

Figure 16. Q-582 shows selectivity over PCa cancer cells. **a) Q-582** significantly reduced the viability of PCa C4-2 cells at low micromolar concentrations. **b)** In sharp contrast, **Q-582** only slightly affected the cell viability of normal prostatic epithelial RWPE-1 cells until its concentration was increased up to 15.0 μM. PCa C4-2 and RWPE-1 cells were treated with indicated drugs for 72 h. Cell viability was analyzed by using MTT assay. Each experiment was independently repeated three times. Bars represent mean ± SEM. *** indicates P<0.001.

Prodrug selectivity was assessed and exemplified by using the model compound **Q-582**. **Q-582** didn't affect the viability of human peripheral blood mononuclear cells (PBMNCs) when treated with same drug concentrations as used in AML MV4-11 cells (This experiment was done my our collaborator Dr. Ge's group, data are not shown). In our study, we demonstrated selectivity by using PCa C4-2 and normal prostate RWPE-1 cells. As shown in **Figure 16a**, **Q-582** reduced C4-2 cell viability with an IC_{50} value at 4.15±0.393 μM. As a prodrug, it was less potent than SAHA (IC_{50} 0.44±0.032 μM). In normal prostate cells, **Q-582** failed to influence cell viability at doses lower than 10.0 μM, and

when the dose was increased to 15.0 μM, **Q-582** reduced cell viability by merely 15% (**Figure 16b**). Therefore, we conclude that the designed prodrug approach (exemplified using **Q-582)** harbors selectivity to cancer cells (AML or PCa cells) over normal cells.

3.5. Experimental procedures

3.5.1. Cell lines, antibodies and reagents

The acute myeloid leukemia (AML) cell lines MV4-11 and U937 were obtained from the American Type Culture Collection. MV4-11 and U937 cells were cultured in RPMI 1640 media supplemented with 10% (v/v) fetal bovine serum (Sigma, F8067), L-glutamine (2 mM), penicillin (100 U/mL) and streptomycin (100 μg/mL). Cultures were maintained in a humidified atmosphere containing 5% CO_2/95% air at 37°C. Antibodies used in this study are as follows. Anti-acetyl-histone 4 (Cell Signaling Technology, cat# 2591), anti-acetyl-α-tubulin (Cell Signaling Technology, Cat# 5335), anti-GAPDH (Santa Cruz, Cat# Sc-25778), and anti-rabbit IgG, HRP-linked antibody (Cell Signaling Technology, cat# 7040). Lipopolysaccharides (LPS, L2654), superoxide dismutase (SOD, S5395), glutathione ethyl ester (GSHEE, G1404), catalase (C1345), 4-Chloromethylphenyl acetate (432881), Xanthine (X4002) and Xanthine Oxidase (X1875) were

purchased from Sigma (St. Louis, MO, USA). 4-Chloromethylphenylboronic acid (BB-2333) was purchased from Combi-Blocks (CA, USA). Glutathione (GSH, BP25211) and hydrogen peroxide were purchased from Fisher (NJ, USA). Cytarabine (16069), Buthionine Sulfoximine (BSO, 14484) and PAPA-NONOate (82140) were obtained from Cayman Chemical (Ann Arbor, Michigan, USA). Piperlongumine (P-004) was from INDOFINE Chemical Company (NJ, USA). Vorinostat (SAHA, RV005) was purchased from TSZ Chem. LPS, catalase, GSH, GSHEE, BSO and SOD were dissolved in PBS (pH 7.4) or in phenol-red free RPMI 1640 medium for cell-free incubations or for cell treatment, respectively. All aqueous stock solutions were freshly made and used within one day. Stock solutions of HDACis, prodrugs and other reagents were prepared in DMSO and stored at -20 °C. HDAC fluorimetric assay/drug discovery Kit (BML-AK500) was purchased from Enzo Life Sciences and was used by following the manufacturer's protocols and instructions. MTT ((3-(4,5-dimethyl-2- thiazolyl)-2,5-diphenyltetrazolium bromide, A0357552) was purchased from ACROS (NJ, USA.).

3.5.2. MTT assay

U937 or MV4-11 cells were seeded into 96-well plate (6000-8000 cells/well) and were treated with the indicated compounds, alone or in combination, for 72 h.

The final concentration of DMSO was less than 0.1%. At the end of treatment, the MTT ((3-(4,5-dimethyl-2- thiazolyl)-2,5-diphenyltetrazolium bromide, 0.5 mg/mL) was added to each well, incubated at 37°C for 3 h. Following the incubation, supernatant was removed, DMSO (100 µL) was added and the mixture was incubated at 37°C for 30 min. Absorbance was read at 570 nM using a microplate reader. The wells contain only culture medium and MTT reagent were used as blanks for the plate reader. The values of "relative viable cells" were calculated as $(OD_{treatment}-OD_{background}) /(OD_{control}-OD_{background})$.

3.5.3. Western blotting assay

After drug treatment, U937 or MV4-11 cells were harvested, washed with PBS and lysed in RIPA buffer (150mM NaCl, 50mM Tris–HCl, pH 7.4, 5mM EDTA, 1% NP40, 0.1% SDS) containing 1% PMSF (phenylmethylsulphonyl fluoride, a serine protease inhibitor) for 30min over ice. The debris was removed by centrifuging at 16,000g for 15min at 4°C. The protein concentration of resulted supernatants was determined using Pierce BCA Protein Assay Kit (Thermo Fisher, Cat# 23225). 10-20 µg protein in loading buffer was resolved by electrophoresis on SDS-PAGE and was electrophoretically transferred onto PVDF (polyvinylidenedifluoride) membranes. The 5% nonfat milk was utilized for blockade of non-specific binding. Blots were incubated with primary antibody

(anti-acetyl-histone 4, anti-acetyl-α-tubulin or anti-GAPDH) overnight at 4°C, followed by the incubation of secondary antibody (anti-rabbit IgG) for 1h at room temperature. Immunoreactive bands were visualized with ECL (enhanced chemiluminescence detection kit) on ImageQuant™ LAS 4000 Imager (GE) as described by the manufacturer. Western blots were repeated at least three times, and one representative blot is shown. Density of protein bonds were calculated and analysed by using imageJ software downloaded from National Institute of Health website.

3.5.4. HPLC analysis

Enzymatic incubations were quenched by adding equal volume of MeOH/ACN mixture (v/v, 1:1), followed by centrifugation at 6,000 rpm. The supernatant (10µL) was injected into HPLC for further analysis. HPLC analysis was conducted using a Phenomenex Lunna 3µm C18, 3.5 µm, 150 mm × 3.0 mm column on Agilent 1100 series HPLC instrument. Mobile phase were: solvent A, water containing 0.1% formic acid (FA) and 10% (v/v) CH_3OH; solvent B, 0.1% FA in CH_3CN; flow rate 0.5 mL/min; gradient, 10%B-95%B in 30min.

3.5.5. HDAC enzymatic assay

In vitro HDACs inhibition was measured by using the HDAC fluorimetric assay/drug discovery Kit (Enzo Life Sciences, BML-AK500). The experiment process follows manufacturer's procedures. Briefly, reagents (assay buffer, SAHA or **1-58**, HeLa extract) were added orderly, and then the *Fluor de Lys*® substrate was added and mixed thoroughly to initiate the reaction according to Table 1 in the protocol. After 15min incubation at 37^{o}C, the reaction was stopped by adding the *Fluor de Lys*® developer (50 µl). Fluorescence was read at Ex/Em=360 nm/460 nm.

3.5.6. Statistical analysis

Statistical analyses were performed using GraphPad Prism 5.0. Error bars represent mean ± standard error of the mean (SEM). The differences between sets of data were compared using student's t-test or one-way ANOVA analysis with significant level α=0.05. Asterisks indicate *$P < 0.05$, **$P < 0.01$, ***$P < 0.001$.

3.5.7. Chemistry methods

General Methods for Chemistry. ^{1}H and ^{13}C NMR spectra were obtained using Varian Mercury 600MHz. Chemical shifts are reported as δ values in parts per million (ppm) relative to tetramethylsilane (TMS) for all recorded NMR spectra. All reagents and solvents were obtained from Acros, Fisher or Aldrich without

further purification. Flash column chromatography was performed over 200−300 mesh silica gel. High resolution mass spectral data were collected using a LCT Premier XE KD128 instrument. All compounds submitted for biological testing were found to be >95% pure by analytical HPLC. Purity check was performed via HPLC analysis as described in the chapter 2.

CHAPTER 4 DESIGN, SYNTHESIS, AND BIOLOGICAL CHARACTERIZATION OF DIMERIC PL DERIVATIVES AS ANTI-PCa AGENTS

4.1. Rationale

PL's attractive anti-cancer activities heavily rely on PL structural uniqueness. PL consists of two α,β-unsaturated carbonyl moieties known as "Michael-acceptors", thereby harboring electrophilicity. The functionalities of C2-C3 and C7-C8 olefins are associated with GSH conjugation and protein glutathionylation, and are determinants of the cellular effects of PL (**Figure 3**). Elevated ROS is the critical player mediating anti-cancer activates of PL, which is attributed to C2-C3 olefin functionality[21] as introducing chlorine at C2 notably enhanced ROS production and cytotoxicty[25,26]. C7-C8 olefin is responsible for the covalent modification of GSH-binding proteins, thereby enhancing PL's cytotoxicity[21]. Because of its anti-cancer activities and the intrinsic relationship between electrophilicity and oxidative stress[25], PL has been explored as a versatile anti-cancer agent applying in the electrophilic prooxidant anti-cancer strategy. Additionally, multimeric electrophiles, including dimers of melampomagnolide B [187], dimeric catechol[188], and PL dimers[189], are more cytotoxic than the corresponding monomers in cancer cells. Building on the diverse anti-cancer activities of PL and the higher anti-cancer potency of dimerized or oligomerized electrophiles, we designed and synthesized a class of

dimeric PL derivatives (DiPLs) and hypothesized that the extra electrophilic moiety of DiPLs may facilitate the recognition of oligomeric cellular targets through multivalent interactions[190] or the crosslinking of cellular nucleophiles, which cannot be achieved by increasing concentration of monomeric PL. We envisioned that anti-cancer properties of PL could be significantly enhanced through the design of dimeric derivatives.

4.2. Design and synthesis of DiPLs

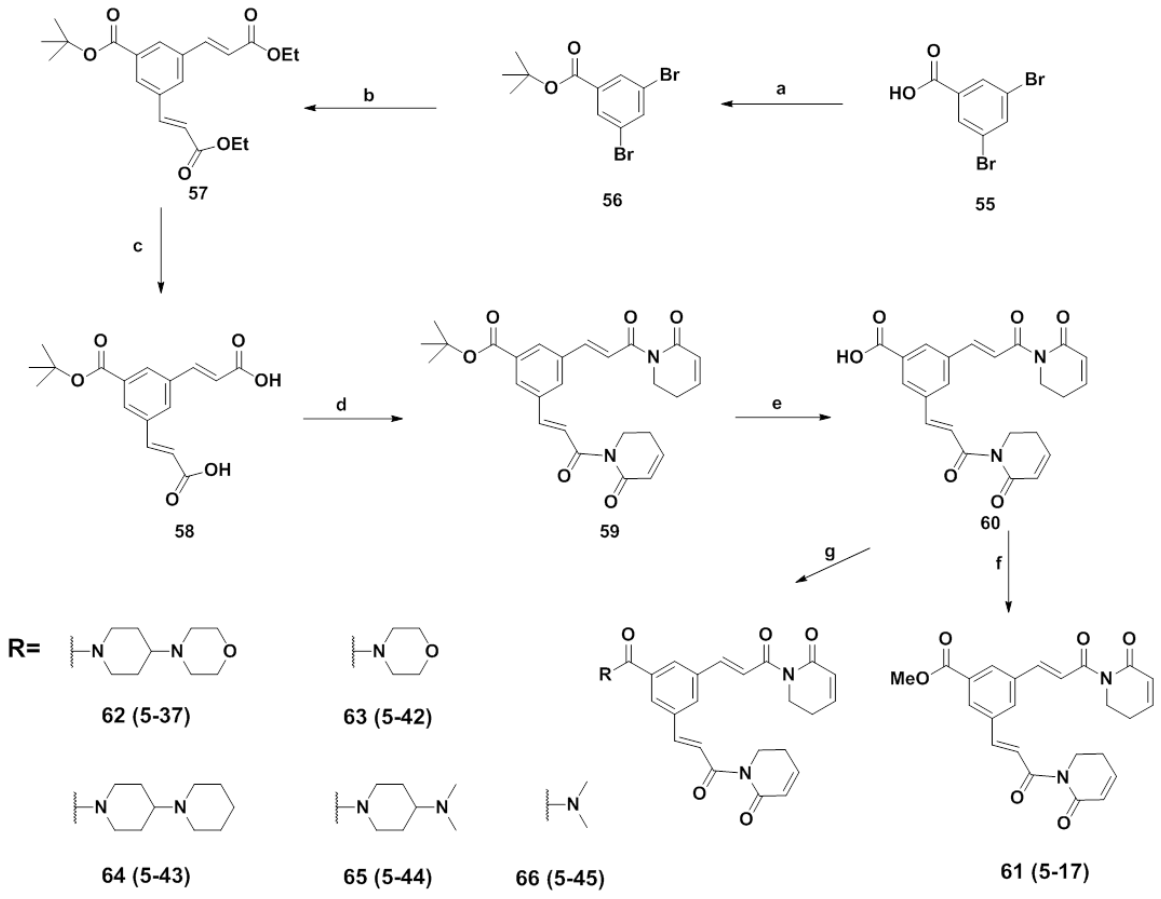

Scheme 4. Synthesis of dimeric PL derivatives (DiPLs). Reagents and conditions:

(a) $(BOC)_2O$, DMAP, *tert*-butanol/THF, 70°C, overnight, 81%; (b) $Pd(OAc)_2$, $P(O\text{-tolyl})_3$, DIPEA, 80°C, anhydrous DMF, overnight, 95%; (c) LiOH, THF/H_2O (v:v 1:1), 91%; (d) (1) pivaloyl chloride, TEA, anhydrous THF, -20°C; (2) *n*-BuLi, anhydrous THF, -78°C, 21%; (e) TFA, DCM, 90%; (f) $TMSCHN_2$, MeOH/ether (v:v 1:1), 26%; (g) HBTU, DIPEA, DMF.

To dimerize PL and test the proof of concept, our group firstly synthesized a PL dimer (**5-17**) by multiplying PL's functional groups (Michael acceptors) on the benzene ring. This structural modification is supported and inspired by three indications: 1) PL-Ben without trimethoxyl groups present shows comparable potency at cancer cell growth inhibition and ROS elevation[25], suggesting the minor involvement of the trimethoxyl groups in PL-related cellular effects. 2) PL-HDACi hybrid **1-58** performs synergistic-to-additive anti-leukemic activity[30], emphasizing feasibility of structural modification at PL benzene ring. 3) The anti-cancer activities of PL may be boosted, as accompanied by the increased number of Michael acceptors[189,191]. PL dimer (e.g., **5-17**) could significantly potentiate interactions with thiol-containing proteins or crosslink cellular nucleophiles, thereby effectively killing cancer cells. Moreover, to optimize physicochemical properties of the PL dimer **5-17**, we increased its hydrophilicity by the coupling of carboxylate of **5-17** with nitrogen-containing heterocycles or amines. Five such dimeric PL derivatives (DiPLs) were prepared. In our study, DiPLs were tested in the CRPC VCaP cells because this cell line is not only

resistant to enzalutamide treatment[192], but also overexpresses AR and AR-Vs, both are key targets for the treatment of CRPC. The positive outcomes from our investigation may support the feasibility of PL-based electrophilic prooxidants in PCa treatment. In addition, given the favorable cytotoxic profile of the **5-17** warhead revealed in this study, the DiPL structure can be further modified, coupled or merged with other chemical functional groups or nanomaterials to further improve potency, tumor localization, and cancer cell selectivity.

The synthetic route of DiPLs (**5-17**, **5-37**, **5-42**, **5-43**, **5-44**, and **5-45**) started with a commercially available compound **55**, which was converted to a acid-labile *t*-butyl ester **56** by using $(BOC)_2O$ and the catalytic amount of DMAP. Without disturbing the *t*-butyl ester group, compound **57** was obtained by reacting compound **56** with two equivalents of ethyl acrylate through Heck reaction[193]. Following basic hydrolysis of ethyl ester groups, compound **58** with two carboxylic acid groups was obtained and was used for the coupling with δ-valerolactam. To prepare compound **59**, we used a strong base, *n*-BuLi, to de-protonate δ-valerolactam, and the pivaloyl chloride to activate the carboxylic acid groups of compound **58**[30]. Next, t-butyl ester group of compound **59** was removed by using TFA and the obtained carboxylic acid was esterified with TMS-diazomethane to afford the methyl ester **60** (**5-17**). In order to explore the SAR and optimize

drug-like properties of the lead compound **5-17**, we also synthesized **62** (**5-37**), **63** (**5-42**), **64** (**5-43**), **65** (**5-44**) and **66** (**5-45**) by coupling **59** with amines 4-morpholinopiperdine, morpholine, 4-piperidinopiperidine, N,N-dimethylpiperidin-4-amine, and dimethylamine, respectively. Synthetic intermediates and final products were characterized by using ^{1}H, ^{13}C NMR and mass spectrometry. Purity of the final products was checked and confirmed by using HPLC analysis.

4.3. Chemistry

Tert-butyl 3,5-dibromobenzoate (56)

The Boc anhydride (2.22 g, 10.2 mmol, 1.5 eq) and compound **55** (1.90 g, 6.80 mmol, commercially available) were dissolved in a mixture of *tert*-butyl alcohol (7 mL) and THF (2 mL). The reaction was stirred for 10 min at room temperature, followed by the addition of DMAP (414.8 mg, 3.4 mmol, 0.5 eq). The reaction was heated up to 70^{o}C overnight. Upon completion, the solvent was evaporated under reduced pressure and the residue was washed with water, extracted with DCM and dried over anhydrous sodium sulfate. The crude product was purified by using column chromatography to afford pure product (eluent hexane; white solid, 1.84 g, yield 81%). ^{1}H NMR (400 MHz, $CDCl_3$): δ (ppm) 8.01 (d, *J*=2.0Hz, 2H), 7.78 (t, *J*=2.0Hz, 1H), 1.58 (s, 9H). ^{13}C NMR (100 MHz, $CDCl_3$):

δ (ppm) 162.97, 137.65, 135.18, 131.191, 122.80, 82.43, 28.06.

Diethyl 3,3'-(5-(tert-butoxycarbonyl)-1,3-phenylene)(2E,2'E)-diacrylate (57)

The compound **56** (2.27 g, 6.77 mmol, 1.0 eq) was dissolved in anhydrous DMF (6 mL) in a flask filled with argon, followed by the addition of ethyl acrylate (1.8 mL, 16.93 mmol, 2.5 eq), $Pd(OAc)_2$ (152.6 mg, 0.68 mmol, 0.1 eq), $P(O\text{-}tolyl)_3$ (410.9 mg, 1.35 mmol, 0.2 eq) and DIPEA (6 mL). The reaction mixture was stirred at 80 ^oC for overnight. After water wash and DCM extraction, the crude product was purified by using silica gel column chromatography (EA/Hexane 1:20) to give the product (slightly yellow solid, 2.4 g, yield 95%). ^1H NMR (400 MHz, $CDCl_3$): δ (ppm) 8.11 (s, 2H), 7.75 (s, 1H), 7.67 (d, *J*=16.0Hz, 2H), 6.50 (d, *J*=16.6Hz, 2H), 4.25(q, *J*=7.2Hz, 4H), 1.60 (s, 9H), 1.33 (t, *J*=14.4Hz, 6H). ^{13}C NMR (100 MHz, $CDCl_3$): δ (ppm) 166.44, 164.47, 142.75, 135.34, 133.47, 130.81, 129.92, 120.22, 81.98, 60.73, 28.13, 14.27.

(2E,2'E)-3,3'-(5-(tert-butoxycarbonyl)-1,3-phenylene)diacrylic acid (58)

Compound **57** (494.2 mg, 1.32 mmol, 1.0 eq) was dissolved in THF/water (10 mL, v:v 1:1). To the stirred solution, the LiOH (95.03 mg, 3.96 mmol, 3.0 eq) water solution was added at room temperature. The reaction underwent for overnight. When reaction was completed, as indicated by TLC plate, 10% citric acid solution was used to acidify the resulting reaction mixture and

adjust pH value to 3-4. DCM was added to extract the potential product, followed by three times wash with brine and dry over Na_2SO_4 for 1 hour. Evaporation of DCM and purification of flush column chromatography (eluent DCM:MeOH 10:1) afford the product. (white solid, 382.0 mg, yield 91%). ^{1}H NMR (400 MHz, C_3D_6O): δ (ppm) 8.31 (s, 1H), 8.22 (d, *J*=1.2Hz, 2H), 7.77 (d, *J*=16.0Hz, 2H), 6.75 (d, *J*=16.4Hz, 2H), 1.63 (s, 9H). ^{13}C NMR (100 MHz, C_3D_6O): δ (ppm) 166.60, 164.21, 142.91, 135.76, 133.61, 130.65, 130.11, 120.52, 81.35, 27.35.

Tert-butyl 3,5-bis((E)-3-oxo-3-(6-oxo-3,6-dihydropyridin-1(2H)-yl)prop-1-en-1-yl)benzoate (59)

Step 1: To a solution of compound **58** (267.1 mg, 0.84 mmol, 1.0 eq) in anhydrous THF (5 mL) were slowly added pivaloyl chloride (0.12 mL, 1.85 mmol, 2.2 eq) and TEA (0.21 mL, 1.56 mmol, 2.5 eq) at -20 ^{o}C. After 1h, the resulted reaction mixture was ready to use for next step without purification. Step 2: The unsaturated valerolactam (256.3 mg, 2.64 mmol, 3.1 eq) was dissolved in anhydrous THF (5 mL). Dry ice-ethanol bath was prepared to cool temperature down to -78 ^{o}C. The *n*-BuLi (2.5 M in hexane, 1.32 mL, 3.3 mmol, 3.9 eq) was added to the lactam THF solution, stirring for 1h. To this stirred solution, the mixture prepared in step 1 was added dropwise by using a syringe at -78 ^{o}C. After 4h, saturated NH_4Cl was added to quench the reaction and to neutralize

excessive *n*-BuLi. THF was removed and the residue was extracted with DCM. The combined organic solution was dried over anhydrous sodium sulfate. The concentrated crude product was purified by using silica gel chromatography (eluent EA:Hexane 2:1) to afford product (yellow solid, 84.0 mg, yield 21%). ^{1}H NMR (400 MHz, $CDCl_3$): δ (ppm) 8.11 (s, 2H), 7.86 (s, 1H), 7.71 (d, *J*=19.2Hz, 2H), 7.50 (d, *J*=27.6Hz, 2H), 6.91-6.70 (m, 2H), 6.03 (d, *J*=9.6Hz, 2H), 4.02 (t, *J*=6.8Hz, 4H), 2.46-2.48 (m, 4H), 1.20 (s, 9H). ^{13}C NMR (100 MHz, $CDCl_3$): δ (ppm) 168.61, 165.67, 164.68, 145.62, 141.55, 135.91, 133.29, 130.90, 130.23, 125.68, 123.66, 81.75, 41.68, 27.57, 24.76.

3,5-bis((E)-3-oxo-3-(6-oxo-3,6-dihydropyridin-1(2H)-yl)prop-1-en-1-yl)benzoic acid (60)

To a solution of compound **59** (95.2 mg, 0.2 mmol, 1.0 eq) in DCM (10 mL) was slowly added TFA (0.5 mL) at room temperature. The reaction was completed in 2 hours and monitored by using TLC. DCM was removed under reduced pressure followed by column chromatography (eluent DCM:MeOH 40:1), which eventually gave pure product. (white solid, 75.6 mg, yield 90%). ^{1}H NMR (600 MHz, DMSO-d_6): δ (ppm) 8.16 (s, 1H), 8.15 (s, 2H), 7.61 (d, *J*=15.6Hz, 2H), 7.44 (d, *J*=15.6Hz, 2H), 7.08-7.11 (m, 2H), 6.00 (dd, *J*1=9.6, *J*2=1.2 Hz, 2H), 3.88 (t, *J*=6.6Hz, 4H), 2.45-2.47 (m, 4H). ^{13}C NMR (125 MHz, DMSO-d_6): δ (ppm) 168.49,

166.97, 165.93, 18.25, 139.93, 136.44, 132.70, 132.34, 129.61, 125.00, 124.79, 41.97, 24.75.

Methyl 3,5-bis((E)-3-oxo-3-(6-oxo-3,6-dihydropyridin-1(2H)-yl)prop-1-en-1-yl) benzoate (5-17)

The compound **60** (54.6 mg, 0.13 mmol, 1.0 eq) was dissolved in 11 mL mixture of MeOH and ether (10:1 v:v), followed by addition of trimethylsilyldiazomethane (2 M in diethyl ether, 0.07 mL, 1.2 eq) under ice-cold water bath. The reaction underwent at room temperature for overnight and then extracted with DCM and dried over sodium sulfate. The column purification (eluent EA:Hexane 1:1) affords product. (colorless oil, 14.7 mg, yield 26%). ^{1}H NMR (600 MHz, $CDCl_3$): δ (ppm) 8.30 (s, 2H), 7.86 (s, 1H), 7.72 (d, *J*=15.6Hz, 2H), 7.52 (d, *J*=15.0Hz, 2H), 6.93-6.96 (m, 2H), 6.04 (dd, *J*1=9.6Hz, *J*2=1.2Hz, 2H), 4.02 (t, *J*=6.6Hz, 4H), 3.93 (s, 3H), 2.47-2.50 (m, 4H). ^{13}C NMR (125 MHz, DMSO-d_6): δ (ppm) 168.57, 166.11, 165.76, 145.74, 141.36, 136.08, 132.03, 131.45, 130.00, 125.67, 123.80, 52.45, 41.68, 24.77. HRMS (ESI): calcd. for $[C_{24}H_{23}N_2O_6+H]^+$, 435.1556; found, 435.1541.

1,1'-((2E,2'E)-3,3'-(5-(4-morpholinopiperidine-1-carbonyl)-1,3-phenylene)bis(acryloyl))bis(5,6-dihydropyridin-2(1H)-one) (5-37)

To the solution of compound **60** (100.8 mg, 0.24 mmol, 1.0 eq) dissolved in

DMF (5 mL) were added HBTU (110 mg, 0.29 mmol, 1.2 eq), 4-morpholinopiperdine (44.2 mg, 0.26 mmol, 1.1 eq), and DIPEA (0.05 mL, 0.29 mmol, 1.2 eq) at room temperature. After 4 hours, the resulting reaction was extracted with DCM, washed with saturated NaCl solution, and purified by using flash chromatography (DCM:MeOH 30:1) to afford **5-37** (colorless oil, 75.6 mg, yield 55%). ^{1}H NMR (600 MHz, $CDCl_3$): δ (ppm) 7.71 (s, 1H), 7.66 (d, *J*=16.2Hz, 2H), 7.55 (s, 2H), 7.47 (d, *J*=15.6Hz, 2H), 6.92-6.95 (m, 2H), 6.01 (d, *J*=10.2Hz, 2H), 4.68-4.70 (m, 1H), 4.02 (t, *J*=6.6Hz, 4H), 3.70-3.71 (m, 4H), 3.01-3.03 (m, 1H), 2.81-2.85 (m, 1H), 2.52-2.56 (m, 4H), 2.44-2.47 (m, 6H), 1.95-1.99 (m, 1H), 1.77-1.79 (m, 1H), 1.54-1.56 (1H), 1.41-1.49 (m, 1H). ^{13}C NMR (125 MHz, $CDCl_3$): δ (ppm) 168.86, 168.51, 165.77, 145.82, 141.41, 137.33, 136.14, 129.15, 127.25, 125.62, 123.73, 67.16, 61.71, 49.69, 46.94, 41.69, 28.94, 24.75. HRMS (ESI): calcd. for $[C_{32}H_{36}N_4O_6+H]^+$, 573.2713; found, 573.2722.

1,1'-((2E,2'E)-3,3'-(5-(morpholine-4-carbonyl)-1,3-phenylene)bis(acryloyl))bis (5,6-dihydropyridin-2(1H)-one) (5-42)

5-42 was synthesized by following the previously described procedures for **5-37**. The compound **60** (58.8 mg, 0.14 mmol, 1.0 eq) was mixed with HBTU (63.8 mg, 0.17 mmol, 1.2 eq), morpholine (13.4 mg, 0.15 mmol, 1.1 eq) and DIPEA (0.03 mL, 0.17 mmol, 1.2 eq) to eventually afford the pure product **5-42**.

(colorless oil, 26.0 mg, yield 38%). ^{1}H NMR (600 MHz, $CDCl_3$): δ (ppm) 7.72 (s, 1H), 7.69 (d, *J*=15.6Hz, 2H), 7.56 (s, 2H), 7.48 (d, *J*=15.6Hz, 2H), 6.93-6.96 (m, 2H), 6.01-6.04 (m, 2H), 4.02 (t, *J*=6.6Hz, 4H), 3.71-3.81 (m, 4H), 3.61-3.63 (m, 2H), 3.40-3.42 (m, 2H), 2.46-2.49 (m, 4H). ^{13}C NMR (125 MHz, $CDCl_3$): δ (ppm) 169.07, 168.47, 165.78, 145.82, 141.25, 136.66, 136.27, 129.35, 127.36, 125.63, 123.87, 66.80, 48.18, 41.65, 24.75. HRMS (ESI): calcd. for $[C_{27}H_{27}N_3O_6+H]^+$, 490.1978; found, 490.1995.

1,1'-((2E,2'E)-3,3'-(5-([1,4'-bipiperidine]-1'-carbonyl)-1,3-phenylene)bis(acryloyl))bis(5,6-dihydropyridin-2(1H)-one) (5-43)

5-43 was synthesized by following the previously described procedures for **5-37**. The compound **60** (54.6 mg, 0.13 mmol, 1.0 eq) was mixed with HBTU (57.3 mg, 0.15 mmol, 1.2 eq), 4-piperidinopiperidine (24 mg, 0.14 mmol, 1.1 eq) and DIPEA (0.03 mL, 0.15 mmol, 1.2 eq) to eventually afford the pure product **5-43**. (white solid, 45.2 mg, yield 61%). ^{1}H NMR (600 MHz, DMSO-d_6): δ (ppm) 8.00 (s, 1H), 7.65 (s, 2H), 7.59 (d, *J*=16.2Hz, 2H), 7.42 (d, *J*=15.6Hz, 2H), 7.08-7.11 (m, 2H), 5.94-5.96 (d, 2H), 4.50-4.53 (m, 1H), 3.88 (t, *J*=6.6Hz, 4H) 3.55-3.57 (m, 1H), 3.29-3.36 (m, 2H), 3.00-3.06 (m, 1H), 2.71-2.75 (m, 2H), 2.51-2.68 (m, 1H), 2.44-2.48 (m, 4H), 1.82-1.89 (m, 1H), 1.68-1.74 (m, 1H), 1.44-1.56 (m, 7H), 1.38-1.42 (m, 2H). ^{13}C NMR (125 MHz, DMSO-d_6): δ (ppm) 168.60, 168.16,

165.89, 148.25, 140.18, 138.09, 136.22, 128.65, 127.57, 124.85, 124.77, 62.31, 55.37, 49.95, 46.92, 42.00, 24.77. HRMS (ESI): calcd. for $[C_{33}H_{38}N_4O_5+H]^+$, 571.2935; found, 571.2920.

1,1'-((2E,2'E)-3,3'-(5-(4-(dimethylamino)piperidine-1-carbonyl)-1,3-phenylene)bis(acryloyl))bis(5,6-dihydropyridin-2(1H)-one) (5-44)

5-44 was synthesized by following the previously described procedures for **5-37**. The compound **60** (54.6 mg, 0.13 mmol, 1.0 eq) was mixed with HBTU (57.3 mg, 0.15 mmol, 1.2 eq), N,N-dimethylpiperidin-4-amine (28.1 mg, 0.14 mmol, 1.1 eq) and DIPEA (0.03 mL, 0.15 mmol, 1.2 eq) to eventually afford the pure product **5-44**. (white solid, 4.8 mg, yield 7%). ^{1}H NMR (600 MHz, $CDCl_3$): δ (ppm) 7.72 (s, 1H), 7.67 (d, *J*=15.6Hz, 2H), 7.58 (s, 2H), 7.48 (d, *J*=15.6Hz, 2H), 6.94-6.97 (m, 2H), 6.01-6.03 (d, *J*=9.6Hz, 2H), 4.71-4.78 (m, 1H), 4.02 (t, *J*=6.6Hz, 4H), 3.01-3.09 (m, 1H), 2.76-2.84 (m, 1H), 2.47-2.49 (m, 10H), 2.11-2.18 (m, 2H), 1.98-2.08 (m, 1H), 1.84-1.88 (m, 1H), 1.59-1.62 (m, 1H), 1.49-1.55 (m, 1H). ^{13}C NMR (125 MHz, $CDCl_3$): δ (ppm) 168.92, 168.53, 165.77, 145.74, 141.45, 137.30, 136.15, 129.18, 127.29, 125.68, 123.73, 62.00, 46.97, 41.65, 41.29, 29.69, 24.77. HRMS (ESI): calcd. for $[C_{30}H_{34}N_4O_5+H]^+$, 531.2607; found, 531.2617.

N,N-dimethyl-3,5-bis((E)-3-oxo-3-(6-oxo-3,6-dihydropyridin-1(2H)-yl)prop-1-en-1-yl)benzamide (5-45)

5-45 was synthesized by following the previously described procedures for **5-37**. The compound **60** (54.6 mg, 0.13 mmol, 1.0 eq) was mixed with HBTU (57.3 mg, 0.15 mmol, 1.2 eq), Dimethylamine THF solution (0.07 mL, 0.14 mmol, 1.1 eq) and DIPEA (0.03 mL, 0.15 mmol, 1.2 eq) to eventually afford the pure product **5-45**. (colorless oil, 26.8 mg, yield 46%). ^{1}H NMR (600 MHz, $CDCl_3$): δ (ppm) 7.70 (s, 1H), 7.68 (d, *J*=15.6Hz, 2H), 7.58 (s, 2H), 7.48 (d, *J*=15.6Hz, 2H), 6.92-6.95 (m, 2H), 6.02 (d, *J*=10.2Hz, 2H), 4.02 (t, *J*=6.6Hz, 4H), 3.10 (s, 3H), 2.95 (s, 3H), 2.45-2.49 (m, 4H). ^{13}C NMR (125 MHz, $CDCl_3$): δ (ppm) 170.30, 168.53, 165.77, 145.77, 141.53, 137.71, 136.04, 129.15, 127.35, 125.64, 123.60, 41.64, 39.55, 35.31, 24.76. HRMS (ESI): calcd. for $[C_{25}H_{25}N_3O_5+H]^+$, 448.1872; found, 448.1863.

4.4. Biological characterization

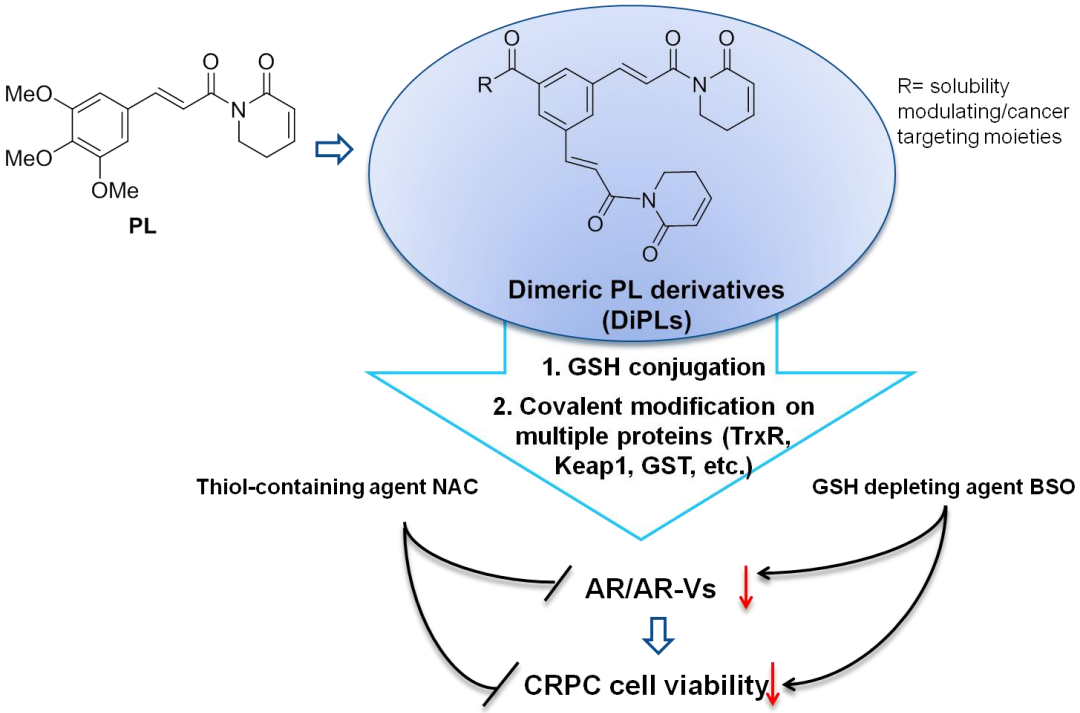

Figure 17. Schematic summary of biological activities of DiPLs.

4.4.1. Cytotoxicity vs. selectivity

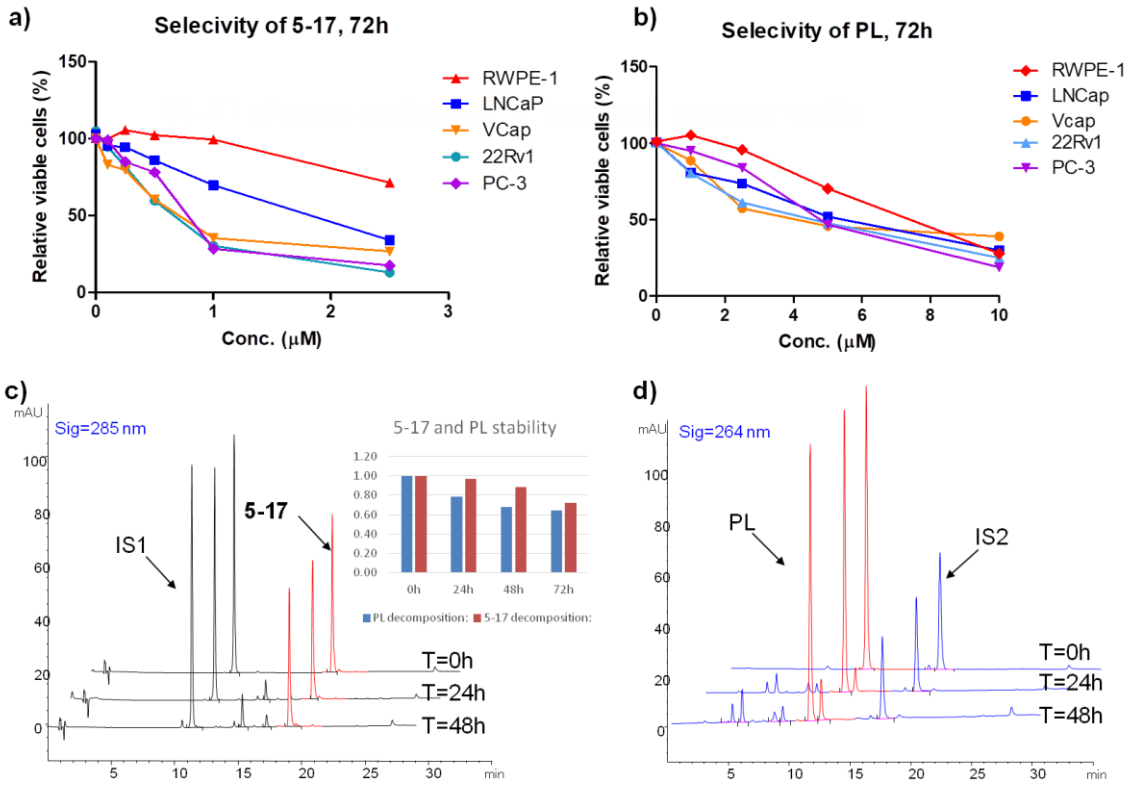

Figure 18. 5-17 selectively reduces viability of PCa cells and is stable in PBS buffer. PCa cells were treated with **5-17 a)** or **PL b)** at indicated concentrations for 72 h. Chemical stability of **5-17 c)** or PL **d)** was monitored by using HPLC. **5-17** (100 μM) and PL (100 μM) was dissolved in PBS buffer and incubated at 37°C, respectively. 3,4,5-Trimethoxybenzoic acid was used as internal standard 1(IS1), and benzophenone was used as internal standard 2 (IS2).

Table 3 IC_{50}s of PL and **5-17** against various PCa cell lines

Cell line[a] / Drugs[b]	LNCaP	VCaP	22Rv1	PC-3	RWPE-1
5-17 (nM)	1767±212	557±49.4	589.3±72.2	829.5±165	>2500[c]
PL (nM)	5137±406	4360±178.1	3984±254	5325±690	8260±1291

[a] Cells were treated with each drug for 72h, and cell viability was analyzed by using MTT assay.

[b] Each experiment was independently repeated three times, and data are represented as mean ± SEM.

[c] RWPE-1 cell viability was reduced by 29% when treated with **5-17** at maximum 2500nM for 72h.

To investigate if the newly synthesized **5-17** has selectivity and broad anti-PCa spectrum, we used androgen-dependent LNCaP (AR mutant T877A), CRPC 22Rv1 (AR mutant H875Y, AR-Vs), CRPC VCaP (WT-AR, AR-Vs), CRPC PC-3 (AR negative) and normal prostatic RWPE-1 cells. Cells were treated with **5-17** or PL for three days, and cell viability was assessed by using MTT assay. As shown in **Figure 18a** and **18b**, in agreement with published PL cytotoxic profile[3], PL efficiently reduced the viability of various PCa cell lines, and PL also suppressed the growth of RWPE-1 cells, suggesting its weak selectivity over PCa cells (**Table 3**). **5-17** was shown pan-anti-PCa activities and 3~8 fold more potent than PL in reducing the viability PCa cells (**Table 3**). It is noteworthy that **5-17** hardly decreased whereas PL reduced viability of RWPE-1 cells by 29% at the concentrations where the VCaP cell viability was decreased by 50%. Besides, the addition of the second electrophilic moiety didn't increase the instability of **5-17** in contrast with PL, as measured in PBS buffer by using HPLC (**Figure 18c** and **18d**). Therefore, these preliminary results have shown that, compared to PL, **5-17** is a relatively stable electrophile and has potent and selective anti-PCa activities.

4.4.2. DiPL induces ROS accumulation, depletes GSH, and inhibits TrxR in VCaP cells

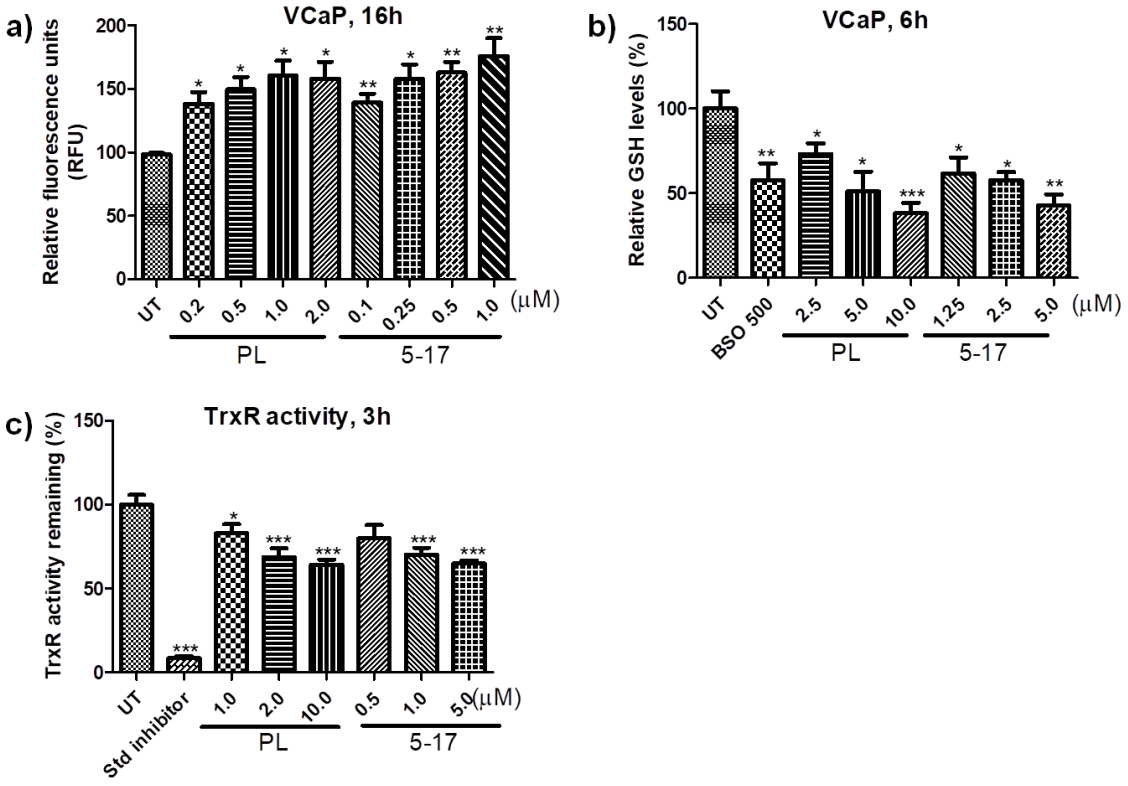

Figure 19. 5-17 increases ROS levels, depletes GSH pool, and inhibits TrxR. **a)** VCaP cells were treated with PL or **5-17** at indicated concentrations for 16h. ROS level was measured by using H_2DCFDA and normalized by vehicle control. **b)** Intracellular GSH was measured by using monochlorobimane and normalized by vehicle control. BSO (500μM) was used as the positive control. **c)** TrxR enzymatic activity was measured by using the TrxR enzymatic kit and normalized by vehicle control. VCaP cells were treated with the standard inhibitor solution, PL, or **5-17** for 3 h, followed by cell lysis and TrxR enzymatic activity measurement. Each experiment was independently performed three times, and the bar represents mean ± SEM. *P < 0.05, **P < 0.01, ***P< 0.001.

Since PL is reported to elevate ROS levels[3], consume GSH pool[3], and inhibit antioxidant enzyme TrxR[19], we tested if **5-17** has similar effects as PL.

VCaP cells were tested with PL or **5-17**, and intracellular ROS level was measured at the 16h time point by using H_2DCFDA. As shown in **Figure 19a**, PL and **5-17** could dramatically increase ROS level up to ~1.8 fold at the highest concentration when compared to the untreated group. It is noted that only half dose of **5-17** was needed to reach the same increased ROS level as PL, which suggests that augmented ROS-inducing capacity of **5-17** may stem from the doubled Michael acceptors. Besides, PL consumes intracellular GSH pool by conjugating GSH at C2 position of C2-C3 olefin[3,33,19], so we also investigated if **5-17** can decrease intracellular GSH content. GSH is involved in scavenging ROS, reducing disulfide bond, and detoxifying endo/exogenous electrophile[194]. As shown in **Figure 19b**, both PL and **5-17** efficiently decreased intracellular GSH in 6h, and **5-17** was twice as efficient as PL, suggesting that **5-17**-induced GSH consumption may be attributed to the double electrophilic moieties. Since PL was previously identified as a potent inhibitor of TrxR1[19], we also evaluated **5-17**'s effect on this antioxidant enzyme TrxR. TrxR is a selenocysteine-containing protein and known to reduce the thioredoxin (Trx). TrxR inhibition may promote NADPH oxidase (NOX) activity, thereby elevating the level of $O_2^{\bullet-}$ and H_2O_2[195]. Therefore, TrxR has emerged as a promising target for anti-cancer therapy[196]. In our study, **5-17** was also found to inhibit TrxR enzyme activity in a

concentration-dependent manner. Inhibition of TrxR by PL was similar in magnitude to those of **5-17** at half concentrations (**Figure 19c**), suggesting that the second electrophilic moiety of **5-17** appears not to affect whereas increase the odds of binding to TrxR, which is in accordance with the finding that it is the electrophilic moiety of PL that binds to TrxR[19]. Taken together, **5-17**, as a result of doubling of electrophilic moieties compared to PL, is twice as potent as PL in ROS enhancement, GSH consumption and TrxR inhibition.

4.4.3. Cytotoxicity of DiPL is influenced by intracellular thiol concentration

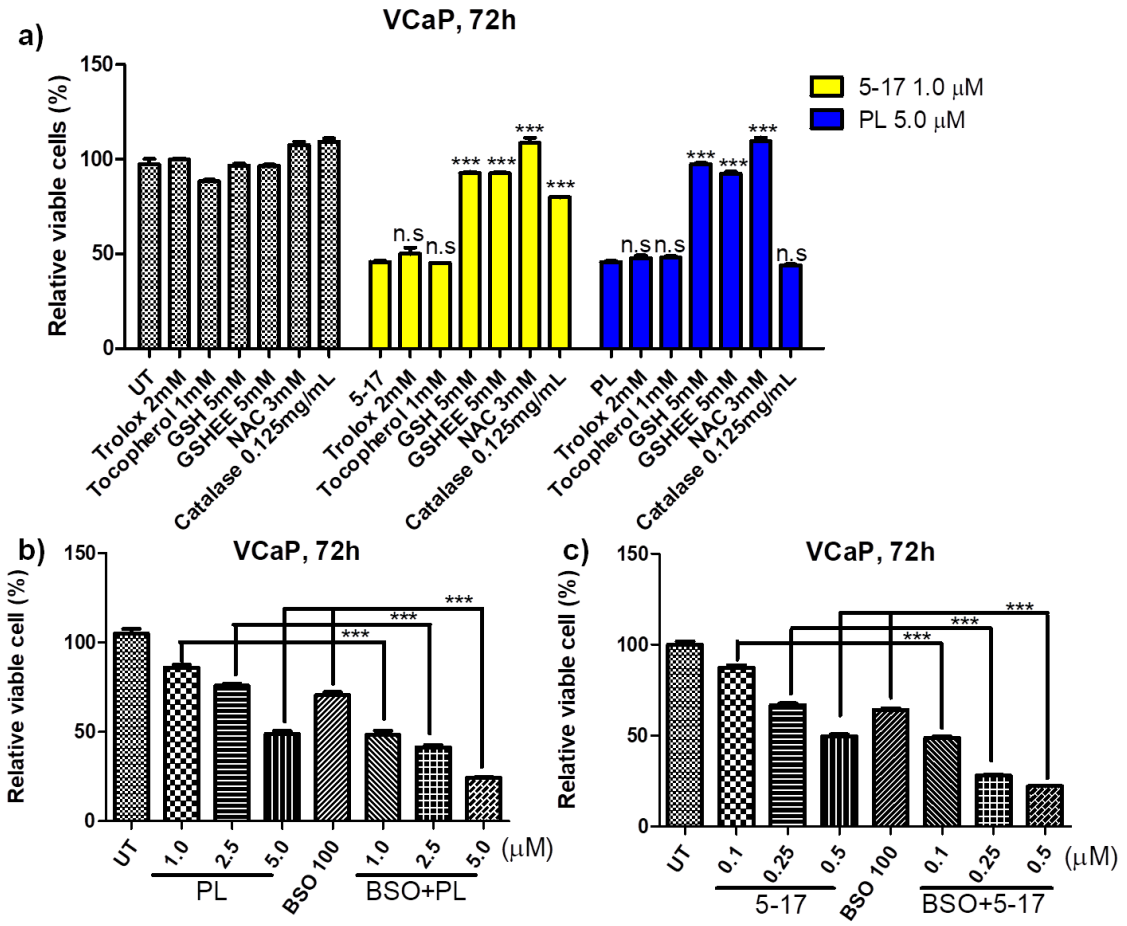

Figure 20. Inhibitory potency of PL or **5-17** on cell viability is influenced by intracellular thiol concentration. **a)** VCaP cells were pretreated with indicated reagents for 2 h, followed by the treatment of **5-17** (1.0 μM) or PL (5.0 μM). VCaP cells were cotreated with PL **b)** or **5-17 c)** for three days following pretreatment (16 h) with BSO (100 μM). Cell viability was analyzed by using MTT assay. Each experiment was independently performed three times, and the bar represents mean ± SEM. n.s indicates no statistical significance. *P < 0.05, **P < 0.01, ***P< 0.001.

Since PL affects cell viability by modifying thiols and ROS elevation, we postulated that free thiol supplement and ROS scavenging may rescue cells from

5-17 or PL treatment. To test this hypothesis, we applied free-thiol substances (e.g., NAC, GSH, and GSHEE), non-thiol antioxidants vitamin E (e.g., tocopherol and trolox), antioxidant enzymes (e.g., catalase) in our study. In agreement with the previous findings[3,197], cell viability reduction caused by PL could be fully reversed by increasing the intracellular free thiol concentration, as observed in NAC, GSH, and GSHEE-treated groups (**Figure 20a**). Vitamin E (tocopherol and trolox) and catalase failed to affect cell viability reduction caused by PL, suggesting that the cell viability reduction was caused by PL-mediated thiol modification rather than ROS[24]. The similar phenomenon was observed for **5-17** except that the catalase addition partially rescued **5-17**-reduced cell viability ***(*Figure 20a**). Since there is no evidence supporting the rapid interaction of PL with catalase, and catalase has been widely used for studying ROS involvement by co-incubating with PL[3,25,197,19], we conclude that this partial rescue may be attributed to intracellular ROS scavenging by catalase rather than sequestration via covalent binding of **5-17** to catalase. Attenuation of cytotoxicity of **5-17** by the catalase suggests that H_2O_2 may play a pronounced role in mediating cytotoxic effects of **5-17**. The explanation may be relevant to increased inhibitory activity of **5-17** against TrxR or other enzymes (e.g., GPX1) responsible for removing H_2O_2. On the other hand, since GSH depletion confers cancer cells higher susceptibility

of cancer cells to electrophilic compounds such as PL and phenethyl isothiocyanate (PEITC)[198,199], we applied a specific GSH synthesis inhibitor, BSO, to assess the effect of free thiols on PL's or **5-17**'s overall activity. We pretreated VCaP cells with BSO (100μM) for 16h, allowing consumption of GSH pool. **5-17** or PL was then added and co-incubated with BSO for three days. The result showed that the BSO pretreatment significantly enhanced cytotoxicity of PL or **5-17** against VCaP cells (**Figure 20b** and **20c**), indicating that GSH depletion makes VCaP cells more susceptible to **5-17** or PL treatment. We concluded that intracellular free thiols protect cancer cells from being damaged by PL or **5-17**, and this protection may be mainly manifested in preventing covalent interactions of PL or **5-17** with thiol-containing proteins.

4.4.4. DiPL decreases AR/AR-V7 protein level in CRPC VCaP cells

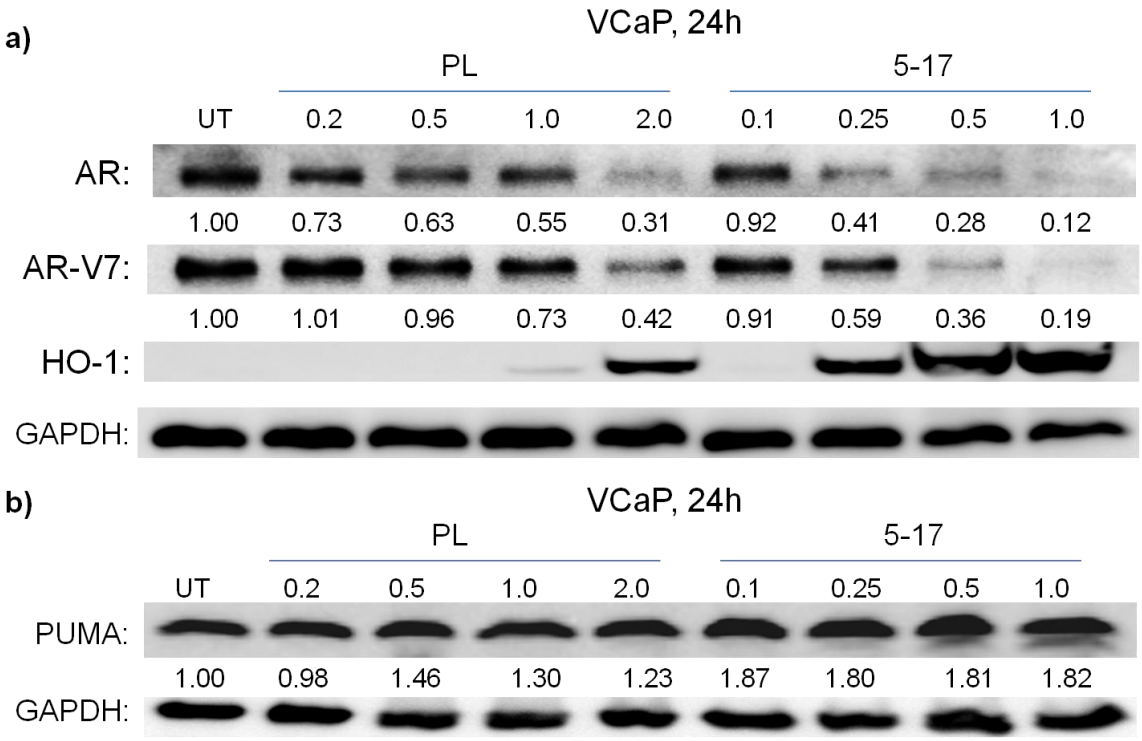

Figure 21. PL or **5-17** decreases AR and AR-V7 and increases HO-1and PUMA protein levels in VCaP cells. **a)** PL or **5-17** decreased the protein level of AR and AR-V7, meanwhile increased OH-1 in a concentration-dependent manner. **b)** PL or **5-17** increased PUMA protein level. VCaP cells were treated with PL or **5-17** at indicated concentrations for 24h, followed by Western Blotting analysis. Each experiment was independently performed three times, and one representative blot was shown.

Next, we assessed the effect of PL or **5-17** on protein targets or oncogenic signaling pathways. AR and AR-Vs are two essential mediators in the progression of CRPC[74,200], and PL was reported to reduce AR and AR-Vs protein level in LNCaP and in PC-3 cells artificially expressing AR-Vs, respectively[5]. Compared to PL, **5-17** more efficiently inhibited PCa cell growth, which inspired us to

hypothesize that **5-17** could be used to design more efficient AR/AR-Vs-depleting agents. In our study, VCaP cells (p53 heterozygous mutant) were used as the cell model to study the AR/AR-Vs depleting effect of **5-17** because of abundant AR and AR-Vs expression in VCaP cells. Experimentally, VCaP cells were incubated with PL or **5-17** for 24h, AR and AR-V7 protein levels were analyzed by using Western Blotting assay. PL could elevate ROS level in many cancer cells and directly react with Keap1 and activate Nrf2-HO-1 pathway in breast cancer cells[24], so HO-1 protein expression was measured in VCaP cells treated with PL or **5-17** since it was recognized as the marker of oxidative stress[201] and the activation of Nrf2 pathway[202]. Additionally, PUMA is a promising drug target and its activation leads to mitochondrial-dependent cell apoptosis[203]. PL was reported to induce apoptosis in cancer cells with wild type and null p53 through activation of PUMA[3], so we also measured the expression level of PUMA. **Figure 21a** shows that both PL or **5-17** downregulated AR and AR-V7 expression in a dose-dependent manner and upregulated PUMA (**Figure 21b**), with **5-17**-induced effects being more prominent than PL-induced. **5-17** at 0.25 μM was sufficient to induce similar AR/AR-V7 depletion as PL at 2.0 μM, correlating with the finding that **5-17** is ~8 fold more effective in reducing VCaP cell viability than PL. HO-1 expression concomitantly upregulated at the doses where AR and AR-V7 notably decreased

(**Figure 21a**). Since PL was reported to covalently modify Keap1 protein, thereby activating Nrf2-HO-1 signaling pathway independently of ROS, these observations suggest that **5-17** is a strong AR/AR-V7 depleting agent and may function as PL in modulating Keap1 protein and inducing PUMA-dependent cell apoptosis independently of ROS. Together with direct ROS elevation (**Figure 19a**) and attenuation of **5-17** cytotoxicity by catalase (**Figure 20a**), it is plausible that ROS participates in pronounced HO-1 upregulation caused by **5-17**. In addition, **5-17** is ~2 fold stronger than PL in ROS induction, GSH depletion, and TrxR inhibition, and ~8 fold stronger than PL in AR/AR-V7 protein reduction, HO-1 induction and cell viability reduction, indicating that doubling electrophilic moieties of PL significantly multiplies its anti-PCa activities.

4.4.5. 5-17 potency is enhanced by incorporating hydrophilic moieties

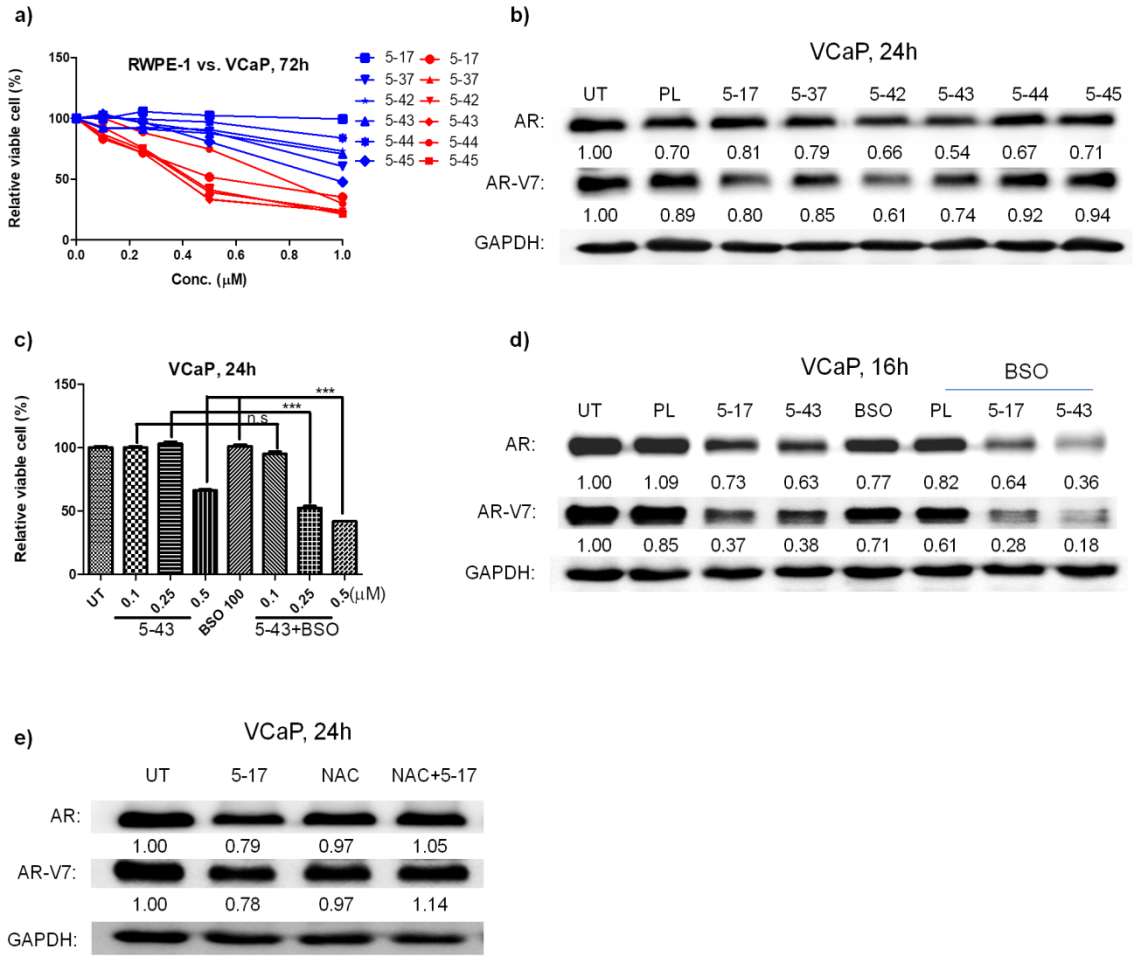

Figure 22. 5-43 is more effective in reducing PCa cell viability and downregulating AR/AR-Vs. **a)** RWPE-1 (blue) and VCaP (red) cells were treated with **5-17** and **5-17** analogs for 72h. Cell viability was analyzed by using MTT assay. **b)** VCaP cells were treated with PL (0.2 μM), **5-17** (0.1 μM), and **5-17** analogs (0.1 μM) for 24h. AR and AR-V7 were detected by using Western Blotting assay. **c)** VCaP cells were co-treated with **5-43** following 16h pretreatment with BSO (100 μM). Cell viability was analyzed by using MTT assay. **d)** VCaP cells were pretreated with BSO (100 μM) for 16h, followed by co-treatment with PL (0.5 μM), **5-17** (0.25 μM), and **5-43** (0.25 μM) for 16h. **e)** NAC treatment fully rescued AR/AR-V7 protein loss caused by **5-17**. VCaP cells were treated with **5-17** (0.1 μM) following 2h pretreatment of NAC (3.0 mM). AR and AR-V7 were detected by using Western Blotting assay. Each experiment was independently performed three times, and the bar represents mean ± SEM. n.s indicates no statistical significance. *P < 0.05,

**P < 0.01, ***P< 0.001.

Next, we refined the **5-17** structure by replacing the methyl ester moiety with multiple hydrophilic entities as **5-17** has relatively high CLogP value (4.34, calculated by using the Chemdraw software), which may limit its bioavailability based on the rational of Lipinski's rule of five, one of which demonstrates LogP<5[204]. To optimize physicochemical properties of **5-17**, we selected a series of morpholine, piperidine and their derivatives with LogP ranging from -0.6 to +0.6, thus producing a class of PL analogs with final CLogP 2~4 (**Table 4**). Moreover, the introduction of these heterocyclic rings or atoms may reveal the tolerability and feasibility of structural modifications on the non-electrophilic moiety of **5-17**, underlying the basis for further modification or incorporation with other chemical scaffolds. VCaP cell model was used to evaluate their overall effects on cell cytotoxicity and AR/ARV-7 expression. Encouragingly, without sacrificing cancer cell selectivity, **5-37**, **5-42**, and **5-43** were 1.0~1.8 fold more potent than **5-17** in reducing VCaP cell viability (**Figure 22a**), with **5-43** being the most potent analog (**Table 4**). **5-45** was slightly more potent while **5-44** was ~1.9 fold less potent than **5-17**. **5-42** and **5-43** more efficiently decreased AR/AR-V7 protein levels than **5-17** at the same dose (0.1 μM) (**Figure 22b**). Given the strongest inhibitory effect of **5-43** on cell viability and AR/AR-V7 expression, **5-43** was selected to pair with

BSO. Since AR and AR-Vs are implicated in progression of CRPC, we further tested if **5-17** or **5-17** analogs affect the expression of AR and AR-Vs, and if their effects are influenced by intracellular thiol concentration. As expected, GSH depletion by BSO pretreatment notably enhanced the potency of **5-43** (**Figure 22c**) and accelerated DiPL-induced AR/ARV-7 protein decline (**Figure 22d**). It is noted that **5-43,** compared to PL or **5-17**, downregulated AR/AR-V7 most when combined with BSO (**Figure 22d**), which correlates with the strongest potency of **5-43** against PCa cell viability. **Figure 22e** shows that NAC addition completely abrogated **5-17**-induced AR and AR-V7 protein reduction. The observation, that BSO enhanced whereas NAC reversed **5-17**-induced AR/AR-V7 downregulation, reveals that thiol-modifying property of **5-17** leads to decreased AR/AR-V7 expression. In conclusion, PL and DiPLs reduce cell viability through multiple mechanisms involving Keap1-Nrf2-HO-1 signaling pathway activation, PUMA activation, and AR/AR-V7 downregulation, and these mechanisms stem from PL or DiPL-mediated cellular thiols modification.

Table 4 IC_{50}s of dimeric PL derivatives against VCaP cells.

	5-17[a]	**5-37**[a]	**5-42**[a]	**5-43**[a]	**5-44**[a]	**5-45**[a]
ClogP[b]	4.34	2.78	3.00	4.00	2.72	2.84

IC_{50}s (nM)[c]	557 ±49.4	468.5 ±15.6	464.9 ±60.6	303 ±31.5	1042 ±47.1	518.4 ±21.4

[a] VCaP cells were treated with **5-17** or **5-17** analogs for 72 h. Cell viability was measured by using MTT assay.
[b] ClogP was calculated by using ChemDraw software.
[c] Each experiment was repeated three times. Data are represented as mean ± SEM.

4.5. Experimental procedures

4.5.1. Cell culture

VCaP, LNCaP, PC-3, 22Rv1, and RWPE-1 cells were purchased from the American Type Culture Collection (Manassas, VA, USA). During experiment, PCa cell lines were maintained at 37 °C and incubated under humidified 5% CO_2/95% air in the RPMI media supplemented with 10% (v:v) fetal bovine serum (Sigma, F8067), streptomycin (100 µg/mL), penicillin (100 U/mL), and L-glutamine (2 mM). RWPE-1 cells were cultured in serum-free Keratinocyte-SFM medium supplemented with L-glutamine, EGF (0.005µg/mL) and BPE (0.05mg/mL). (Thermo Fisher, Cat# 17005-042).

4.5.2. Cell viability

PCa cells were seeded into 96-well plates with 6000-12000 cells in each well. The phenol-red free RPMI 1640 medium was supplemented with 10% fetal bovine serum and 1% streptomycin. 20,000 RWPE-1 cells were seeded into each

well of a 96-well plate and incubated serum-free Keratinocyte-SFM medium. All cells were grown at 37°C in a humidified cell incubator with an atmosphere of 5% CO_2/95% air. After 24h cell attachment, cells were treated with graded concentrations of indicated compounds or DMSO vehicle, and the final concentration of DMSO in all treated groups is limited to below 0.1%. The fresh solution of MTT ((3-(4,5-dimethyl-2-thiazolyl)-2,5-diphenyltetrazolium bromide) agent (ACROS, NJ, USA. Cat#A0357552) was added to each well, and incubated with cells for 3h in the 37 °C incubator. Finally, the number of viable cells was quantified by using absorbance reading at 570nm.

4.5.3. Western blotting assay

PCa cells were harvested, washed with PBS and lysed in RIPA buffer (150mM NaCl, 50mM Tris–HCl, pH 7.4, 5mM EDTA, 1% NP40, 0.1% SDS) containing 1% PMSF (phenylmethylsulphonyl fluoride) for 30min over ice. The Pierce BCA Protein Assay Kit was used for protein concentration of resulting supernatants. 40-60ug protein was prepared for SDS gels separation and transfer onto PVDF (polyvinylidenedifluoride) membranes. The 5% nonfat milk was utilized for blockade of non-specific binding. Blots were incubated with anti-AR (Santa Cruz, CA. Cat#sc-816), anti-AR-V7 (Precision, MD. Cat#AG10008), anti-HO-1(Cell Signaling, MA. Cat#70081), anti-PUMA (Cell signaling, MA.

Cat#4976), and anti-GAPDH (FC-335, Santa Cruze, CA. Cat#E0212.) for 16h, followed by conjugation with anti-rabbit IgG (Cell Signaling, MA. Cat#7074) for 1h at room temperature. Immunoreactive bands were visualized with ECL (enhanced chemiluminescence detection kit, Cat#203-16281, PerkinElmer.Inc, USA). Densitometry assay was performed by using imageJ software.

4.5.4. HPLC analysis

The indicated compound was dissolved in PBS. The 10μL solution was injected into HPLC for analysis. HPLC analysis was conducted using a Phenomenex Lunna 3μm C18, 3.5 μm, 150 mm × 3.0 mm column on Agilent 1100 series HPLC instrument. Mobile phase uses 10% CH_3OH (0.1% formic acid, A) and CH_3CN (0.1% formic acid, B) with flow rate 0.5 mL/min and 10%B-95%B in 30min gradient.

4.5.5. Intracellular ROS measurement

VCaP cells (10,000 cells/well) were seeded into black 96-well plates and cultured in 10% FBS RPMI 1640 medium for 48h. After culture medium removal and PBS wash (1X), 20μM H_2DCFDA (C400, ThermoFisher, USA) dissolved in 2% FBS medium was added and incubated with cells for 30 min at 37 ^oC in the dark. Cell groups without H_2DCFDA treatment are set as blank. After 30min, cells were washed with PBS (1X) to remove H_2DCFDA. The fluorescence reading was

obtained at Ex/Em=497 nm/527 nm. The reading was set as baseline. Next, cells were treated with tested compounds for 16h, followed by reading at Ex/Em=497 nm/527 m. Fold change= [Reading (sample)- Reading (blank) / Reading (baseline)- Reading (blank)]

4.5.6. Intracellular GSH content measurement

VCaP cells (10,000 cells/well) were seeded to 96-well plates and cultured in 10% FBS RPMI 1640 medium for 24h. BSO (0.5 μM), PL (2.5, 5.0, 10 μM), and **5-17** (1.25, 2.5, 5.0 μM) were added and incubated with cells for 6h. After medium removal and PBS wash (1X), monochlorobimane (100 μM, 69899, Sigma, USA) was added and incubated with cells for 30min at 37^{o}C. Following PBS wash (1X) and culture medium addition, fluorescence was measured in a plate reader at Ex/Em=360$\pm$40 nM/460$\pm$40 nM.

4.5.7. TrxR enzymatic assay

VCaP cells were seeded in 6-well plates with 2.6x10^{6} per well and cultured in 10% FBS RPMI 1640 medium for 48h. Cells were treated with PL (1.0, 2.0, 10.0 μM) and **5-17** (0.5, 1.0, 5.0 μM) for 3h. Following medium removal and PBS wash (2X), cells were scraped off, transferred to tubes, centrifuged at 100g for 5 min. After removing supernatant, RIPA lysis buffer (50 μL) was added and incubated with cells for 30min at 4 ^{o}C. Cell lysate was obtained by centrifuging at 10,000g for

15min. The Pierce BCA Protein Assay Kit was used for protein concentration of resulting supernatants. The amount of enzyme activity was measured and calculated according to the manufacture's standard protocol (CS0170, Sigma, USA). Briefly, the spectrophotometer at 412nM was set up using an enzymatic kinetic program (Delay=120s, interval=10s, the number of reading=6). 180 µL working buffer was added to each well of a 96-well plate. Other components, including TrxR enzyme, assay buffer (1X), TrxR standard inhibitor solution, and DTNB, were added based on the Table 2 of the protocol.

4.5.8. Statistical analysis

GraphPad Prism 5.0 was utilized for statistical analysis. Results are represented as means ± standard error of the mean (SEM). The differences between sets of data were analyzed with student's t-test or one-way ANOVA Bonferroni post test. Significant level was set as α=0.05. Asterisks indicate *P < 0.05, **P < 0.01, ***P < 0.001.

4.5.9. Chemistry methods

General Methods for Chemistry. ^{1}H and ^{13}C NMR spectra were obtained using Varian Mercury 600MHz. Chemical shifts are reported as δ values in parts per million (ppm) relative to tetramethylsilane (TMS) for all recorded NMR spectra. All reagents and solvents were obtained from Acros, Fisher or Aldrich without

further purification. Flash column chromatography was performed over 200−300 mesh silica gel. High resolution mass spectral data were collected using a LCT Premier XE KD128 instrument. All compounds submitted for biological testing were found to be >95% pure by analytical HPLC. Purity check was performed via HPLC analysis as described in the chapter 2.

CHAPTER 5 CONCLUSION

PL is an electrophilic anti-cancer natural product that selectively kills malignant cells over non-malignant cells in preclinical models[2-3]. Through non-covalent or covalent interactions, PL inactivates multiple oncogenic pathways (e.g., NF-κB,[22] Keap1[24] and Akt/mTOR[6]) and suppresses key components of cellular antioxidant defense systems (e.g., GSH, GST[3] and TrxR[205]). These actions result in pleiotropic anti-cancer effects and *in vivo* efficacy in animal models[205]. We envisioned that PL is a promising lead for anti-cancer drug discovery, and PL derivatives with higher potency and strengthened safety profiles represent a new generation of anti-AML/anti-PCa agents that perturb oncogenic networks rather than single oncotarget.

We performed three strategies to enhance anti-AML or anti-PCa selectivity and potency of PL derivatives: 1) To design PL-HDACi hybrid drugs (e.g., compound **1-58**) based on the synergistic anti-AML interactions between PL and the HDACi (e.g., SAHA) (**Chapter 2**)[30]; 2) Aimed to further improve cancer selectivity and drug bioavailability, we designed ROS/PNT-activated hydroxamic acid HDACi prodrugs, and used this approach to equip the previously obtained PL-HDACis (**Chapter 3**); 3) To dimerize the PL pharmacophore to generate a dimeric PL (DiPL) warhead, as exemplified by a lead compound **5-17** (**Chapter 4**). Both **1-58** and **5-17** are significantly more potent than PL in inhibiting AML or PCa

cell proliferation and display broad anti-AML/anti-PCa activities in high-risk and treatment-resistant cell lines.

In **Chapter 2**, PL was paired with SAHA at ratio 1:1, and this combination showed synergism against AML cell lines, which supported our proposal that anti-cancer activities of PL can be enhanced by adding HDACi (eg., SAHA) through their cooperative and complementary cellular effects. Inspired by this finding and the analysis of anti-cancer SAR of PL, we designed PL-HDACi hybrid molecule **1-58** by merging PL and SAHA into one single molecule. **1-58** was more potent than PL or SAHA alone and their combination at inhibiting AML cell growth. To dissect SAR of **1-58**, we applied chemistry and biology strategies. Chemically, we synthesized **3-98** or **3-35** by introducing an electron-withdrawing chlorine atom at the C2 position of PL moiety of **3-31** or **1-58**, respectively. **3-98** or **3-31** was obtained by eliminating C7-C8 olefins of PL pharmacophore of **3-35** or **1-58**, respectively. As expected, **3-35** or **3-98** was more potent than **1-58** or **3-31**, due to the enhanced electrophilicity at the C3 position. **3-35** is the most potent because of co-existence of C7-C8 and chlorinated C2-C3 olefins, which also contributes to non-selective cytotoxicity toward normal MCF-10A cells. Biologically, we validated that both PL and HDACi pharmacophores are necessary to maintain the overall anti-leukemic activity of hybrid **1-58**. The function of PL pharmacophore is to

interfere with antioxidant defense system. HDACi pharmacophore is responsible for downregulating DNA-repair enzymes such as CHK1 and RAD51, increasing pro-apoptotic proteins (e.g., Bim), and decreasing anti-apoptotic proteins (e.g., XIAP). These effects collectively favor enhanced DNA damage and apoptotic death of PL-HDACi hybrid drugs. In summary, we demonstrated the potent anti-leukemic activity of PL and HDACi combination, and further designed a PL-HDACi hybrid drug class based on the synergistic anti-AML interactions of PL and SAHA. Given the higher potency than parental drugs and the selectivity between AML and normal cells, the representative hybrid drug **1-58** is a promising anti-leukemic lead compound for further optimization.

The epigenetic deregulation of AML makes HDACi an attractive “targeted” drug class for disease treatment. However, the clinical use of hydroxamic acid-based HDACis is frequently hindered by undesired cardiovascular and gastrointestinal toxicity, as well as fast elimination and poor tissue penetration. These challenges prompt us to design HDACi prodrugs and eventually applied this methodology to PL-HDACi hybrid drugs. Occurrence of acute myeloid leukemia (AML) results in abundant endogenous ROS/RNS sources in AML cells and in disease-relevant microenvironments. In **Chapter 3**, prodrug approach was designed accordingly by masking the hydroxamic acid zinc binding group with

H_2O_2/PNT-sensitive, self-immolative aryl boronic acid moiety. Model prodrugs **Q-582** and **Q-523** were derived from FDA-approved SAHA and the previously reported PL-HDACi **1-58**, respectively. We demonstrated that these prodrugs are specifically activated by H_2O_2 or PNT, leading to intracellular release of active HDACi and inhibition of AML cell proliferation. Consistent with the mechanism of activation, intracellular activities of prodrugs were increased or reduced by ROS/PNT inducers and scavengers, respectively. **Q-582** and **Q-523** also enhanced the potency of chemotherapy drug cytarabine, supporting potentials of pairing this prodrug class with conventional chemotherapy drugs. In addition, **Q-582** displayed promising selectivity as it is well tolerated in normal PBMNCs and prostate epithelial RWPE-1 cells compared to AML and PCa cell lines, respectively. Given the broad pharmacological effects of HDACi and the critical pathological roles of ROS and PNT in various human diseases, including cancer, neurodegenerative diseases and metabolic disorders[206], H_2O_2 and PNT-activated HDACi prodrugs may be utilized in broader scope other than AML, e.g., in the treatment of solid tumors and non-cancer indications.

Intrinsic electrophilicity is the chemical foundation of PL-induced anti-cancer effects. Although “targeted covalent inhibitors”[207], a drug class that carries thiol-reactive electrophile, are being used for cancer treatment (e.g.,

EGFR inhibitor afatinib[208] and BTK inhibitor ibrutinib[209]), clinical utilization of general electrophiles to target multiple oncogenic pathways is still rare. In this area, APR-246 spontaneously converts to electrophilic methylene quinuclidinone (MQ) at physiological pH[210], and was tested in phase I/IIa blood cancer (including AML) and prostate cancer trials. It showed encouraging safety profiles and signs of clinical efficacy[211]. Moreover, APR-246 is currently being assessed in more oncology trials either alone or in combination with other drugs (e.g., Dabrafenib, NCT03391050). Despite limited success, clinical use of electrophilic compounds is concerned due to potential non-selective protein modification, DNA alkylation and toxicity to normal cells. From this point of view, the success of multi-target electrophiles in cancer treatment is ultimately relied on their selective cytotoxicity and whether drug uptake/distribution in tumor tissues can be dramatically improved via conjugating with tumor-homing moieties or by drug delivery techniques. A recent study shows that highly toxic monomethyl auristatin E (pM potency) can be selectively uptaken by prostate cancer cells via conjugating the compound to a cancer cell-selective aptamer[212]. These examples support a workflow for discovering PL-based cancer treatments: to discover PL derivatives with higher potency and selectivity followed by conjugating the PL-derived "warhead" to cancer-targeting moieties.

Compared to parental compound, dimerization or oligomerization of an electrophile could result in derivatives with higher biological potency. Possible explanations include 1) containing more than one copy of electrophilic moiety in single molecule; 2) recognizing oligomeric cellular targets through multivalent interactions[190]; 3) crosslinking of cellular nucleophiles. Some of these MOAs (mechanism of action), e.g., multivalent binding or crosslinking of cellular targets cannot be realized by simply increasing concentration of an electrophilic compound. Numerous anti-cancer multimeric electrophiles have been reported, such as dimers of melampomagnolide B as potent growth inhibitors of hematological and solid tumor cell lines[187], dimeric catechol as DNA crosslinking agent[188], and more specifically, PL oligomers[21] or dimers[189] are more cytotoxic than PL in cancer cells. Inspired by these works, in **chapter 4**, we designed new DiPLs by incorporating two PL pharmacophores onto the phenyl ring of benzoic acid at 3 and 5 positions, and the carboxylate group (**5-17**) is suitable for further conjugation to improve water solubility and/or cancer-targeting properties.

As the first step to explore DiPL-derived anti-AML and anti-PCa agents, a small library of DiPLs was synthesized to test if this new scaffold can more potently inhibits growth and oncogenic pathways than PL in AML or PCa cells without sacrificing selectivity. We also attached water solubility-enhancing polar

moieties, such as nitrogen-containing heterocycles to DiPL, to investigate if changing physiochemical properties could impact anti-cancer potency and selectivity. The anti-AML activities were tested in collaborator's (Dr. Yubin Ge) lab, and the anti-PCa activities was a focus in **Chapter 4** of this thesis. AR signaling is the primary drug target for PCa treatment. VCaP cell line expresses abundant full length AR and AR-V7 and was selected as a cell culture model to test cell growth inhibition and AR downregulation properties of DiPLs. DiPL **5-17** more potently inhibited VCaP cell growth than PL, reflected by significantly lowered IC_{50} (557 nM *vs.* 4360 nM). **5-17** also retained cancer cell selectivity, more than 4-fold difference were seen between the IC_{50} values in VCaP and in the non-cancerous RWPE1 cells. Under the same experimental conditions, the PL-induced differential effects between VCaP and RWPE-1 cells was less than 2-fold. Compared to **5-17**, DiPLs (e.g., **5-42** and **5-43**) more effectively downregulated AR and AR-V7 expression as measured using Western blot assays. To correlate cellular activity with electrophilicity of DiPLs, we showed that both cell growth inhibition and AR/AR-V7 downregulation were significantly enhanced by GSH synthesis inhibitor BSO. Apparently, decreased cellular GSH content reduced intracellular GSH conjugation, making DiPLs access protein target more easily. Overall, our current work identified novel DiPL (e.g., **5-17** and **5-43**) scaffolds as

potent and cancer-selective “warhead” that can be used for designing DiPL-based cancer-targeting conjugates to further improve safety profiles.

REFERENCES

1. Chatterjee, A.; Dutta, C. P., Alkaloids of Piper longum Linn. I. Structure and synthesis of piperlongumine and piperlonguminine. *Tetrahedron* **1967,** *23* (4), 1769-81.

2. Bezerra, D. P.; Pessoa, C.; de Moraes, M. O.; Saker-Neto, N.; Silveira, E. R.; Costa-Lotufo, L. V., Overview of the therapeutic potential of piplartine (piperlongumine). *European journal of pharmaceutical sciences : official journal of the European Federation for Pharmaceutical Sciences* **2013,** *48* (3), 453-63.

3. Raj, L.; Ide, T.; Gurkar, A. U.; Foley, M.; Schenone, M.; Li, X.; Tolliday, N. J.; Golub, T. R.; Carr, S. A.; Shamji, A. F.; Stern, A. M.; Mandinova, A.; Schreiber, S. L.; Lee, S. W., Selective killing of cancer cells by a small molecule targeting the stress response to ROS. *Nature* **2011,** *475* (7355), 231-4.

4. Adams, D. J.; Boskovic, Z. V.; Theriault, J. R.; Wang, A. J.; Stern, A. M.; Wagner, B. K.; Shamji, A. F.; Schreiber, S. L., Discovery of small-molecule enhancers of reactive oxygen species that are nontoxic or cause genotype-selective cell death. *ACS chemical biology* **2013,** *8* (5), 923-9.

5. Golovine, K. V.; Makhov, P. B.; Teper, E.; Kutikov, A.; Canter, D.; Uzzo, R. G.; Kolenko, V. M., Piperlongumine induces rapid depletion of the androgen receptor in human prostate cancer cells. *The Prostate* **2013,** *73* (1), 23-30.

6. Makhov, P.; Golovine, K.; Teper, E.; Kutikov, A.; Mehrazin, R.; Corcoran, A.;

Tulin, A.; Uzzo, R. G.; Kolenko, V. M., Piperlongumine promotes autophagy via inhibition of Akt/mTOR signalling and mediates cancer cell death. *British journal of cancer* **2014,** *110* (4), 899-907.

7. Ginzburg, S.; Golovine, K. V.; Makhov, P. B.; Uzzo, R. G.; Kutikov, A.; Kolenko, V. M., Piperlongumine inhibits NF-kappaB activity and attenuates aggressive growth characteristics of prostate cancer cells. *The Prostate* **2014,** *74* (2), 177-86.

8. Song, X.; Gao, T.; Lei, Q.; Zhang, L.; Yao, Y.; Xiong, J., Piperlongumine Induces Apoptosis in Human Melanoma Cells Via Reactive Oxygen Species Mediated Mitochondria Disruption. *Nutrition and cancer* **2018**, 1-10.

9. Seok, J. S.; Jeong, C. H.; Petriello, M. C.; Seo, H. G.; Yoo, H.; Hong, K.; Han, S. G., Piperlongumine decreases cell proliferation and the expression of cell cycle-associated proteins by inhibiting Akt pathway in human lung cancer cells. *Food and Chemical Toxicology* **2018,** *111*, 9-18.

10. Jin, H.-O.; Park, J.-A.; Kim, H.-A.; Chang, Y. H.; Hong, Y. J.; Park, I.-C.; Lee, J. K., Piperlongumine downregulates the expression of HER family in breast cancer cells. *Biochemical and biophysical research communications* **2017,** *486* (4), 1083-1089.

11. Randhawa, H.; Kibble, K.; Zeng, H.; Moyer, M. P.; Reindl, K. M., Activation of ERK signaling and induction of colon cancer cell death by piperlongumine.

Toxicology in vitro : an international journal published in association with BIBRA **2013,** *27* (6), 1626-33.

12. Pei, S.; Minhajuddin, M.; Callahan, K. P.; Balys, M.; Ashton, J. M.; Neering, S. J.; Lagadinou, E. D.; Corbett, C.; Ye, H.; Liesveld, J. L.; O'Dwyer, K. M.; Li, Z.; Shi, L.; Greninger, P.; Settleman, J.; Benes, C.; Hagen, F. K.; Munger, J.; Crooks, P. A.; Becker, M. W.; Jordan, C. T., Targeting aberrant glutathione metabolism to eradicate human acute myelogenous leukemia cells. *The Journal of biological chemistry* **2013,** *288* (47), 33542-58.

13. Han, S. S.; Han, S.; Kamberos, N. L., Piperlongumine inhibits the proliferation and survival of B-cell acute lymphoblastic leukemia cell lines irrespective of glucocorticoid resistance. *Biochemical and biophysical research communications* **2014,** *452* (3), 669-75.

14. Alpay, M.; Yurdakok-Dikmen, B.; Kismali, G.; Sel, T., Antileukemic effects of piperlongumine and alpha lipoic acid combination on Jurkat, MEC1 and NB4 cells in vitro. *Journal of cancer research and therapeutics* **2016,** *12* (2), 556-60.

15. Kang, Q.; Yan, S., Piperlongumine reverses doxorubicin resistance through the PI3K/Akt signaling pathway in K562/A02 human leukemia cells. *Experimental and therapeutic medicine* **2015,** *9* (4), 1345-1350.

16. Dhillon, H.; Chikara, S.; Reindl, K. M., Piperlongumine induces pancreatic

cancer cell death by enhancing reactive oxygen species and DNA damage. *Toxicology reports* **2014,** *1*, 309-318.

17. Chen, Y. J.; Kuo, C. C.; Ting, L. L.; Lu, L. S.; Lu, Y. C.; Cheng, A. J.; Lin, Y. T.; Chen, C. H.; Tsai, J. T.; Chiou, J. F., Piperlongumine inhibits cancer stem cell properties and regulates multiple malignant phenotypes in oral cancer. *Oncology letters* **2018,** *15* (2), 1789-1798.

18. Liu, D.; Qiu, X. Y.; Wu, X.; Hu, D. X.; Li, C. Y.; Yu, S. B.; Pan, F.; Chen, X. Q., Piperlongumine suppresses bladder cancer invasion via inhibiting epithelial mesenchymal transition and F-actin reorganization. *Biochemical and biophysical research communications* **2017,** *494* (1-2), 165-172.

19. Zou, P.; Xia, Y.; Ji, J.; Chen, W.; Zhang, J.; Chen, X.; Rajamanickam, V.; Chen, G.; Wang, Z.; Chen, L.; Wang, Y.; Yang, S.; Liang, G., Piperlongumine as a direct TrxR1 inhibitor with suppressive activity against gastric cancer. *Cancer letters* **2016,** *375* (1), 114-126.

20. Golovine, K.; Makhov, P.; Naito, S.; Raiyani, H.; Tomaszewski, J.; Mehrazin, R.; Tulin, A.; Kutikov, A.; Uzzo, R. G.; Kolenko, V. M., Piperlongumine and its analogs down-regulate expression of c-Met in renal cell carcinoma. *Cancer biology & therapy* **2015,** *16* (5), 743-9.

21. Adams, D. J.; Dai, M.; Pellegrino, G.; Wagner, B. K.; Stern, A. M.; Shamji, A. F.;

Schreiber, S. L., Synthesis, cellular evaluation, and mechanism of action of piperlongumine analogs. *Proceedings of the National Academy of Sciences of the United States of America* **2012,** *109* (38), 15115-20.

22. Han, J. G.; Gupta, S. C.; Prasad, S.; Aggarwal, B. B., Piperlongumine chemosensitizes tumor cells through interaction with cysteine 179 of IkappaBalpha kinase, leading to suppression of NF-kappaB-regulated gene products. *Molecular cancer therapeutics* **2014,** *13* (10), 2422-35.

23. Sun, L. D.; Wang, F.; Dai, F.; Wang, Y. H.; Lin, D.; Zhou, B., Development and mechanism investigation of a new piperlongumine derivative as a potent anti-inflammatory agent. *Biochemical pharmacology* **2015,** *95* (3), 156-69.

24. Lee, H. N.; Jin, H. O.; Park, J. A.; Kim, J. H.; Kim, J. Y.; Kim, B.; Kim, W.; Hong, S. E.; Lee, Y. H.; Chang, Y. H.; Hong, S. I.; Hong, Y. J.; Park, I. C.; Surh, Y. J.; Lee, J. K., Heme oxygenase-1 determines the differential response of breast cancer and normal cells to piperlongumine. *Molecules and cells* **2015,** *38* (4), 327-35.

25. Yan, W. J.; Wang, Q.; Yuan, C. H.; Wang, F.; Ji, Y.; Dai, F.; Jin, X. L.; Zhou, B., Designing piperlongumine-directed anticancer agents by an electrophilicity-based prooxidant strategy: A mechanistic investigation. *Free radical biology & medicine* **2016,** *97*, 109-123.

26. Zhang, Y.; Ma, H.; Wu, Y.; Wu, Z.; Yao, Z.; Zhang, W.; Zhuang, C.; Miao, Z.,

Novel non-trimethoxylphenyl piperlongumine derivatives selectively kill cancer cells. *Bioorganic & medicinal chemistry letters* **2017,** *27* (11), 2308-2312.

27. Poli, G.; Schaur, R. J., 4-Hydroxynonenal in the pathomechanisms of oxidative stress. *IUBMB life* **2000,** *50* (4-5), 315-21.

28. Armstrong, J. S.; Steinauer, K. K.; Hornung, B.; Irish, J. M.; Lecane, P.; Birrell, G. W.; Peehl, D. M.; Knox, S. J., Role of glutathione depletion and reactive oxygen species generation in apoptotic signaling in a human B lymphoma cell line. *Cell death and differentiation* **2002,** *9* (3), 252-63.

29. Forman, H. J., Reactive oxygen species and alpha,beta-unsaturated aldehydes as second messengers in signal transduction. *Annals of the New York Academy of Sciences* **2010,** *1203*, 35-44.

30. Liao, Y.; Niu, X.; Chen, B.; Edwards, H.; Xu, L.; Xie, C.; Lin, H.; Polin, L.; Taub, J. W.; Ge, Y.; Qin, Z., Synthesis and Antileukemic Activities of Piperlongumine and HDAC Inhibitor Hybrids against Acute Myeloid Leukemia Cells. *Journal of medicinal chemistry* **2016,** *59* (17), 7974-90.

31. Xiong, X. X.; Liu, J. M.; Qiu, X. Y.; Pan, F.; Yu, S. B.; Chen, X. Q., Piperlongumine induces apoptotic and autophagic death of the primary myeloid leukemia cells from patients via activation of ROS-p38/JNK pathways. *Acta pharmacologica Sinica* **2015,** *36* (3), 362-74.

32. Thongsom, S.; Suginta, W.; Lee, K. J.; Choe, H.; Talabnin, C., Piperlongumine induces G2/M phase arrest and apoptosis in cholangiocarcinoma cells through the ROS-JNK-ERK signaling pathway. *Apoptosis : an international journal on programmed cell death* **2017,** *22* (11), 1473-1484.

33. Harshbarger, W.; Gondi, S.; Ficarro, S. B.; Hunter, J.; Udayakumar, D.; Gurbani, D.; Singer, W. D.; Liu, Y.; Li, L.; Marto, J. A.; Westover, K. D., Structural and Biochemical Analyses Reveal the Mechanism of Glutathione S-Transferase Pi 1 Inhibition by the Anti-cancer Compound Piperlongumine. *The Journal of biological chemistry* **2017,** *292* (1), 112-120.

34. Jarvius, M.; Fryknas, M.; D'Arcy, P.; Sun, C.; Rickardson, L.; Gullbo, J.; Haglund, C.; Nygren, P.; Linder, S.; Larsson, R., Piperlongumine induces inhibition of the ubiquitin-proteasome system in cancer cells. *Biochemical and biophysical research communications* **2013,** *431* (2), 117-23.

35. Karki, K.; Hedrick, E.; Kasiappan, R.; Jin, U. H.; Safe, S., Piperlongumine Induces Reactive Oxygen Species (ROS)-Dependent Downregulation of Specificity Protein Transcription Factors. *Cancer prevention research* **2017,** *10* (8), 467-477.

36. Gong, L. H.; Chen, X. X.; Wang, H.; Jiang, Q. W.; Pan, S. S.; Qiu, J. G.; Mei, X. L.; Xue, Y. Q.; Qin, W. M.; Zheng, F. Y.; Shi, Z.; Yan, X. J., Piperlongumine induces

apoptosis and synergizes with cisplatin or paclitaxel in human ovarian cancer cells. *Oxidative medicine and cellular longevity* **2014,** *2014*, 906804.

37. Zou, P.; Chen, M.; Ji, J.; Chen, W.; Chen, X.; Ying, S.; Zhang, J.; Zhang, Z.; Liu, Z.; Yang, S.; Liang, G., Auranofin induces apoptosis by ROS-mediated ER stress and mitochondrial dysfunction and displayed synergistic lethality with piperlongumine in gastric cancer. *Oncotarget* **2015,** *6* (34), 36505-21.

38. Li, J.; Sharkey, C. C.; King, M. R., Piperlongumine and immune cytokine TRAIL synergize to promote tumor death. *Scientific reports* **2015,** *5*, 9987.

39. Cullen, P., Case of splenitis acutus in which the serum of the blood drawn from the arm had the appearance of milk. *Edinburgh Medical Journal* **1811,** *7*, 169-71.

40. Kampen, K. R., The discovery and early understanding of leukemia. *Leukemia research* **2012,** *36* (1), 6-13.

41. McKenna, S. J., Leukemia. *Oral surgery, oral medicine, oral pathology, oral radiology, and endodontics* **2000,** *89* (2), 137-9.

42. Horner, M.; Ries, L.; Krapcho, M.; Neyman, N.; Aminou, R.; Howlader, N.; Altekruse, S.; Feuer, E.; Huang, L.; Mariotto, A., SEER Cancer Statistics Review, 1975-2006, National Cancer Institute. Bethesda, MD. 2009.

43. Dohner, H.; Estey, E. H.; Amadori, S.; Appelbaum, F. R.; Buchner, T.; Burnett,

A. K.; Dombret, H.; Fenaux, P.; Grimwade, D.; Larson, R. A.; Lo-Coco, F.; Naoe, T.; Niederwieser, D.; Ossenkoppele, G. J.; Sanz, M. A.; Sierra, J.; Tallman, M. S.; Lowenberg, B.; Bloomfield, C. D.; European, L., Diagnosis and management of acute myeloid leukemia in adults: recommendations from an international expert panel, on behalf of the European LeukemiaNet. *Blood* **2010,** *115* (3), 453-74.

44. Ward, E.; DeSantis, C.; Robbins, A.; Kohler, B.; Jemal, A., Childhood and adolescent cancer statistics, 2014. *CA Cancer J Clin* **2014,** *64* (2), 83-103.

45. Dohner, H.; Weisdorf, D. J.; Bloomfield, C. D., Acute Myeloid Leukemia. *The New England journal of medicine* **2015,** *373* (12), 1136-52.

46. Tamamyan, G.; Kadia, T.; Ravandi, F.; Borthakur, G.; Cortes, J.; Jabbour, E.; Daver, N.; Ohanian, M.; Kantarjian, H.; Konopleva, M., Frontline treatment of acute myeloid leukemia in adults. *Critical reviews in oncology/hematology* **2017,** *110*, 20-34.

47. Disease, G. B. D.; Injury, I.; Prevalence, C., Global, regional, and national incidence, prevalence, and years lived with disability for 310 diseases and injuries, 1990-2015: a systematic analysis for the Global Burden of Disease Study 2015. *Lancet* **2016,** *388* (10053), 1545-1602.

48. Siegel, R.; Jemal, A., Cancer facts & figures 2015. *American Cancer Society. Cancer Facts & Figures* **2015**.

49. Society, A. C., Cancer Facts & Figures 2017. American Cancer Society Atlanta, GA: 2017.

50. Kahn, J. M.; Keegan, T. H.; Tao, L.; Abrahao, R.; Bleyer, A.; Viny, A. D., Racial disparities in the survival of American children, adolescents, and young adults with acute lymphoblastic leukemia, acute myelogenous leukemia, and Hodgkin lymphoma. *Cancer* **2016,** *122* (17), 2723-30.

51. Howlander, N.; Noone, A.; Krapcho, M., SEER Cancer Statistics Review, 1975-2011, National Cancer Institute, Bethesda, MD. Based on November 2013 SEER data submission, posted to the SEER Web site, April 2014. 2016.

52. Arber, D. A.; Orazi, A.; Hasserjian, R.; Thiele, J.; Borowitz, M. J.; Le Beau, M. M.; Bloomfield, C. D.; Cazzola, M.; Vardiman, J. W., The 2016 revision to the World Health Organization classification of myeloid neoplasms and acute leukemia. *Blood* **2016,** *127* (20), 2391-405.

53. Melnick, A.; Licht, J. D., Deconstructing a disease: RARalpha, its fusion partners, and their roles in the pathogenesis of acute promyelocytic leukemia. *Blood* **1999,** *93* (10), 3167-215.

54. Schlenk, R. F.; Dohner, K., Impact of new prognostic markers in treatment decisions in acute myeloid leukemia. *Current opinion in hematology* **2009,** *16* (2), 98-104.

55. Schlenk, R. F.; Dohner, H., Genomic applications in the clinic: use in treatment paradigm of acute myeloid leukemia. *Hematology. American Society of Hematology. Education Program* **2013,** *2013*, 324-30.

56. Marcucci, G.; Haferlach, T.; Dohner, H., Molecular genetics of adult acute myeloid leukemia: prognostic and therapeutic implications. *Journal of clinical oncology : official journal of the American Society of Clinical Oncology* **2011,** *29* (5), 475-86.

57. Patel, J. P.; Gonen, M.; Figueroa, M. E.; Fernandez, H.; Sun, Z.; Racevskis, J.; Van Vlierberghe, P.; Dolgalev, I.; Thomas, S.; Aminova, O.; Huberman, K.; Cheng, J.; Viale, A.; Socci, N. D.; Heguy, A.; Cherry, A.; Vance, G.; Higgins, R. R.; Ketterling, R. P.; Gallagher, R. E.; Litzow, M.; van den Brink, M. R.; Lazarus, H. M.; Rowe, J. M.; Luger, S.; Ferrando, A.; Paietta, E.; Tallman, M. S.; Melnick, A.; Abdel-Wahab, O.; Levine, R. L., Prognostic relevance of integrated genetic profiling in acute myeloid leukemia. *The New England journal of medicine* **2012,** *366* (12), 1079-89.

58. Fathi, A. T.; Abdel-Wahab, O., Mutations in epigenetic modifiers in myeloid malignancies and the prospect of novel epigenetic-targeted therapy. *Advances in hematology* **2012,** *2012*, 469592.

59. Dombret, H., Gene mutation and AML pathogenesis. *Blood* **2011,** *118* (20),

5366-7.

60. Kelly, L. M.; Liu, Q.; Kutok, J. L.; Williams, I. R.; Boulton, C. L.; Gilliland, D. G., FLT3 internal tandem duplication mutations associated with human acute myeloid leukemias induce myeloproliferative disease in a murine bone marrow transplant model. *Blood* **2002,** *99* (1), 310-8.

61. Kelly, L. M.; Kutok, J. L.; Williams, I. R.; Boulton, C. L.; Amaral, S. M.; Curley, D. P.; Ley, T. J.; Gilliland, D. G., PML/RARalpha and FLT3-ITD induce an APL-like disease in a mouse model. *Proceedings of the National Academy of Sciences of the United States of America* **2002,** *99* (12), 8283-8.

62. Shih, A. H.; Abdel-Wahab, O.; Patel, J. P.; Levine, R. L., The role of mutations in epigenetic regulators in myeloid malignancies. *Nature reviews. Cancer* **2012,** *12* (9), 599-612.

63. Bousquet, M.; Harris, M. H.; Zhou, B.; Lodish, H. F., MicroRNA miR-125b causes leukemia. *Proceedings of the National Academy of Sciences of the United States of America* **2010,** *107* (50), 21558-63.

64. Phan, V. T.; Shultz, D. B.; Truong, B. T.; Blake, T. J.; Brown, A. L.; Gonda, T. J.; Le Beau, M. M.; Kogan, S. C., Cooperation of cytokine signaling with chimeric transcription factors in leukemogenesis: PML-retinoic acid receptor alpha blocks growth factor-mediated differentiation. *Molecular and cellular biology* **2003,** *23*

(13), 4573-85.

65. Irwin, M. E.; Rivera-Del Valle, N.; Chandra, J., Redox control of leukemia: from molecular mechanisms to therapeutic opportunities. *Antioxidants & redox signaling* **2013,** *18* (11), 1349-83.

66. Dombret, H.; Gardin, C., An update of current treatments for adult acute myeloid leukemia. *Blood* **2016,** *127* (1), 53-61.

67. Ries, L.; Melbert, D.; Krapcho, M.; Stinchcomb, D.; Howlander, N.; Horner, M.; Mariotto, A.; Miller, B.; Feuer, E.; Altekruse, S., SEER Cancer Statistics Review, 1975–2014; National Cancer Institute: Bethesda, MD, USA.

68. Siegel, R. L.; Miller, K. D.; Jemal, A., Cancer Statistics, 2017. *CA Cancer J Clin* **2017,** *67* (1), 7-30.

69. Ohlmann, C. H., [Chemotherapy of prostate cancer]. *Der Urologe. Ausg. A* **2015,** *54* (10), 1461-9; quiz 1470.

70. Huggins, C.; Hodges, C. V., Studies on prostatic cancer. I. The effect of castration, of estrogen and androgen injection on serum phosphatases in metastatic carcinoma of the prostate. *CA Cancer J Clin* **1972,** *22* (4), 232-40.

71. Wein, A. J.; Kavoussi, L. R.; Novick, A. C.; Partin, A. W.; Peters, C. A., *Campbell-Walsh Urology*. Elsevier Health Sciences: 2011.

72. Harris, W. P.; Mostaghel, E. A.; Nelson, P. S.; Montgomery, B., Androgen

deprivation therapy: progress in understanding mechanisms of resistance and optimizing androgen depletion. *Nature clinical practice. Urology* **2009,** *6* (2), 76-85.

73. Chandrasekar, T.; Yang, J. C.; Gao, A. C.; Evans, C. P., Mechanisms of resistance in castration-resistant prostate cancer (CRPC). *Translational andrology and urology* **2015,** *4* (3), 365-80.

74. Yuan, X.; Cai, C.; Chen, S.; Chen, S.; Yu, Z.; Balk, S. P., Androgen receptor functions in castration-resistant prostate cancer and mechanisms of resistance to new agents targeting the androgen axis. *Oncogene* **2014,** *33* (22), 2815-25.

75. Organization, W. H., GLOBOCAN 2012: Estimated cancer incidence, mortality and prevalence worldwide in 2012. *Lyon, France: International Agency for Research on Cancer* **2014**.

76. Jernberg, E.; Bergh, A.; Wikstrom, P., Clinical relevance of androgen receptor alterations in prostate cancer. *Endocrine connections* **2017,** *6* (8), R146-R161.

77. Watson, P. A.; Chen, Y. F.; Balbas, M. D.; Wongvipat, J.; Socci, N. D.; Viale, A.; Kim, K.; Sawyers, C. L., Constitutively active androgen receptor splice variants expressed in castration-resistant prostate cancer require full-length androgen receptor. *Proceedings of the National Academy of Sciences of the United States of America* **2010,** *107* (39), 16759-65.

78. Hu, R.; Dunn, T. A.; Wei, S.; Isharwal, S.; Veltri, R. W.; Humphreys, E.; Han, M.; Partin, A. W.; Vessella, R. L.; Isaacs, W. B.; Bova, G. S.; Luo, J., Ligand-independent androgen receptor variants derived from splicing of cryptic exons signify hormone-refractory prostate cancer. *Cancer research* **2009,** *69* (1), 16-22.

79. Brinkmann, A. O.; Klaasen, P.; Kuiper, G. G.; van der Korput, J. A.; Bolt, J.; de Boer, W.; Smit, A.; Faber, P. W.; van Rooij, H. C.; Geurts van Kessel, A.; et al., Structure and function of the androgen receptor. *Urological research* **1989,** *17* (2), 87-93.

80. Lallous, N.; Dalal, K.; Cherkasov, A.; Rennie, P. S., Targeting alternative sites on the androgen receptor to treat castration-resistant prostate cancer. *International journal of molecular sciences* **2013,** *14* (6), 12496-519.

81. Ford, O. H., 3rd; Gregory, C. W.; Kim, D.; Smitherman, A. B.; Mohler, J. L., Androgen receptor gene amplification and protein expression in recurrent prostate cancer. *The Journal of urology* **2003,** *170* (5), 1817-21.

82. Waltering, K. K.; Urbanucci, A.; Visakorpi, T., Androgen receptor (AR) aberrations in castration-resistant prostate cancer. *Molecular and cellular endocrinology* **2012,** *360* (1-2), 38-43.

83. Gregory, C. W.; Johnson, R. T., Jr.; Mohler, J. L.; French, F. S.; Wilson, E. M.,

Androgen receptor stabilization in recurrent prostate cancer is associated with hypersensitivity to low androgen. *Cancer research* **2001,** *61* (7), 2892-8.

84. Gioeli, D.; Mandell, J. W.; Petroni, G. R.; Frierson, H. F., Jr.; Weber, M. J., Activation of mitogen-activated protein kinase associated with prostate cancer progression. *Cancer research* **1999,** *59* (2), 279-84.

85. Mellinghoff, I. K.; Vivanco, I.; Kwon, A.; Tran, C.; Wongvipat, J.; Sawyers, C. L., HER2/neu kinase-dependent modulation of androgen receptor function through effects on DNA binding and stability. *Cancer cell* **2004,** *6* (5), 517-27.

86. Mo, W.; Zhang, J.; Li, X.; Meng, D.; Gao, Y.; Yang, S.; Wan, X.; Zhou, C.; Guo, F.; Huang, Y.; Amente, S.; Avvedimento, E. V.; Xie, Y.; Li, Y., Identification of novel AR-targeted microRNAs mediating androgen signalling through critical pathways to regulate cell viability in prostate cancer. *PloS one* **2013,** *8* (2), e56592.

87. Murata, T.; Takayama, K.; Katayama, S.; Urano, T.; Horie-Inoue, K.; Ikeda, K.; Takahashi, S.; Kawazu, C.; Hasegawa, A.; Ouchi, Y.; Homma, Y.; Hayashizaki, Y.; Inoue, S., miR-148a is an androgen-responsive microRNA that promotes LNCaP prostate cell growth by repressing its target CAND1 expression. *Prostate cancer and prostatic diseases* **2010,** *13* (4), 356-61.

88. Shi, X. B.; Xue, L.; Yang, J.; Ma, A. H.; Zhao, J.; Xu, M.; Tepper, C. G.; Evans, C. P.; Kung, H. J.; deVere White, R. W., An androgen-regulated miRNA

suppresses Bak1 expression and induces androgen-independent growth of prostate cancer cells. *Proceedings of the National Academy of Sciences of the United States of America* **2007,** *104* (50), 19983-8.

89. Titus, M. A.; Schell, M. J.; Lih, F. B.; Tomer, K. B.; Mohler, J. L., Testosterone and dihydrotestosterone tissue levels in recurrent prostate cancer. *Clinical cancer research : an official journal of the American Association for Cancer Research* **2005,** *11* (13), 4653-7.

90. Montgomery, R. B.; Mostaghel, E. A.; Vessella, R.; Hess, D. L.; Kalhorn, T. F.; Higano, C. S.; True, L. D.; Nelson, P. S., Maintenance of intratumoral androgens in metastatic prostate cancer: a mechanism for castration-resistant tumor growth. *Cancer research* **2008,** *68* (11), 4447-54.

91. Hofland, J.; van Weerden, W. M.; Dits, N. F.; Steenbergen, J.; van Leenders, G. J.; Jenster, G.; Schroder, F. H.; de Jong, F. H., Evidence of limited contributions for intratumoral steroidogenesis in prostate cancer. *Cancer research* **2010,** *70* (3), 1256-64.

92. Cai, C.; Wang, H.; Xu, Y.; Chen, S.; Balk, S. P., Reactivation of androgen receptor-regulated TMPRSS2:ERG gene expression in castration-resistant prostate cancer. *Cancer research* **2009,** *69* (15), 6027-32.

93. de Bono, J. S.; Logothetis, C. J.; Molina, A.; Fizazi, K.; North, S.; Chu, L.; Chi,

K. N.; Jones, R. J.; Goodman, O. B., Jr.; Saad, F.; Staffurth, J. N.; Mainwaring, P.; Harland, S.; Flaig, T. W.; Hutson, T. E.; Cheng, T.; Patterson, H.; Hainsworth, J. D.; Ryan, C. J.; Sternberg, C. N.; Ellard, S. L.; Flechon, A.; Saleh, M.; Scholz, M.; Efstathiou, E.; Zivi, A.; Bianchini, D.; Loriot, Y.; Chieffo, N.; Kheoh, T.; Haqq, C. M.; Scher, H. I.; Investigators, C.-A.-. Abiraterone and increased survival in metastatic prostate cancer. *The New England journal of medicine* **2011,** *364* (21), 1995-2005.

94. Scher, H. I.; Fizazi, K.; Saad, F.; Taplin, M. E.; Sternberg, C. N.; Miller, K.; de Wit, R.; Mulders, P.; Chi, K. N.; Shore, N. D.; Armstrong, A. J.; Flaig, T. W.; Flechon, A.; Mainwaring, P.; Fleming, M.; Hainsworth, J. D.; Hirmand, M.; Selby, B.; Seely, L.; de Bono, J. S.; Investigators, A., Increased survival with enzalutamide in prostate cancer after chemotherapy. *The New England journal of medicine* **2012,** *367* (13), 1187-97.

95. Antonarakis, E. S.; Lu, C.; Wang, H.; Luber, B.; Nakazawa, M.; Roeser, J. C.; Chen, Y.; Mohammad, T. A.; Chen, Y.; Fedor, H. L.; Lotan, T. L.; Zheng, Q.; De Marzo, A. M.; Isaacs, J. T.; Isaacs, W. B.; Nadal, R.; Paller, C. J.; Denmeade, S. R.; Carducci, M. A.; Eisenberger, M. A.; Luo, J., AR-V7 and resistance to enzalutamide and abiraterone in prostate cancer. *The New England journal of medicine* **2014,** *371* (11), 1028-38.

96. Mostaghel, E. A.; Marck, B. T.; Plymate, S. R.; Vessella, R. L.; Balk, S.; Matsumoto, A. M.; Nelson, P. S.; Montgomery, R. B., Resistance to CYP17A1 inhibition with abiraterone in castration-resistant prostate cancer: induction of steroidogenesis and androgen receptor splice variants. *Clinical cancer research : an official journal of the American Association for Cancer Research* **2011,** *17* (18), 5913-25.

97. Masiello, D.; Cheng, S.; Bubley, G. J.; Lu, M. L.; Balk, S. P., Bicalutamide functions as an androgen receptor antagonist by assembly of a transcriptionally inactive receptor. *The Journal of biological chemistry* **2002,** *277* (29), 26321-6.

98. Farla, P.; Hersmus, R.; Trapman, J.; Houtsmuller, A. B., Antiandrogens prevent stable DNA-binding of the androgen receptor. *Journal of cell science* **2005,** *118* (Pt 18), 4187-98.

99. Bohl, C. E.; Gao, W.; Miller, D. D.; Bell, C. E.; Dalton, J. T., Structural basis for antagonism and resistance of bicalutamide in prostate cancer. *Proceedings of the National Academy of Sciences of the United States of America* **2005,** *102* (17), 6201-6.

100. Chen, C. D.; Welsbie, D. S.; Tran, C.; Baek, S. H.; Chen, R.; Vessella, R.; Rosenfeld, M. G.; Sawyers, C. L., Molecular determinants of resistance to antiandrogen therapy. *Nature medicine* **2004,** *10* (1), 33-9.

101. Efstathiou, E.; Titus, M.; Wen, S.; Hoang, A.; Karlou, M.; Ashe, R.; Tu, S. M.; Aparicio, A.; Troncoso, P.; Mohler, J.; Logothetis, C. J., Molecular characterization of enzalutamide-treated bone metastatic castration-resistant prostate cancer. *European urology* **2015,** *67* (1), 53-60.

102. Robinson, D.; Van Allen, E. M.; Wu, Y. M.; Schultz, N.; Lonigro, R. J.; Mosquera, J. M.; Montgomery, B.; Taplin, M. E.; Pritchard, C. C.; Attard, G.; Beltran, H.; Abida, W.; Bradley, R. K.; Vinson, J.; Cao, X.; Vats, P.; Kunju, L. P.; Hussain, M.; Feng, F. Y.; Tomlins, S. A.; Cooney, K. A.; Smith, D. C.; Brennan, C.; Siddiqui, J.; Mehra, R.; Chen, Y.; Rathkopf, D. E.; Morris, M. J.; Solomon, S. B.; Durack, J. C.; Reuter, V. E.; Gopalan, A.; Gao, J.; Loda, M.; Lis, R. T.; Bowden, M.; Balk, S. P.; Gaviola, G.; Sougnez, C.; Gupta, M.; Yu, E. Y.; Mostaghel, E. A.; Cheng, H. H.; Mulcahy, H.; True, L. D.; Plymate, S. R.; Dvinge, H.; Ferraldeschi, R.; Flohr, P.; Miranda, S.; Zafeiriou, Z.; Tunariu, N.; Mateo, J.; Perez-Lopez, R.; Demichelis, F.; Robinson, B. D.; Schiffman, M.; Nanus, D. M.; Tagawa, S. T.; Sigaras, A.; Eng, K. W.; Elemento, O.; Sboner, A.; Heath, E. I.; Scher, H. I.; Pienta, K. J.; Kantoff, P.; de Bono, J. S.; Rubin, M. A.; Nelson, P. S.; Garraway, L. A.; Sawyers, C. L.; Chinnaiyan, A. M., Integrative clinical genomics of advanced prostate cancer. *Cell* **2015,** *161* (5), 1215-28.

103. Dehm, S. M.; Schmidt, L. J.; Heemers, H. V.; Vessella, R. L.; Tindall, D. J.,

Splicing of a novel androgen receptor exon generates a constitutively active androgen receptor that mediates prostate cancer therapy resistance. *Cancer research* **2008,** *68* (13), 5469-77.

104. Aarnisalo, P.; Palvimo, J. J.; Janne, O. A., CREB-binding protein in androgen receptor-mediated signaling. *Proceedings of the National Academy of Sciences of the United States of America* **1998,** *95* (5), 2122-7.

105. McEwan, I. J.; Gustafsson, J., Interaction of the human androgen receptor transactivation function with the general transcription factor TFIIF. *Proceedings of the National Academy of Sciences of the United States of America* **1997,** *94* (16), 8485-90.

106. Carter, B. S.; Bova, G. S.; Beaty, T. H.; Steinberg, G. D.; Childs, B.; Isaacs, W. B.; Walsh, P. C., Hereditary prostate cancer: epidemiologic and clinical features. *The Journal of urology* **1993,** *150* (3), 797-802.

107. Lee, J.; Demissie, K.; Lu, S. E.; Rhoads, G. G., Cancer incidence among Korean-American immigrants in the United States and native Koreans in South Korea. *Cancer control : journal of the Moffitt Cancer Center* **2007,** *14* (1), 78-85.

108. Bratt, O., Hereditary prostate cancer: clinical aspects. *The Journal of urology* **2002,** *168* (3), 906-13.

109. Johns, L. E.; Houlston, R. S., A systematic review and meta-analysis of

familial prostate cancer risk. *BJU international* **2003,** *91* (9), 789-94.

110. Lichtenstein, P.; Holm, N. V.; Verkasalo, P. K.; Iliadou, A.; Kaprio, J.; Koskenvuo, M.; Pukkala, E.; Skytthe, A.; Hemminki, K., Environmental and heritable factors in the causation of cancer--analyses of cohorts of twins from Sweden, Denmark, and Finland. *The New England journal of medicine* **2000,** *343* (2), 78-85.

111. Shand, R. L.; Gelmann, E. P., Molecular biology of prostate-cancer pathogenesis. *Current opinion in urology* **2006,** *16* (3), 123-31.

112. Goode, E. L.; Stanford, J. L.; Peters, M. A.; Janer, M.; Gibbs, M.; Kolb, S.; Badzioch, M. D.; Hood, L.; Ostrander, E. A.; Jarvik, G. P., Clinical characteristics of prostate cancer in an analysis of linkage to four putative susceptibility loci. *Clinical cancer research : an official journal of the American Association for Cancer Research* **2001,** *7* (9), 2739-49.

113. Xu, J.; Dimitrov, L.; Chang, B. L.; Adams, T. S.; Turner, A. R.; Meyers, D. A.; Eeles, R. A.; Easton, D. F.; Foulkes, W. D.; Simard, J.; Giles, G. G.; Hopper, J. L.; Mahle, L.; Moller, P.; Bishop, T.; Evans, C.; Edwards, S.; Meitz, J.; Bullock, S.; Hope, Q.; Hsieh, C. L.; Halpern, J.; Balise, R. N.; Oakley-Girvan, I.; Whittemore, A. S.; Ewing, C. M.; Gielzak, M.; Isaacs, S. D.; Walsh, P. C.; Wiley, K. E.; Isaacs, W. B.; Thibodeau, S. N.; McDonnell, S. K.; Cunningham, J. M.; Zarfas, K. E.;

Hebbring, S.; Schaid, D. J.; Friedrichsen, D. M.; Deutsch, K.; Kolb, S.; Badzioch, M.; Jarvik, G. P.; Janer, M.; Hood, L.; Ostrander, E. A.; Stanford, J. L.; Lange, E. M.; Beebe-Dimmer, J. L.; Mohai, C. E.; Cooney, K. A.; Ikonen, T.; Baffoe-Bonnie, A.; Fredriksson, H.; Matikainen, M. P.; Tammela, T.; Bailey-Wilson, J.; Schleutker, J.; Maier, C.; Herkommer, K.; Hoegel, J. J.; Vogel, W.; Paiss, T.; Wiklund, F.; Emanuelsson, M.; Stenman, E.; Jonsson, B. A.; Gronberg, H.; Camp, N. J.; Farnham, J.; Cannon-Albright, L. A.; Seminara, D.; Consortium, A., A combined genomewide linkage scan of 1,233 families for prostate cancer-susceptibility genes conducted by the international consortium for prostate cancer genetics. *American journal of human genetics* **2005,** *77* (2), 219-29.

114. Eeles, R.; Goh, C.; Castro, E.; Bancroft, E.; Guy, M.; Al Olama, A. A.; Easton, D.; Kote-Jarai, Z., The genetic epidemiology of prostate cancer and its clinical implications. *Nature reviews. Urology* **2014,** *11* (1), 18-31.

115. Al Olama, A. A.; Kote-Jarai, Z.; Giles, G. G.; Guy, M.; Morrison, J.; Severi, G.; Leongamornlert, D. A.; Tymrakiewicz, M.; Jhavar, S.; Saunders, E.; Hopper, J. L.; Southey, M. C.; Muir, K. R.; English, D. R.; Dearnaley, D. P.; Ardern-Jones, A. T.; Hall, A. L.; O'Brien, L. T.; Wilkinson, R. A.; Sawyer, E.; Lophatananon, A.; Oncology, U. K. G. P. C. S. C. B. A. o. U. S. S. o.; cancer, U. K. P. t. f.; Treatment study, C.; Horwich, A.; Huddart, R. A.; Khoo, V. S.; Parker, C. C.; Woodhouse, C.

J.; Thompson, A.; Christmas, T.; Ogden, C.; Cooper, C.; Donovan, J. L.; Hamdy, F. C.; Neal, D. E.; Eeles, R. A.; Easton, D. F., Multiple loci on 8q24 associated with prostate cancer susceptibility. *Nature genetics* **2009,** *41* (10), 1058-60.

116. Amundadottir, L. T.; Sulem, P.; Gudmundsson, J.; Helgason, A.; Baker, A.; Agnarsson, B. A.; Sigurdsson, A.; Benediktsdottir, K. R.; Cazier, J. B.; Sainz, J.; Jakobsdottir, M.; Kostic, J.; Magnusdottir, D. N.; Ghosh, S.; Agnarsson, K.; Birgisdottir, B.; Le Roux, L.; Olafsdottir, A.; Blondal, T.; Andresdottir, M.; Gretarsdottir, O. S.; Bergthorsson, J. T.; Gudbjartsson, D.; Gylfason, A.; Thorleifsson, G.; Manolescu, A.; Kristjansson, K.; Geirsson, G.; Isaksson, H.; Douglas, J.; Johansson, J. E.; Balter, K.; Wiklund, F.; Montie, J. E.; Yu, X.; Suarez, B. K.; Ober, C.; Cooney, K. A.; Gronberg, H.; Catalona, W. J.; Einarsson, G. V.; Barkardottir, R. B.; Gulcher, J. R.; Kong, A.; Thorsteinsdottir, U.; Stefansson, K., A common variant associated with prostate cancer in European and African populations. *Nature genetics* **2006,** *38* (6), 652-8.

117. Yeager, M.; Orr, N.; Hayes, R. B.; Jacobs, K. B.; Kraft, P.; Wacholder, S.; Minichiello, M. J.; Fearnhead, P.; Yu, K.; Chatterjee, N.; Wang, Z.; Welch, R.; Staats, B. J.; Calle, E. E.; Feigelson, H. S.; Thun, M. J.; Rodriguez, C.; Albanes, D.; Virtamo, J.; Weinstein, S.; Schumacher, F. R.; Giovannucci, E.; Willett, W. C.; Cancel-Tassin, G.; Cussenot, O.; Valeri, A.; Andriole, G. L.; Gelmann, E. P.;

Tucker, M.; Gerhard, D. S.; Fraumeni, J. F., Jr.; Hoover, R.; Hunter, D. J.; Chanock, S. J.; Thomas, G., Genome-wide association study of prostate cancer identifies a second risk locus at 8q24. *Nature genetics* **2007,** *39* (5), 645-9.

118. Ahmadiyeh, N.; Pomerantz, M. M.; Grisanzio, C.; Herman, P.; Jia, L.; Almendro, V.; He, H. H.; Brown, M.; Liu, X. S.; Davis, M.; Caswell, J. L.; Beckwith, C. A.; Hills, A.; Macconaill, L.; Coetzee, G. A.; Regan, M. M.; Freedman, M. L., 8q24 prostate, breast, and colon cancer risk loci show tissue-specific long-range interaction with MYC. *Proceedings of the National Academy of Sciences of the United States of America* **2010,** *107* (21), 9742-6.

119. Kote-Jarai, Z.; Leongamornlert, D.; Tymrakiewicz, M.; Field, H.; Guy, M.; Al Olama, A. A.; Morrison, J.; O'Brien, L.; Wilkinson, R.; Hall, A.; Sawyer, E.; Muir, K.; Hamdy, F.; Donovan, J.; Neal, D.; Easton, D.; Eeles, R., Mutation analysis of the MSMB gene in familial prostate cancer. *British journal of cancer* **2010,** *102* (2), 414-8.

120. Kote-Jarai, Z.; Amin Al Olama, A.; Leongamornlert, D.; Tymrakiewicz, M.; Saunders, E.; Guy, M.; Giles, G. G.; Severi, G.; Southey, M.; Hopper, J. L.; Sit, K. C.; Harris, J. M.; Batra, J.; Spurdle, A. B.; Clements, J. A.; Hamdy, F.; Neal, D.; Donovan, J.; Muir, K.; Pharoah, P. D.; Chanock, S. J.; Brown, N.; Benlloch, S.; Castro, E.; Mahmud, N.; O'Brien, L.; Hall, A.; Sawyer, E.; Wilkinson, R.; Easton, D.

F.; Eeles, R. A., Identification of a novel prostate cancer susceptibility variant in the KLK3 gene transcript. *Human genetics* **2011,** *129* (6), 687-94.

121. Kote-Jarai, Z.; Olama, A. A.; Giles, G. G.; Severi, G.; Schleutker, J.; Weischer, M.; Campa, D.; Riboli, E.; Key, T.; Gronberg, H.; Hunter, D. J.; Kraft, P.; Thun, M. J.; Ingles, S.; Chanock, S.; Albanes, D.; Hayes, R. B.; Neal, D. E.; Hamdy, F. C.; Donovan, J. L.; Pharoah, P.; Schumacher, F.; Henderson, B. E.; Stanford, J. L.; Ostrander, E. A.; Sorensen, K. D.; Dork, T.; Andriole, G.; Dickinson, J. L.; Cybulski, C.; Lubinski, J.; Spurdle, A.; Clements, J. A.; Chambers, S.; Aitken, J.; Gardiner, R. A.; Thibodeau, S. N.; Schaid, D.; John, E. M.; Maier, C.; Vogel, W.; Cooney, K. A.; Park, J. Y.; Cannon-Albright, L.; Brenner, H.; Habuchi, T.; Zhang, H. W.; Lu, Y. J.; Kaneva, R.; Muir, K.; Benlloch, S.; Leongamornlert, D. A.; Saunders, E. J.; Tymrakiewicz, M.; Mahmud, N.; Guy, M.; O'Brien, L. T.; Wilkinson, R. A.; Hall, A. L.; Sawyer, E. J.; Dadaev, T.; Morrison, J.; Dearnaley, D. P.; Horwich, A.; Huddart, R. A.; Khoo, V. S.; Parker, C. C.; Van As, N.; Woodhouse, C. J.; Thompson, A.; Christmas, T.; Ogden, C.; Cooper, C. S.; Lophatonanon, A.; Southey, M. C.; Hopper, J. L.; English, D. R.; Wahlfors, T.; Tammela, T. L.; Klarskov, P.; Nordestgaard, B. G.; Roder, M. A.; Tybjaerg-Hansen, A.; Bojesen, S. E.; Travis, R.; Canzian, F.; Kaaks, R.; Wiklund, F.; Aly, M.; Lindstrom, S.; Diver, W. R.; Gapstur, S.; Stern, M. C.; Corral, R.; Virtamo, J.; Cox, A.; Haiman, C. A.; Le

Marchand, L.; Fitzgerald, L.; Kolb, S.; Kwon, E. M.; Karyadi, D. M.; Orntoft, T. F.; Borre, M.; Meyer, A.; Serth, J.; Yeager, M.; Berndt, S. I.; Marthick, J. R.; Patterson, B.; Wokolorczyk, D.; Batra, J.; Lose, F.; McDonnell, S. K.; Joshi, A. D.; Shahabi, A.; Rinckleb, A. E.; Ray, A.; Sellers, T. A.; Lin, H. Y.; Stephenson, R. A.; Farnham, J.; Muller, H.; Rothenbacher, D.; Tsuchiya, N.; Narita, S.; Cao, G. W.; Slavov, C.; Mitev, V.; Easton, D. F.; Eeles, R. A.; Oncology, U. K. G. P. C. S. C. B. A. o. U. S. S. o.; Uk ProtecT Study Collaborators, T. A. P. C. B.; Consortium, P., Seven prostate cancer susceptibility loci identified by a multi-stage genome-wide association study. *Nature genetics* **2011,** *43* (8), 785-91.

122. Toyokuni, S.; Okamoto, K.; Yodoi, J.; Hiai, H., Persistent oxidative stress in cancer. *FEBS letters* **1995,** *358* (1), 1-3.

123. Ames, B. N.; Shigenaga, M. K.; Hagen, T. M., Oxidants, antioxidants, and the degenerative diseases of aging. *Proceedings of the National Academy of Sciences of the United States of America* **1993,** *90* (17), 7915-22.

124. Meister, A., On the discovery of glutathione. *Trends in biochemical sciences* **1988,** *13* (5), 185-8.

125. Hayes, J. D.; Pulford, D. J., The glutathione S-transferase supergene family: regulation of GST and the contribution of the isoenzymes to cancer chemoprotection and drug resistance. *Critical reviews in biochemistry and*

molecular biology **1995,** *30* (6), 445-600.

126. Cairns, P.; Esteller, M.; Herman, J. G.; Schoenberg, M.; Jeronimo, C.; Sanchez-Cespedes, M.; Chow, N. H.; Grasso, M.; Wu, L.; Westra, W. B.; Sidransky, D., Molecular detection of prostate cancer in urine by GSTP1 hypermethylation. *Clinical cancer research : an official journal of the American Association for Cancer Research* **2001,** *7* (9), 2727-30.

127. Nelson, W. G.; De Marzo, A. M.; DeWeese, T. L., The molecular pathogenesis of prostate cancer: Implications for prostate cancer prevention. *Urology* **2001,** *57* (4 Suppl 1), 39-45.

128. Lin, X.; Tascilar, M.; Lee, W. H.; Vles, W. J.; Lee, B. H.; Veeraswamy, R.; Asgari, K.; Freije, D.; van Rees, B.; Gage, W. R.; Bova, G. S.; Isaacs, W. B.; Brooks, J. D.; DeWeese, T. L.; De Marzo, A. M.; Nelson, W. G., GSTP1 CpG island hypermethylation is responsible for the absence of GSTP1 expression in human prostate cancer cells. *The American journal of pathology* **2001,** *159* (5), 1815-26.

129. Bastian, P. J.; Ellinger, J.; Schmidt, D.; Wernert, N.; Wellmann, A.; Muller, S. C.; von Rucker, A., GSTP1 hypermethylation as a molecular marker in the diagnosis of prostatic cancer: is there a correlation with clinical stage, Gleason grade, PSA value or age? *European journal of medical research* **2004,** *9* (11),

523-7.

130. Nelson, C. P.; Kidd, L. C.; Sauvageot, J.; Isaacs, W. B.; De Marzo, A. M.; Groopman, J. D.; Nelson, W. G.; Kensler, T. W., Protection against 2-hydroxyamino-1-methyl-6-phenylimidazo[4,5-b]pyridine cytotoxicity and DNA adduct formation in human prostate by glutathione S-transferase P1. *Cancer research* **2001,** *61* (1), 103-9.

131. Bostwick, D. G.; Liu, L.; Brawer, M. K.; Qian, J., High-grade prostatic intraepithelial neoplasia. *Reviews in urology* **2004,** *6* (4), 171-9.

132. Hokaiwado, N.; Takeshita, F.; Naiki-Ito, A.; Asamoto, M.; Ochiya, T.; Shirai, T., Glutathione S-transferase Pi mediates proliferation of androgen-independent prostate cancer cells. *Carcinogenesis* **2008,** *29* (6), 1134-8.

133. Yu, D. S.; Hsieh, D. S.; Chang, S. Y., Increasing expression of GST-pi MIF, and ID1 genes in chemoresistant prostate cancer cells. *Archives of andrology* **2006,** *52* (4), 275-81.

134. Ruzza, P.; Rosato, A.; Rossi, C. R.; Floreani, M.; Quintieri, L., Glutathione transferases as targets for cancer therapy. *Anti-cancer agents in medicinal chemistry* **2009,** *9* (7), 763-77.

135. Mottet, N.; Bellmunt, J.; Briers, E.; Van den Bergh, R.; Bolla, M.; Van Casteren, N.; Cornford, P.; Culine, S.; Joniau, S.; Lam, T., Guidelines on prostate

cancer. *European urology* **2014,** *65* (1), 124-37.

136. Tilki, D.; Schaeffer, E. M.; Evans, C. P., Understanding Mechanisms of Resistance in Metastatic Castration-resistant Prostate Cancer: The Role of the Androgen Receptor. *European urology focus* **2016,** *2* (5), 499-505.

137. Yoo, S.; Choi, S. Y.; You, D.; Kim, C. S., New drugs in prostate cancer. *Prostate international* **2016,** *4* (2), 37-42.

138. Schieber, M.; Chandel, N. S., ROS function in redox signaling and oxidative stress. *Current biology : CB* **2014,** *24* (10), R453-62.

139. Cairns, R. A.; Harris, I. S.; Mak, T. W., Regulation of cancer cell metabolism. *Nature reviews. Cancer* **2011,** *11* (2), 85-95.

140. Schumacker, P. T., Reactive oxygen species in cancer cells: live by the sword, die by the sword. *Cancer cell* **2006,** *10* (3), 175-6.

141. Liou, G. Y.; Storz, P., Reactive oxygen species in cancer. *Free radical research* **2010,** *44* (5), 479-96.

142. Singh, J.; Petter, R. C.; Baillie, T. A.; Whitty, A., The resurgence of covalent drugs. *Nature reviews. Drug discovery* **2011,** *10* (4), 307-17.

143. (a) Pollyea, D. A.; Gutman, J. A.; Gore, L.; Smith, C. A.; Jordan, C. T., Targeting acute myeloid leukemia stem cells: a review and principles for the development of clinical trials. *Haematologica* **2014,** *99* (8), 1277-84; (b) Barabe, F.;

Kennedy, J. A.; Hope, K. J.; Dick, J. E., Modeling the initiation and progression of human acute leukemia in mice. *Science* **2007,** *316* (5824), 600-4.

144. Gu, W.; Roeder, R. G., Activation of p53 sequence-specific DNA binding by acetylation of the p53 C-terminal domain. *Cell* **1997,** *90* (4), 595-606.

145. Chen, L.-f.; Fischle, W.; Verdin, E.; Greene, W. C., Duration of nuclear NF-κB action regulated by reversible acetylation. *Science* **2001,** *293* (5535), 1653-1657.

146. Glozak, M.; Seto, E., Histone deacetylases and cancer. *Oncogene* **2007,** *26* (37), 5420-5432.

147. Deroanne, C. F.; Bonjean, K.; Servotte, S.; Devy, L.; Colige, A.; Clausse, N.; Blacher, S.; Verdin, E.; Foidart, J.-M.; Nusgens, B. V., Histone deacetylases inhibitors as anti-angiogenic agents altering vascular endothelial growth factor signaling. *Oncogene* **2002,** *21* (3), 427-436.

148. Medina, V.; Edmonds, B.; Young, G. P.; James, R.; Appleton, S.; Zalewski, P. D., Induction of caspase-3 protease activity and apoptosis by butyrate and trichostatin A (inhibitors of histone deacetylase): dependence on protein synthesis and synergy with a mitochondrial/cytochrome c-dependent pathway. *Cancer Research* **1997,** *57* (17), 3697-3707.

149. Bolden, J. E.; Peart, M. J.; Johnstone, R. W., Anticancer activities of

histone deacetylase inhibitors. *Nature reviews Drug discovery* **2006,** *5* (9), 769-784.

150. Petruccelli, L. A.; Dupere-Richer, D.; Pettersson, F.; Retrouvey, H.; Skoulikas, S.; Miller, W. H., Jr., Vorinostat induces reactive oxygen species and DNA damage in acute myeloid leukemia cells. *PloS one* **2011,** *6* (6), e20987.

151. Robert, C.; Rassool, F. V., HDAC inhibitors: roles of DNA damage and repair. *Advances in cancer research* **2012,** *116*, 87-129.

152. Munshi, A.; Kurland, J. F.; Nishikawa, T.; Tanaka, T.; Hobbs, M. L.; Tucker, S. L.; Ismail, S.; Stevens, C.; Meyn, R. E., Histone deacetylase inhibitors radiosensitize human melanoma cells by suppressing DNA repair activity. *Clinical cancer research : an official journal of the American Association for Cancer Research* **2005,** *11* (13), 4912-22.

153. Xie, C.; Drenberg, C.; Edwards, H.; Caldwell, J. T.; Chen, W.; Inaba, H.; Xu, X.; Buck, S. A.; Taub, J. W.; Baker, S. D.; Ge, Y., Panobinostat enhances cytarabine and daunorubicin sensitivities in AML cells through suppressing the expression of BRCA1, CHK1, and Rad51. *PloS one* **2013,** *8* (11), e79106.

154. Kuo, Y. H.; Qi, J.; Cook, G. J., Regain control of p53: Targeting leukemia stem cells by isoform-specific HDAC inhibition. *Experimental hematology* **2016,** *44* (5), 315-21.

155. Zhang, B.; Strauss, A. C.; Chu, S.; Li, M.; Ho, Y.; Shiang, K. D.; Snyder, D. S.; Huettner, C. S.; Shultz, L.; Holyoake, T.; Bhatia, R., Effective targeting of quiescent chronic myelogenous leukemia stem cells by histone deacetylase inhibitors in combination with imatinib mesylate. *Cancer cell* **2010,** *17* (5), 427-42.

156. Garcia-Manero, G.; Yang, H.; Bueso-Ramos, C.; Ferrajoli, A.; Cortes, J.; Wierda, W. G.; Faderl, S.; Koller, C.; Morris, G.; Rosner, G.; Loboda, A.; Fantin, V. R.; Randolph, S. S.; Hardwick, J. S.; Reilly, J. F.; Chen, C.; Ricker, J. L.; Secrist, J. P.; Richon, V. M.; Frankel, S. R.; Kantarjian, H. M., Phase 1 study of the histone deacetylase inhibitor vorinostat (suberoylanilide hydroxamic acid [SAHA]) in patients with advanced leukemias and myelodysplastic syndromes. *Blood* **2008,** *111* (3), 1060-6.

157. Zhou, L.; Zhang, Y.; Chen, S.; Kmieciak, M.; Leng, Y.; Lin, H.; Rizzo, K.; Dumur, C.; Ferreira-Gonzalez, A.; Dai, Y., A regimen combining the Wee1 inhibitor AZD1775 with HDAC inhibitors targets human acute myeloid leukemia cells harboring various genetic mutations. *Leukemia* **2015,** *29* (4), 807-818.

158. Dai, Y.; Chen, S.; Kmieciak, M.; Zhou, L.; Lin, H.; Pei, X. Y.; Grant, S., The novel Chk1 inhibitor MK-8776 sensitizes human leukemia cells to HDAC inhibitors by targeting the intra-S checkpoint and DNA replication and repair. *Molecular cancer therapeutics* **2013,** *12* (6), 878-89.

159. Hartwell, K. A.; Miller, P. G.; Mukherjee, S.; Kahn, A. R.; Stewart, A. L.; Logan, D. J.; Negri, J. M.; Duvet, M.; Jaras, M.; Puram, R.; Dancik, V.; Al-Shahrour, F.; Kindler, T.; Tothova, Z.; Chattopadhyay, S.; Hasaka, T.; Narayan, R.; Dai, M.; Huang, C.; Shterental, S.; Chu, L. P.; Haydu, J. E.; Shieh, J. H.; Steensma, D. P.; Munoz, B.; Bittker, J. A.; Shamji, A. F.; Clemons, P. A.; Tolliday, N. J.; Carpenter, A. E.; Gilliland, D. G.; Stern, A. M.; Moore, M. A. S.; Scadden, D. T.; Schreiber, S. L.; Ebert, B. L.; Golub, T. R., Niche-based screening identifies small-molecule inhibitors of leukemia stem cells. *Nature chemical biology* **2013,** *9* (12), 840-848.

160. Okamoto, S.; Narita, T.; Sasanuma, H.; Takeda, S.; Masunaga, S.; Bessho, T.; Tano, K., Impact of DNA repair pathways on the cytotoxicity of piperlongumine in chicken DT40 cell-lines. *Genes & cancer* **2014,** *5* (7-8), 285-92.

161. Dhillon, H.; Chikara, S.; Reindl, K. M., Piperlongumine induces pancreatic cancer cell death by enhancing reactive oxygen species and DNA damage. *Toxicology reports* **2014,** *1*, 309-318.

162. Shrivastava, S.; Kulkarni, P.; Thummuri, D.; Jeengar, M. K.; Naidu, V. G.; Alvala, M.; Redddy, G. B.; Ramakrishna, S., Piperlongumine, an alkaloid causes inhibition of PI3 K/Akt/mTOR signaling axis to induce caspase-dependent apoptosis in human triple-negative breast cancer cells. *Apoptosis : an*

international journal on programmed cell death **2014,** *19* (7), 1148-64.

163. Meunier, B., Hybrid Molecules with a Dual Mode of Action: Dream or Reality?†. *Accounts of chemical research* **2007,** *41* (1), 69-77.

164. Wu, Y.; Min, X.; Zhuang, C.; Li, J.; Yu, Z.; Dong, G.; Yao, J.; Wang, S.; Liu, Y.; Wu, S.; Zhu, S.; Sheng, C.; Wei, Y.; Zhang, H.; Zhang, W.; Miao, Z., Design, synthesis and biological activity of piperlongumine derivatives as selective anticancer agents. *European journal of medicinal chemistry* **2014,** *82*, 545-51.

165. Winter, D. K.; Drouin, A.; Lessard, J.; Spino, C., Photochemical rearrangement of N-chlorolactams: a route to N-heterocycles through concerted ring contraction. *The Journal of organic chemistry* **2010,** *75* (8), 2610-8.

166. Kawanaka, Y.; Kobayashi, K.; Kusuda, S.; Tatsumi, T.; Murota, M.; Nishiyama, T.; Hisaichi, K.; Fujii, A.; Hirai, K.; Nishizaki, M.; Naka, M.; Komeno, M.; Nakai, H.; Toda, M., Design and synthesis of orally bioavailable inhibitors of inducible nitric oxide synthase. synthesis and biological evaluation of dihydropyridin-2(1H)-imines and 1,5,6,7-tetrahydro-2H-azepin-2-imines. *Bioorganic & medicinal chemistry* **2003,** *11* (5), 689-702.

167. Thein, M. S.; Ershler, W. B.; Jemal, A.; Yates, J. W.; Baer, M. R., Outcome of older patients with acute myeloid leukemia: an analysis of SEER data over 3 decades. *Cancer* **2013,** *119* (15), 2720-7.

168. Quintas-Cardama, A.; Santos, F. P.; Garcia-Manero, G., Histone deacetylase inhibitors for the treatment of myelodysplastic syndrome and acute myeloid leukemia. *Leukemia* **2011,** *25* (2), 226-35.

169. Kirschbaum, M. H.; Foon, K. A.; Frankel, P.; Ruel, C.; Pulone, B.; Tuscano, J. M.; Newman, E. M., A phase 2 study of belinostat (PXD101) in patients with relapsed or refractory acute myeloid leukemia or patients over the age of 60 with newly diagnosed acute myeloid leukemia: a California Cancer Consortium Study. *Leuk Lymphoma* **2014,** *55* (10), 2301-4.

170. (a) Gryder, B. E.; Sodji, Q. H.; Oyelere, A. K., Targeted cancer therapy: giving histone deacetylase inhibitors all they need to succeed. *Future medicinal chemistry* **2012,** *4* (4), 505-24; (b) Subramanian, S.; Bates, S. E.; Wright, J. J.; Espinoza-Delgado, I.; Piekarz, R. L., Clinical Toxicities of Histone Deacetylase Inhibitors. *Pharmaceuticals (Basel)* **2010,** *3* (9), 2751-2767.

171. (a) Silhar, P.; Eubanks, L. M.; Seki, H.; Pellett, S.; Javor, S.; Tepp, W. H.; Johnson, E. A.; Janda, K. D., Targeting botulinum A cellular toxicity: a prodrug approach. *Journal of medicinal chemistry* **2013,** *56* (20), 7870-9; (b) Daniel, K. B.; Sullivan, E. D.; Chen, Y.; Chan, J. C.; Jennings, P. A.; Fierke, C. A.; Cohen, S. M., Dual-Mode HDAC Prodrug for Covalent Modification and Subsequent Inhibitor Release. *Journal of medicinal chemistry* **2015,** *58* (11), 4812-21.

172. Schlimme, S.; Hauser, A. T.; Carafa, V.; Heinke, R.; Kannan, S.; Stolfa, D. A.; Cellamare, S.; Carotti, A.; Altucci, L.; Jung, M.; Sippl, W., Carbamate prodrug concept for hydroxamate HDAC inhibitors. *ChemMedChem* **2011,** *6* (7), 1193-8.

173. Zielonka, J.; Sikora, A.; Hardy, M.; Joseph, J.; Dranka, B. P.; Kalyanaraman, B., Boronate probes as diagnostic tools for real time monitoring of peroxynitrite and hydroperoxides. *Chemical research in toxicology* **2012,** *25* (9), 1793-9.

174. Sikora, A.; Zielonka, J.; Lopez, M.; Joseph, J.; Kalyanaraman, B., Direct oxidation of boronates by peroxynitrite: mechanism and implications in fluorescence imaging of peroxynitrite. *Free radical biology & medicine* **2009,** *47* (10), 1401-7.

175. Mann, B. S.; Johnson, J. R.; Cohen, M. H.; Justice, R.; Pazdur, R., FDA approval summary: vorinostat for treatment of advanced primary cutaneous T-cell lymphoma. *The oncologist* **2007,** *12* (10), 1247-52.

176. (a) Er, T. K.; Tsai, S. M.; Wu, S. H.; Chiang, W.; Lin, H. C.; Lin, S. F.; Wu, S. H.; Tsai, L. Y.; Liu, T. Z., Antioxidant status and superoxide anion radical generation in acute myeloid leukemia. *Clinical biochemistry* **2007,** *40* (13-14), 1015-9; (b) Zhou, F. L.; Zhang, W. G.; Wei, Y. C.; Meng, S.; Bai, G. G.; Wang, B. Y.; Yang, H. Y.; Tian, W.; Meng, X.; Zhang, H.; Chen, S. P., Involvement of oxidative

stress in the relapse of acute myeloid leukemia. *J Biol Chem* **2010,** *285* (20), 15010-5; (c) Hole, P. S.; Zabkiewicz, J.; Munje, C.; Newton, Z.; Pearn, L.; White, P.; Marquez, N.; Hills, R. K.; Burnett, A. K.; Tonks, A.; Darley, R. L., Overproduction of NOX-derived ROS in AML promotes proliferation and is associated with defective oxidative stress signaling. *Blood* **2013,** *122* (19), 3322-30.

177. Sieracki, N. A.; Gantner, B. N.; Mao, M.; Horner, J. H.; Ye, R. D.; Malik, A. B.; Newcomb, M. E.; Bonini, M. G., Bioluminescent detection of peroxynitrite with a boronic acid-caged luciferin. *Free radical biology & medicine* **2013,** *61*, 40-50.

178. Passaro, D.; Di Tullio, A.; Abarrategi, A.; Rouault-Pierre, K.; Foster, K.; Ariza-McNaughton, L.; Montaner, B.; Chakravarty, P.; Bhaw, L.; Diana, G.; Lassailly, F.; Gribben, J.; Bonnet, D., Increased Vascular Permeability in the Bone Marrow Microenvironment Contributes to Disease Progression and Drug Response in Acute Myeloid Leukemia. *Cancer Cell* **2017,** *32* (3), 324-341 e6.

179. Gediya, L. K.; Chopra, P.; Purushottamachar, P.; Maheshwari, N.; Njar, V. C., A new simple and high-yield synthesis of suberoylanilide hydroxamic acid and its inhibitory effect alone or in combination with retinoids on proliferation of human prostate cancer cells. *Journal of medicinal chemistry* **2005,** *48* (15), 5047-51.

180. Wang, L.; Xie, S.; Ma, L.; Chen, Y.; Lu, W., 10-Boronic acid substituted

camptothecin as prodrug of SN-38. *Eur J Med Chem* **2016,** *116*, 84-89.

181. Das, B. C.; Thapa, P.; Karki, R.; Schinke, C.; Das, S.; Kambhampati, S.; Banerjee, S. K.; Van Veldhuizen, P.; Verma, A.; Weiss, L. M.; Evans, T., Boron chemicals in diagnosis and therapeutics. *Future medicinal chemistry* **2013,** *5* (6), 653-76.

182. Hulsman, N.; Medema, J. P.; Bos, C.; Jongejan, A.; Leurs, R.; Smit, M. J.; de Esch, I. J.; Richel, D.; Wijtmans, M., Chemical insights in the concept of hybrid drugs: the antitumor effect of nitric oxide-donating aspirin involves a quinone methide but not nitric oxide nor aspirin. *Journal of medicinal chemistry* **2007,** *50* (10), 2424-31.

183. Lippert, A. R.; Van de Bittner, G. C.; Chang, C. J., Boronate oxidation as a bioorthogonal reaction approach for studying the chemistry of hydrogen peroxide in living systems. *Accounts of chemical research* **2011,** *44* (9), 793-804.

184. Zheng, S.; Guo, S.; Zhong, Q.; Zhang, C.; Liu, J.; Yang, L.; Zhang, Q.; Wang, G., Biocompatible Boron-Containing Prodrugs of Belinostat for the Potential Treatment of Solid Tumors. *ACS medicinal chemistry letters* **2018,** *9* (2), 149-154.

185. Bose, P.; Grant, S., Rational Combinations of Targeted Agents in AML. *J Clin Med* **2015,** *4* (4), 634-64.

186. Garcia-Manero, G.; Tambaro, F. P.; Bekele, N. B.; Yang, H.; Ravandi, F.; Jabbour, E.; Borthakur, G.; Kadia, T. M.; Konopleva, M. Y.; Faderl, S.; Cortes, J. E.; Brandt, M.; Hu, Y.; McCue, D.; Newsome, W. M.; Pierce, S. R.; de Lima, M.; Kantarjian, H. M., Phase II trial of vorinostat with idarubicin and cytarabine for patients with newly diagnosed acute myelogenous leukemia or myelodysplastic syndrome. *J Clin Oncol* **2012,** *30* (18), 2204-10.

187. Janganati, V.; Ponder, J.; Jordan, C. T.; Borrelli, M. J.; Penthala, N. R.; Crooks, P. A., Dimers of Melampomagnolide B Exhibit Potent Anticancer Activity against Hematological and Solid Tumor Cells. *Journal of medicinal chemistry* **2015,** *58* (22), 8896-906.

188. Bai, M.; Huang, J.; Zheng, X.; Song, Z.; Tang, M.; Mao, W.; Yuan, L.; Wu, J.; Weng, X.; Zhou, X., Highly selective suppression of melanoma cells by inducible DNA cross-linking agents: bis(catechol) derivatives. *Journal of the American Chemical Society* **2010,** *132* (43), 15321-7.

189. Zarko V. Boskovic, M. M. H., Drew J. Adams, Mingji Dai, Stuart L. Schreiber, Synthesis of piperlogs and analysis of their effects on cells. *Tetrahedron* **2013,** *69*, 7559-7567.

190. Tanaka, M.; Roberts, J. M.; Seo, H. S.; Souza, A.; Paulk, J.; Scott, T. G.; DeAngelo, S. L.; Dhe-Paganon, S.; Bradner, J. E., Design and characterization of

bivalent BET inhibitors. *Nature chemical biology* **2016,** *12* (12), 1089-1096.

191. Roy, D.; Parthasarathi, R.; Maiti, B.; Subramanian, V.; Chattaraj, P., Electrophilicity as a possible descriptor for toxicity prediction. *Bioorganic & medicinal chemistry* **2005,** *13* (10), 3405-3412.

192. Li, Y.; Chan, S. C.; Brand, L. J.; Hwang, T. H.; Silverstein, K. A.; Dehm, S. M., Androgen receptor splice variants mediate enzalutamide resistance in castration-resistant prostate cancer cell lines. *Cancer research* **2013,** *73* (2), 483-9.

193. Heck, R.; Nolley Jr, J., Palladium-catalyzed vinylic hydrogen substitution reactions with aryl, benzyl, and styryl halides. *The Journal of organic chemistry* **1972,** *37* (14), 2320-2322.

194. Chakravarthi, S.; Jessop, C. E.; Bulleid, N. J., The role of glutathione in disulphide bond formation and endoplasmic-reticulum-generated oxidative stress. *EMBO reports* **2006,** *7* (3), 271-5.

195. Anestal, K.; Prast-Nielsen, S.; Cenas, N.; Arner, E. S., Cell death by SecTRAPs: thioredoxin reductase as a prooxidant killer of cells. *PloS one* **2008,** *3* (4), e1846.

196. Urig, S.; Becker, K., On the potential of thioredoxin reductase inhibitors for cancer therapy. *Seminars in cancer biology* **2006,** *16* (6), 452-65.

197. Halasi, M.; Wang, M.; Chavan, T. S.; Gaponenko, V.; Hay, N.; Gartel, A. L., ROS inhibitor N-acetyl-L-cysteine antagonizes the activity of proteasome inhibitors. *The Biochemical journal* **2013,** *454* (2), 201-8.

198. Huang, B. K.; Langford, T. F.; Sikes, H. D., Using sensors and generators of H2O2 to elucidate the toxicity mechanism of piperlongumine and phenethyl isothiocyanate. *Antioxidants & redox signaling* **2016,** *24* (16), 924-938.

199. Zhu, C.; Hu, W.; Wu, H.; Hu, X., No evident dose-response relationship between cellular ROS level and its cytotoxicity–a paradoxical issue in ROS-based cancer therapy. *Scientific reports* **2014,** *4*.

200. Sprenger, C. C.; Plymate, S. R., The link between androgen receptor splice variants and castration-resistant prostate cancer. *Hormones & cancer* **2014,** *5* (4), 207-17.

201. Applegate, L. A.; Luscher, P.; Tyrrell, R. M., Induction of heme oxygenase: a general response to oxidant stress in cultured mammalian cells. *Cancer research* **1991,** *51* (3), 974-8.

202. Furfaro, A. L.; Traverso, N.; Domenicotti, C.; Piras, S.; Moretta, L.; Marinari, U. M.; Pronzato, M. A.; Nitti, M., The Nrf2/HO-1 Axis in Cancer Cell Growth and Chemoresistance. *Oxidative medicine and cellular longevity* **2016,** *2016*, 1958174.

203. Yu, J.; Zhang, L., PUMA, a potent killer with or without p53. *Oncogene* **2008,** *27 Suppl 1*, S71-83.

204. Lipinski, C. A.; Lombardo, F.; Dominy, B. W.; Feeney, P. J., Experimental and computational approaches to estimate solubility and permeability in drug discovery and development settings. *Advanced drug delivery reviews* **2012,** *64*, 4-17.

205. Zou, P.; Xia, Y.; Ji, J.; Chen, W.; Zhang, J.; Chen, X.; Rajamanickam, V.; Chen, G.; Wang, Z.; Chen, L.; Wang, Y.; Yang, S.; Liang, G., Piperlongumine as a direct TrxR1 inhibitor with suppressive activity against gastric cancer. *Cancer letters* **2016,** *375* (1), 114-26.

206. (a) Falkenberg, K. J.; Johnstone, R. W., Histone deacetylases and their inhibitors in cancer, neurological diseases and immune disorders. *Nat Rev Drug Discov* **2014,** *13* (9), 673-91; (b) Christensen, D. P.; Dahllof, M.; Lundh, M.; Rasmussen, D. N.; Nielsen, M. D.; Billestrup, N.; Grunnet, L. G.; Mandrup-Poulsen, T., Histone deacetylase (HDAC) inhibition as a novel treatment for diabetes mellitus. *Mol Med* **2011,** *17* (5-6), 378-90.

207. Baillie, T. A., Targeted Covalent Inhibitors for Drug Design. *Angewandte Chemie* **2016,** *55* (43), 13408-13421.

208. FDA approves afatinib for advanced lung cancer. *Oncology* **2013,** *27* (8),

813-4.

209. de Claro, R. A.; McGinn, K. M.; Verdun, N.; Lee, S.-L.; Chiu, H.-J.; Saber, H.; Brower, M. E.; Chang, C. G.; Pfuma, E.; Habtemariam, B., FDA approval: ibrutinib for patients with previously treated mantle cell lymphoma and previously treated chronic lymphocytic leukemia. *Clinical Cancer Research* **2015,** *21* (16), 3586-3590.

210. Lambert, J. M.; Gorzov, P.; Veprintsev, D. B.; Soderqvist, M.; Segerback, D.; Bergman, J.; Fersht, A. R.; Hainaut, P.; Wiman, K. G.; Bykov, V. J., PRIMA-1 reactivates mutant p53 by covalent binding to the core domain. *Cancer cell* **2009,** *15* (5), 376-88.

211. Lehmann, S.; Bykov, V. J.; Ali, D.; Andren, O.; Cherif, H.; Tidefelt, U.; Uggla, B.; Yachnin, J.; Juliusson, G.; Moshfegh, A.; Paul, C.; Wiman, K. G.; Andersson, P. O., Targeting p53 in vivo: a first-in-human study with p53-targeting compound APR-246 in refractory hematologic malignancies and prostate cancer. *Journal of clinical oncology : official journal of the American Society of Clinical Oncology* **2012,** *30* (29), 3633-9.

212. Powell Gray, B.; Kelly, L.; Ahrens, D. P.; Barry, A. P.; Kratschmer, C.; Levy, M.; Sullenger, B. A., Tunable cytotoxic aptamer-drug conjugates for the treatment of prostate cancer. *Proceedings of the National Academy of Sciences of the*

United States of America **2018**.

ABSTRACT

DISCOVERY OF PIPERLONGUMINE DERIVATIVES AS ANTI-LEUKEMIC AND ANTI-PROSTATE CANCER AGENTS

by

Yi Liao

August 2018

Advisor: Dr. Zhihui Qin

Major: Pharmaceutical Science

Degree: Doctor of Philosophy

Piperlongumine (PL) is an electrophilic anti-cancer natural product. Through non-covalent or covalent interactions with cellular targets, PL inactivates multiple oncogenic pathways and suppresses key components of cellular anti-oxidant/anti-electrophile defense systems. These actions result in pleiotropic anticancer effects and are expected to be effective to heterogeneous acute myeloid leukemia (AML) and prostate cancer (PCa). We applied two approaches to enhance the anticancer potency of PL: 1) To design PL-histone deacetylase inhibitor hybrid drugs (PL-HDACis; e.g., **1-58**), and 2) To dimerize PL pharmacophore to generate a dimeric PL (DiPL) warhead that is suitable for further conjugation (e.g., **5-17**). Both **1-58** and **5-17** were significantly more potent than PL in inhibiting AML or PCa cell proliferation and displayed broad

anti-AML/anti-PCa activities in high-risk and treatment-resistant cell lines. In the PL-HDACi hybrid drugs, both PL and HDACi structural components are essential for cooperatively inducing significant DNA damage and apoptosis in AML cells: PL moiety interferes cellular GSH defense, and the HDACi functionality suppresses DNA repair and antiapoptotic pathways. The chemical reactivity of PL pharmacophore strongly affected potency and selectivity profiles. In PCa VCaP cells, compared to PL, dimeric PL derivatives (DiPLs) more potently inhibited VCaP cell growth without sacrificing selectivity, and more effectively downregulated expression of androgen receptor (AR) and AR splice variant 7 (AR-V7). Both growth inhibition and AR/AR-V7 downregulation were significantly enhanced by GSH synthesis inhibitor BSO, demonstrating the critical role of electrophilicity of DiPL in drug-caused cellular effects. In order to improve disease selectivity and drug bioavailability of the newly obtained HDACi hybrid drugs, H_2O_2/peroxynitrite (PNT)-activated hydroxamic acid HDACi prodrugs were designed. Model compounds **Q-523** and **Q-582** were activated in AML cells to release cytotoxic HDACis, evidenced by inducing acetylation markers and reducing viability of AML cells. Intracellular activation and anti-leukemic activities of prodrug were increased or decreased by ROS/PNT inducers and scavengers, respectively. **Q-582** and **Q-523** also enhanced the potency of chemotherapy drug

cytarabine in AML cells, supporting the potentials of this prodrug class in combinatorial treatment. These prototype hybrid molecules, DiPLs and H_2O_2/PNT-activated HDACi prodrugs may serve as new leads for anticancer drug discovery.

AUTOBIOGRAPHICAL STATEMENT

YI LIAO

Education

Ph.D., Pharmaceutical Science, Medicinal Chemistry. Wayne State University, Detroit, USA. 2013-2018

B.S., Chemical biology, South-Central University for Nationalities (SCUEC), Wuhan, China. 2009-2013

Awards and Honors

- National Scholarship, Ministry of Education of China. 2010/2011
- The First Prize Scholarship, School of Pharmacy, SCUEC, China. 2010/2011
- Outstanding Bachelor's Thesis, Hubei Province, China. 2013
- The Rumble Fellowship, Wayne State University, USA. 2016
- Outstanding Student Poster Presentation Award, School of pharmacy, Wayne State University, USA. 2016
- Travel Awards, School of Pharmacy, Wayne State University, USA. 2017
- Frank O. Taylor scholarship, Wayne State University, USA. 2018

Publications

- **Liao Y**, Niu X, Chen B, et al. Synthesis and Antileukemic Activities of Piperlongumine and HDAC Inhibitor Hybrids against Acute Myeloid Leukemia Cells. Journal of Medicinal Chemistry, 2016, 59 (17): 7974-7990.

Poster Presentation

- **Yi Liao**, Xiaoja Nu, Bailing Chen, Yubin Ge*, Zhihui Qin*. *Discovery of Piperlongumine-Histone Deacetylase Inhibitor Hybrids as Potent Antileukemic Agents against Acute Myeloid Leukemia Cells*. The 13th Annual Research Forum, Wayne State University, Detroit, MI, 2015/10/05.
- **Yi Liao**, Liping Xu, Zhihui Qin*. *Michael Acceptor-equipped EPI-001 analogs reduce AR transcriptional activity, AR-V7 expression and cell proliferation in prostate cancer cells.* The 14th Annual Research Forum, Wayne State University, Detroit, MI, 2016/11/01. And the 49th Annual Pharmaceutics Graduate Student Research Meeting. University of Michigan, Ann Arbor, MI, 2017/06/15-2017/06/17.
- **Yi Liao**, Liping Xu, Zhihui Qin*. *ROS/RNS-activated hydroxamic acid HDAC inhibitor prodrugs inhibit proliferation of acute myeloid leukemia cells*. The 15th Annual Research Forum, Wayne State University, Detroit, MI, 2017/11/01. And the 36th National Medicinal Chemistry Symposium, Nashville, TN, 2018/04/29-2018/05/02.